CHARACTERIZATION OF PROTEIN TYROSINE PHOSPHATASE ε

by

Ian Granville Melhado

B.Sc., Simon Fraser University, 1988

A THESIS SUBMITTED IN PARTIAL FULFILMENT OF
THE REQUIREMENTS FOR THE DEGREE OF

DOCTOR OF PHILOSOPHY

in

THE FACULTY OF GRADUATE STUDIES

(Department of Medicine)

THE UNIVERSITY OF BRITISH COLUMBIA

July 1999

Abstract

Protein tyrosine phosphatases have been shown to play an important role in immune cell regulation. This study focused upon identifying PTPases that were regulated during inflammation. Using PCR mediated differential hybridization PTPε was identified as a candidate PTPase mRNA upregulated by pro-inflammatory stimuli. Northern blotting analysis confirmed that the message for this PTPase was induced by a limited number of stimuli in cells of the monocyte/macrophage lineage. With the development of highly specific polyclonal antibodies, monocyte/macrophage derived PTPε was observed as a 72/74 kDa doublet. p72/74PTPε was found to possess PTPase activity *in vitro*, predominantly within the cytosol, and its expression was observed to be regulated during cellular differentiation. Further characterization of PTPε indicated that the PTPase was phosphorylated and tyrosine phosphorylation could be induced *in vivo*. Tyrosine phosphorylation was found to induce the association of the small adapter protein GRB2 with PTPε in pervanadate treated cells. These observations and others pointed to a novel isoform of the previously described transmembrane PTPε PTPase.

An *in vitro* analysis of recombinant PTPε was undertaken to characterize the PTPase activity of the enzyme. This analysis revealed that the PTPase had a pH optimum

of 5.6. PTPε exhibited some substrate specificity especially when compared to other recombinant PTPases such as CD45 and PTPα. From the preceding analysis and the fact that the closely related PTPα appears to show specificity for $pp60^{c\text{-}src}$, the *src* family kinases were the signaling proteins initially investigated as potential *in vivo* substrates of PTPε.

By utilizing cDNAs encoding both transmembrane and non-transmembrane isforms of PTPε, PTPases were introduced into mammalian cells. In the case of transmembrane PTPε, various mutants were characterized *in vivo*. These studies revealed that p100/110PTPε is a highly glycosylated membrane protein, found predominantly at cell-cell junctions. While p100/110PTPε was capable of associating with and modulating the phosphotyrosine content and kinase activity of the *src* family kinase members $pp60^{c\text{-}src}$ and $pp59^{fyn}$ p72/74PTPε was not. This phenomenon may be explained by the observation that the localization of p72/74PTPε was to the nucleus and not the plasma membrane where *src* family kinases are found.

Finally, the PTPε homologue was reported to contain a SH3 binding site, however, this site was not conserved in PTPε. A proline residue was introduced at position F112 and resulted in the reconstitution of an SH3 domain-binding site thus turning PTPε into a PTPα like molecule. PTPεF112P exhibited altered substrate specificity showing increased activity towards *src* family kinases and reduced activity towards the *in vivo* substrate CrkII.

Table of Contents

List of Tables and Figures

Chapter 1

Chapter 3

Chapter 4

Chapter 5

Chapter 6

Abbreviations

AMLV	Abelson murine leukemia virus
ATP	Adenosine triphosphate
BPV	Bovine papilloma virus
CD	cluster differentiation
CMV	cytomegalovirus
CSF-1R	colony stimulating factor receptor
DNA	deoxyribonucleic acid
ECM	extracellular matrix
EGF-R	epidermal growth factor receptor
GAP	GTPase activating protein
GRB2	growth factor receptor bound protein 2
GST	Glutathione S Transferase
HEK	human embryonal kidney
ICAM-1	intracellular adhesion molecule 1
Ig	immunoglobulin
IL	interleukin
IPTG	isopropyl-1-thio-β-D-galactopyranoside
LAR	leukocyte common antigen related protein

MAb	monoclonal antibody
MAP kinase	mitogen activated protein kinase
MMTV	mouse mammory tumour viruse
PBS	phosphate buffered salin
PCR	polymerase chain reaction
PDGF-R	platelet-derived growth factor
PH	pleckstrin homology
PI3K	phosphatidylinositol-3-kinase
PKC	protein kinase C
PLCγ1	phospholipase C gamma 1
PMA	phorbol myristate acetate
PTB	phosphoprotein binding
PTP	protein tyrosine phosphatase
PTPase	protein tyrosine phosphatase
PTK	protein tyrosine kinase
RNA	ribonucleic acid
SDS-PAGE	sodium dodecyl sulfate – polyacrylamide gel electrophoresis
SH2	src homology 2
SH3	src homolgy 3
SYP	SH2-containing tyrosine phosphatase
TCR	T cell receptor
TNF-α	tumour necrosis factor alpha

Acknowledgements

I am indebted to a number of people who aided me during the course of this thesis. In particular I would like to thank Nicola Melhado (Mann) and the Mann family for all their support. I am forever grateful to Frank Jirik for encouragement and unwavering support during years prior to and during this course of study. A special thanks to Nicole Janzen a life long friend and co-worker, to Dr. Donald Semenuik, Gloria and Bruce Thomson, and my advisory committee. I would also like to acknowledge Ken Harder for collaborative efforts, discussions and assistance with the F112P mutants, Scott Pownall for assistance in expression of the cytosolic isoform of PTPε and the remaining Jirik lab for continued support during the past 5 years. Finally, I would like acknowledge the solid support of my family, Vernal, Barbera, Mark and Joy with a special thank you to Caroline Proctor.

Chapter 1

Introduction

With the discovery by Sefton, Hunter and Beemon in 1979 of the cellular homologue of *v-src*, the kinase within the Rous sarcoma virus responsible for the tumorigenicity of the infectious particle, the family of signaling proteins now known as protein kinases was catapulted to the forefront of cancer research (figure 1.1). Further work by Collett *et al.*, 1980 culminated in the report that the tumorigenic activity in the Rous sarcoma virus was a kinase specific for protein tyrosine residues. Despite the critical importance of tyrosine phosphorylation for differentiation and intracellular regulatory events associated with cell growth it was demonstrated to only constitute 0.1% of the phosphate on proteins within a cell. In contrast, serine and threonine phosphorylations were found to comprise greater than 99% of the polypeptide associated phosphate within the cell. Based on these observations, it was assumed that serine and

threonine phosphorylation was the most important phosphorylation type with respect to physiological events occuring within cells. This may account for the fact that the serine and threonine kinases were initially the most widely studied of protein kinases. The work of Collett *et al.*, 1980 however, indicated that although tyrosine phosphate was relatively rare, a single tyrosine kinase was capable of inducing single step transformation of susceptible cells. Thereafter, numerous groups reported that virally transformed homologues of cellular protein tyrosine kinases were the tumorigenic agents within the genomes of a number of different cancer inducing viruses (Rohrschneider *et al.*, 1979, Yoshida *et al.*, 1980). For example, the *fyn, lyn, abl, fes,* and erbB moleucles were all found to be tyrosine kinases present within the genomes of cancer causing retroviruses. In searching viral genomes for 'hijacked' signaling proteins, it rapidly became evident the viral counterparts of the cellular genes often led to truncated proteins or molecules containing amino acid substitutions. The sites of these mutations often yielded important biochemical information with respect to gene function since many of the mutations gave rise to abnormal protein products constituitive activation, abnormal dimerization or altered subcellular localization. Thus, tyrosine kinases play a crutial role in the regulation of intracellular signal transduction mechanisms and likely modulate key cellular processes.

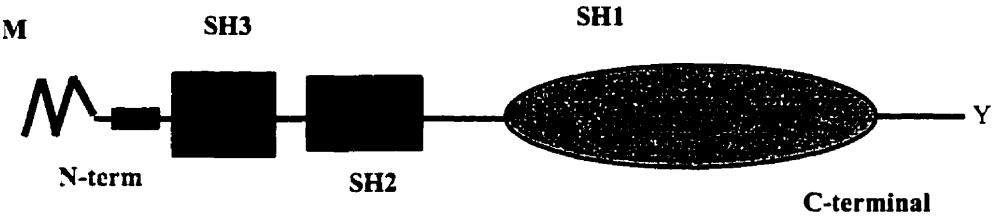

Figure 1.1 Illustration of the *src* family of tyrosine kinases. M denotes meristylation of the N terminus. N-term is the unique N-terminal region of this family of kinases. SH3 is the *src* homology 3 domain, SH2 the *src* homology 2 domain and SH1 the *src* homology 1 or kinase domain which contains the enzyme active site as well as the site for a stimulatory phosphotyrosine residue. The C-terminal tail 'Y' indicates the C-terminal regulatory phosphorylation site

Since the molecular cloning of the first PTPase, PTP1B, the number of members of the PTPase family has grown considerably with the nucleic acid sequences of more than 50 PTPases reported. This family of proteins can be divided into three broad groups (figure 1.2). The dual specificity PTPases, such as mkp1/CL100/3CH314, and CDC25 are predominantly nuclear enzymes having a single catalytic domain (Sun *et al.*, 1993, Guan *et al.*, 1995). These PTPases are characterized by their ability to catalyze the removal of phosphate groups from both threonine and tyrosine residues. The dual specificity PTPases also possess strict substrate specificity and are amongst the few PTPases whose substrates have been identified, these include the erk family of kinases (Guan *et al.*, 1995).

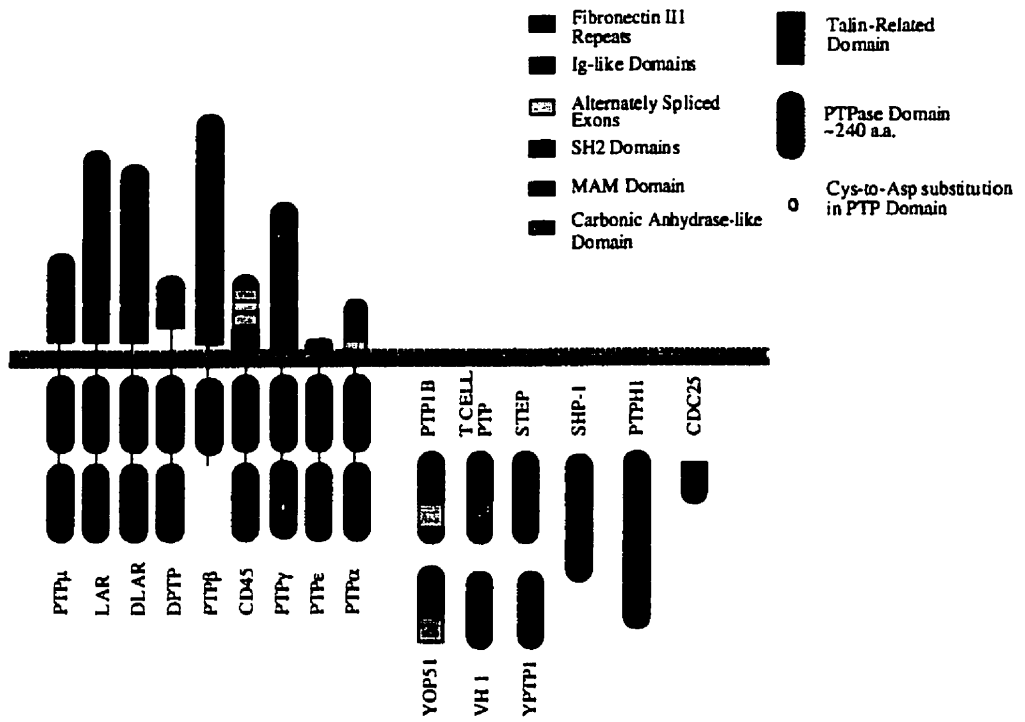

Figure 1.2 The Protein tyrosine phosphatase family. The PTPase family is broken into three broad groups. The transmembrane PTPases, the cytosolic PTPases and the nuclear PTPases. Transmembrane PTPases are characterized by diverse extracellular domains, a transmembrane domain and with the exception of PTPβ tandem catalytic domains. Cytosolic PTPases often contain various signaling domains including SH2 domains and PEST domains. The majority of nuclear PTPases are dual specificity PTPases capable of catalyzing the dephosphorylation of threonine and tyrosine residues.

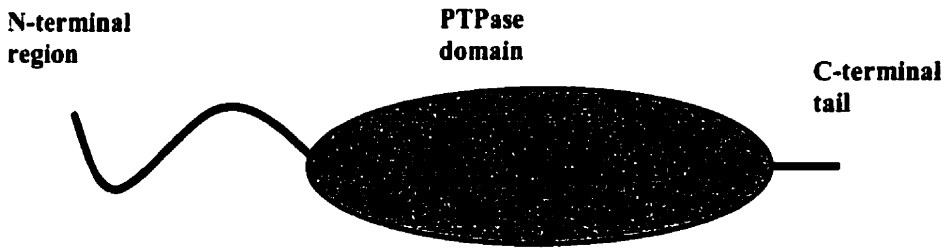

Figure 1.3 Illustration of cytosolic PTPases

The cytosolic PTPases comprise a broad range of PTPases (figure 1.3). As with many other cytosolic molecules involved in cell signaling, this sub-group often has notable protein-protein interaction domains in addition to the single catalytic domain. The SH2 domain containing PTPases SHP-1 and SHP-2, for example, have been shown to interact with a wide variety of activated growth factor receptors either potentiating (SHP-2) or inhibiting (SHP-1) signal transduction cascades emanating from these receptors (Rivard *et al.*, 1995, Su *et al.*, 1996, Tomic *et al.*, 1995, Neel *et al.*, 1997). Ezrin domain containing PTPases, such as PTP-MEG, associate with cytoskeletal proteins and are thought to regulate cellular architecture (Moller & Ullrich *et al.*, 1994). The PDZ domain containing PTPase FAP-1 associates with the Fas receptor blocking the apoptotic signal delivered by FasL (Sato *et al.*, 1995). The cysolic PTPase group also includes PTPases, such as PTP1B and T-cell PTPase that lack known protein interaction domains (Charbonneau *et al.*, 1988, Cool *et al.*, 1989). The activity of PTP1B can be regulated by limited proteolysis of the C-terminal tail (Liu *et al.*,1996). Its functions range from growth factor receptor de-phosphorylation (PTP1B) (Goldstein *et al.*, 1998) to regulation of hematopoiesis (Tremblay *et al* 1998) to control of glucose homeostasis (Kennedy *et al* 1999).

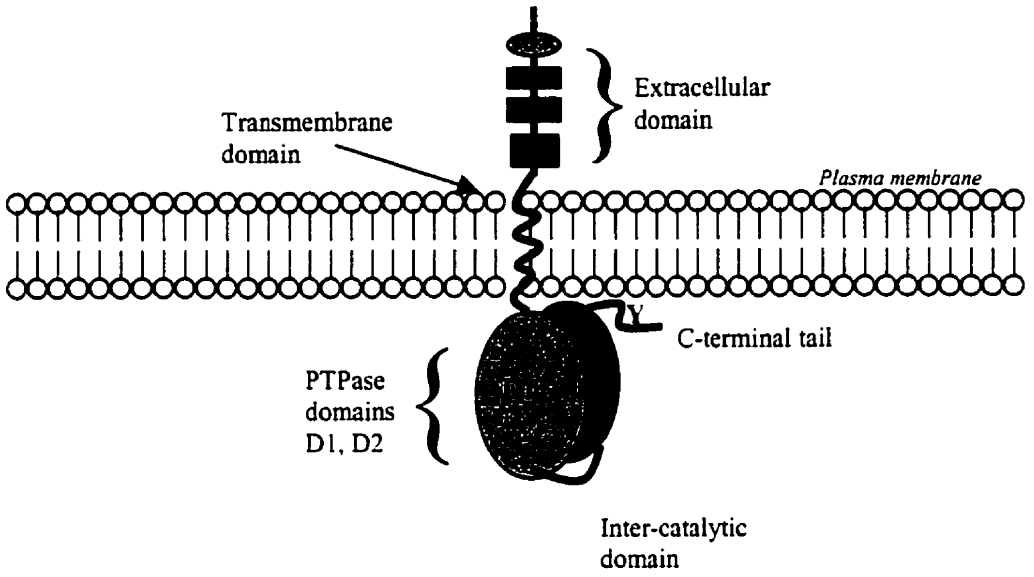

Figure 1.4 Illustration of transmembrane PTPases

The transmembrane or receptor-like PTPases are probably the most diverse sub family of PTPases (figure 1.3). Differentially glycosylated extracellular domains of widely varying size, a single membrane-spanning region and, with the exception RPTPβ, which has a single catalytic domain, tandem catalytic domains distinguishes this group of PTPases. The extra-cellular domains contain an array of common receptor motifs including immunoglobulin superfamily domains and fibronectin type-III repeats. The catalytic domains of this group of PTPases, in contrast, share high degrees of sequence identity (Levy *et al.*, 1993).

The crystal structure of PTPα 's first catalytic domain, as solved by Kurian and Hunter in 1997, indicated that PTPα may exist as inactive homodimers. The hypothesis argues that the membrane proximal region, located before the beginning of the catalytic

domain, forms a unique helical wedge structure. The wedge is capable of insertion into the first catalytic domain of a second PTPase, abrogating the interaction of the enzyme with its substrate through competitive inhibition.

Multiple mRNA splice variants is also a hallmark of this sub-family of PTPases. CD45, otherwise known as leukocyte common antigen (LCA), is an archetypal member of this family, apart from being one of the most widely studied and best understood transmembrane PTPase. With more than five different splice variants giving rise to a number of different isoforms, including T200 and B220, this PTPase exhibits cell lineage-specific isoform expression and function (Streuli *et al.*, 1987, Thomas *et al.*, 1987, Ralph *et al.*, 1987). The T200 isoform, for example, dephosphorylates and activates the membrane associated tyrosine kinase $pp55^{lck}$ in mature T-cells during TCR aggregation, resulting in T lymphocyte activation (Pingel and Thomas 1989, Mustelin *et al.*, 1989, Ostergaard *et al.*, 1989, Mustelin *et al.*, 1990). Dephosphorylation and activation of another *src* kinase family member, $pp53/56^{lyn}$, by the B220 isoform in mature B-cells during BCR aggregation, similarly results in B-cell activation (Katagiri *et al.*, 1995, Yanagi *et al.*, 1996).

As regulators of tyrosine phosphorylated PTKs and their substrates, both receptor and cytosolic protein-tryosine phosphatases have been identified as important regulatory components within signaling complexes (Charbonneau and Tonks, 1992; Stone and Dixon, 1994; Hunter, 1995). Furthermore, a given phosphatase may demonstrate either stimulatory, inhibitory or both effects within specific intracellular signaling pathways

(Feng and Pawson, 1994; Trowbridge and Thomas, 1994). While commonly referred to as "receptor" PTPases the putative ligands for this sub-family of PTPases are largely unknown. With the discovery of the ligand for RPTPβ as the extracellular domain of another RPTPβ molecule on an adjacent cell, many reports have subsequently implicated transmembrane PTPases in the regulation of cell-cell adhesion (Peles *et al.*, 1998). CD45 also possesses an extracellular domain that resembles those of certain adhesion molecules. CD45 is also thought to have a ligand that is bound to the surface of thymic epithelial cells (Thomas personal communication).

The catalytic domains of all known PTPases contain a common active site motif, $(H/V)C(X)_5R(ST)$, that is essential for the hydrolyis of substrates via a common mechanism (figure 1.4). The first step of the reaction involves attack by the thiolate anion of the conserved cysteine residue within the above motif on the phosphate ester, with simultaneous departure of the tyrosyl residue aided by general acid-base catalysis involving an invariant aspartic acid residue. The resulting phosphoenzyme intermediate then undergoes a rate-limiting hydrolysis step to form inorganic phosphate and the free enzyme. The invariant arginine in the signature motif is crucial for binding of the substrate through electrostatic interaction with the phosphate moiety and also for transition state stabilization (Barford *et al.*, 1998, Zhang 1998, Zhao *et al.*, 1998, Denu *et al.*, 1996, Denu *et al.,1996*). The catalytic domain has also recently been shown in some cases to have a broad specificity for phosphorylated moieties. In the case of PTEN, for example, recent reports demonstrate that this PTPase is not only capable of catalyzing

the removal of phosphate groups from tyrosyl residues but also from the 3-position of phosphatidyl inositol (PI) group of phospholipids (Maehama & Dixon 1998).

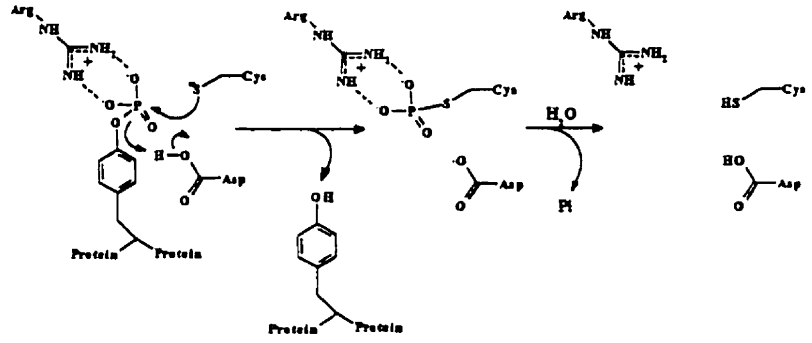

Figure 1.5 Illustration of the catalytic mechanism of PTPases

The first member of the PTPase superfamily of signaling molecules to be characterized in detail was the cytosolic PTPase PTP1B (Charbonneau *et al.*, 1989). Comprised of short N-terminal and C-terminal sequences flanking a single catalytic domain, PTP1B has been shown associate with the rough endoplasmic reticulum through its C-terminus. Its activity can be modulated by limited proteolytic cleavage of its tail (Liu *et al.*, 1996). However, work by Lammers, Moller, and Ullrich in 1997, implicated PTP1B PTPase activity in insulin receptor signaling as well as the signal transduction pathways activated by various other growth factor receptors. It has recently been shown that the stimulation of various cells with growth factors results in a transient increase in the intracellular concentration of H_2O_2 that is required for growth factor-induced protein

tyrosine phosphorylation (Sundaresan *et al.*, 1995, Denu *et al.*, 1998). PTP1B has been implicated in EGF-R signal transduction through a physical association of EGF-R in cells expressing a mutant PTP1B where the catalytic cysteine had been mutated to a serine residue. While the resulting mutant is capable of binding its substrate through phosphotyrosine independent interactions, it is incapable of forming a thio-phosphate ester intermediate. In this way, PTP1B mutant effectively traps the substrate, in this case the EGF-R (Milarski *et al.*, 1993). The effect of H_2O_2 produced in response to epidermal growth factor (EGF) on the activity of protein-tyrosine phosphatase 1B (PTP1B) has been investigated in A431 human epidermoid carcinoma cells. H_2O_2 was shown to inactivate recombinant PTP1B in vitro by oxidizing its catalytic site cysteine. The oxidized enzyme was reactivated more effectively by thioredoxin than by glutaredoxin or glutathione at their physiological concentrations. When the oxidation-state of PTP1B was monitored, oxidized PTP1B reached maximal levels ten minutes after stimulation of cells with EGF and returned to baseline levels by forty minutes, suggesting that the oxidation of PTP1B is reversible in cells. These results elegantly indicated that the activation of a receptor tyrosine kinase by binding of the corresponding growth factor may not be sufficient to increase the steady state level of protein tyrosine phosphorylation in cells and that concurrent inhibition of protein-tyrosine phosphatases by H_2O_2 might also be required (Lee *et al.*, 1998). This observation touches upon the novel methods of regulation that may be discovered in signal transduction systems within the cell. However, it remains to be shown whether this is a common mechanism of PTP regulation *in vivo*.

Shortly after the initial molecular characterization of PTP1B, database searches revealed that CD45 exhibited sequence similarity. Using a variety of molecular cloning techniques, a number of receptor like PTPases have subsequently been described. One of the first in this family was LAR, a molecule that is characterized by tandem catalytic domains and a large extra-cellular domain composed of both fibronectin type-III repeats and Ig domains that are similar to those of the homophilic adhesion molecule NCAM. A role for LAR as well as PTPβ has been reported in axon guidance (Serra-Pages *et al.*, 1998, Holland *et al.*, 1998) and mammary gland development (Serra-Pages *et al.*, 1998). In cultured cells, LAR has been shown to bind to the intracellular, coiled coil LAR-interacting protein at discrete ends of focal adhesions, implicating these proteins in the regulation of cell-matrix interactions (Serra-Pages *et al.*, 1998). Seven LAR-interacting protein homologues have been described in humans and *Caenorhabditis elegans* that make up the liprin gene family (Serra-Pages *et al.*, 1998). Based on sequence similarities and binding characteristics, liprins are subdivided into alpha-type and beta-type liprins. The C-terminal, non-coiled coil regions of alpha-liprins bind to the membrane-distal phosphatase domains of LAR family members, as well as to the C-terminal, non-coiled coil region of beta-liprins (Serra-Pages *et al.*, 1998). Both alpha- and beta-liprins homodimerize via their N-terminal, coiled-coil regions. Liprins are thus multivalent proteins that potentially form complex structures. Co-expression studies indicate that liprin-α_2 alters LAR cellular localization and induces clustering of this PTP which results in localization of LAR family tyrosine phosphatases at specific sites on the plasma membrane, possibly regulating their interaction with the extracellular environment and their association with substrates (Serra-Pages *et al.*, 1998). Such membrane localization

may explain the possible role of LAR in insulin receptor signaling. In this regard, a functional and physical association between LAR and the insulin receptor within endosomes after stimulation has been described (Ahmad and Goldstein 1997). The receptor's activation was observed to influence the affinity of LAR for the receptor. Such results highlight the importance of cellular localization in defining the functions of receptor PTPases. Evidence suggests that individual receptor PTPases may be involved in different signaling pathways dependent upon their proximity to particular molecules within specific signaling complexes. In the case of LAR it is possible that interactions between the extracellular domain and signaling complexes involving cell-cell adhesion occur, in addition to its association with the activated insulin receptor. Thus, it is probable that insulin signals in a cell may be regulated by concurrent signals received by cell-cell or extracellular matrix interactions that are transduced through receptor PTPases.

The hemopoietic cell lineage gives rise to the wide-variety of cell types found in the immune system. Through differentiation, guided by coordination of a complex network of granulocytic and macrophage growth factors and cytokines, hemopoietic progenitors give rise to the cells of the reticuloendothelial system. The reticuloendothelial system includes microglia in the brain, dendtritic cells within the lymph nodes and monocytes which roam the vasculature. At sites of inflammation, it is the monocyte lineage, which responds in collaboration with granulocytes and neutrophils. Following a concentration gradient of chemotactic factors known as chemokines monocytes slow their progress through blood vessels and begin a phase of "rolling adhesion" as cellular

adhesion molecules are upregulated both on monocytes and endothelial cells. At sites of inflammation, monocyte migration is halted and the activated cells invade the tissue. Once activated, monocytes differentiate into macrophages and acquire various functions related to wound healing. Phagocytosis, production of reactive oxygen intermediates and secretion of pro-inflammatory cytokines, such as IL-1 and TNFα, are among the properties displayed be activated macrophages. These functions are also responsible for the symptoms of certain inflammatory autoimmune diseases such as arthritis, multiple sclerosis and lupus. Thus, a better understanding of macrophage signaling and differentiation may yield novel strategies in the treatment of various autoimmune diseases.

There is much evidence supporting the role of various PTKs in the proliferation, differentiation, and function of hemopoietic cells (Chan *et al.*, 1994, Gold & DeFranco, 1994, Ihle, 1995). However, with the exception of molecules such as CD45, the SH2 domain-containing PTPases (Trowbridge & Thomas, 1994; Feng & Pawson, 1994), and the novel tumour suppressor PTPase PTEN, knowledge about the specific functional roles of many PTPases is lacking. With the importance of PTKs and PTPases in many leukocyte functions, we decided to examine which PTPases are upregulated by macrophages after differentiation, thus, providing some insight into the roles PTPases play in macrophage function.

An initial approach in elucidating the role of these molecules has been to establish the spectrum of expressed PTPases, both during cell differentiation as well as in

terminally differentiated cells. Efforts to determine the expression patterns of PTPases in monocytic cells have, for example, capitalized on systems allowing the external control of cellular differentiation. In this respect, the promyelocytic leukemia cell lines U937 and HL-60 have been useful models. In response to various stimuli, HL-60 cells undergo differentiation into various cell types (Collins *et al.*, 1987). Following phorbol-ester treatment, HL-60 cells develop a number of monocyte-like characteristics. In contrast, DMSO treatment results in cells with granulocytic features (Collins *et al.*, 1978; Collins *et al.*, 1987). The regulation of a number of PTPases has been studied during HL-60 differentiation. For example, Uchida *et al.*, (1993), as well as Zhao *et al.*, (1994), described both induction of PTP1C phosphorylation and increases in transcript and protein levels within phorbol-ester stimulated HL-60 cells. In addition, the transcriptional regulation of a number of PTPases, including protein tyrosine phosphatases alpha (PTPα) and epsilon (PTPε) and PTP-MEG2 has been described in the U937 and HL-60 cell lines following phorbol-ester administration (Seimiya *et al.*, 1995). Using the murine macrophage cell line RAW 264.7 as well as primary macrophage cultures as model systems the expression patterns of PTPases was studied further.

PTPε is a member of the family of receptor-like PTPases, which includes PTPα, LAR, and CD45 among others (Charbonneau and Tonks, 1992). PTPε is composed of a protein having two tandem intracellular catalytic domains, a transmembrane segment, and following signal peptide processing, a ~25-residue extracellular domain (Krueger *et al.*, 1990). Within the group of receptor-like PTPases, PTPε bears closest similarity to the widely expressed phosphatase, PTPα (Matthews *et al.*, 1990; Sap *et al.*, 1990; Kaplan *et*

al., 1990; Jirik *et al.*, 1990). The similarity between these two PTPases is striking when the amino acid sequences of the intracellular domains are compared (~85% identity) (figure 3.3.1). In contrast, the extracellular regions of the two molecules are dissimilar, both in length and amino acid sequence (Krueger *et al.*, 1990). Moreover, the expression of PTPε appears to be more restricted in its distribution than that of PTPα (Hendriks *et al.*, 1994; Elson and Leder, 1995a, 1995b). PTPε transcripts were detected in the interleukin (IL)-3-dependent myeloid leukemia cell line DA-3 (Yi *et al.*, 1991), mouse embryonic stem cells (Hendriks *et al.*, 1994), and at low levels in NIH-3T3 cells (Yi *et al.*, 1991). PTPε transcripts were also seen in MEL erythroblastoid leukemia cells, following induction with dimethyl sulfoxide (Kume *et al.*, 1994). PTPε expression was recently discovered in mammary tumor cell lines derived from transgenic mice expressing MMTV-v-Ha-*ras* and MMTV-c-*neu* (Elson and Leder, 1995a).

In a study aimed at characterizing PTPases expressed in cells of hemopoietic origin and in response to pro-inflammatory stimuli, PTPε was identified as a phosphatase upregulated by treatment of adherent cells obtained from murine peritoneal macrophages with LPS or IFNγ. This thesis focuses upon a characterization of PTPε. In Chapter 3, "***The Screen for PTPases Regulated by IFNγ and PTPε Expression in Cells of the Monocyte/Macrophage Lineage***", PTPε expression during monocytic cell differentiation is described. Here, the expression pattern and activity of PTPε was analyzed in phorbol ester-differentiated HL-60 cells. During this study a novel, primarily nuclear and cytosolic fraction-associated, p72/74 isoform of PTPε was identified, the only detectable form of this PTPase expressed in HL-60, Jurkat, and murine peritoneal-exudate cells.

Chapter 4, "***Bacterial Expression and in vitro Substrate Specificity of PTPε and Substrate Specificity of Native PTPε***", describes expression of recombinant PTPε in bacteria. This section details the characterization of *in vitro* substrate specificity of PTPε using synthetic phosphopeptide substrates. The final chapter entitled "***Over-expression of Transmembrane and Non-transmembrane PTPε in Mammalian Cells and the Role of a Putative SH3 Binding Motif in PTPα/PTPε Family of PTPases***" describes the characterization of PTPε isoforms by over-expression in mammalian cells. These studies compare the PTPε isoforms and makes use of the *in vitro* biochemical enzyme analysis in Chapter 4 to direct the search for *in vivo* substrates.

Chapter 2

Materials and Methods

2.1 Materials. Phorbol 12-myristate 13-acetate (PMA) was obtained from Gibco/BRL. Hydrogen peroxide, sodium orthovanadate and other chemicals were obtained from Fisher Scientific.

2.2 Buffers. Buffer A: 25 mM Tris-HCl pH 7.5, 150 mM NaCl, 10 mM 2-mercaptoethanol, 1.0% Triton X-100, soybean trypsin inhibitor 10 μg/ml, leupeptin 1.0 μg/ml, 1 mM phenylmethylsulfonylflouride, and pepstatin 1.0 μg/ml. Buffer B: 50 mM Tris-HCl pH 8.0, 150 mM NaCl, 2.5 mM $CaCl_2$, 10 mM 2-mercaptoethanol. Northern/Southern Hybridization buffer: 25% Formamide, 1.0% BSA, 7.0% SDS, 0.5 M $NaHPO_4$ pH 7.2, 10 mM EDTA. GT buffer: 4M guanidine isothiocyanate, 50 mM MOPS

pH 7.0, 1.0% 2-mercaptoethanol, 1.0% Sarcosyl. 2x Bind buffer: 1M NaCl, 50 mM MOPS pH 7.0, 10 mM EDTA pH 8.0. 1x Wash buffer 150 mM NaCl, 25 mM MOPS pH 7.0, 2 mM EDTA, 0.1% Sarcosyl. TX100 lysis buffer: 100 mM NaCl, 25 mM Tris-HCl pH 7.5, 2 mM EDTA, 1 mM DTT, 1.0% Triton X-100, 10 μg/ml aprotinin, 10 μg/ml bestatin, 10 μg/ml leupeptin, 5 μg/ml pepstatin, 10 μg/ml soybean trypsin inhibitor, 1 mM phenylmethylsulfonyl fluoride, 1 mM Na_3VO_4, 50 mM NaF. RIPA buffer: 100 mM NaCl, 25 mM Tris-HCl pH 7.5, 2 mM EDTA, 1 mM DTT, 1.0% (v/v) Triton X-100, NaF, 0.5% (w/v) Deoxycholate, 0.1% (w/v) SDS, 10 μg/ml aprotinin, 10 μg/ml bestatin, 10 μg/ml leupeptin, 5 μg/ml pepstatin, 10 μg/ml soybean trypsin inhibitor, 1 mM phenylmethylsulfonyl fluoride, 1 mM Na_3VO_4, 50 mM NaF.

2.3 Rapid mRNA purification. Cells or tissue were homogenized in 1-5 ml of GT buffer using a 22G needle and syringe or tissue homogenizer. Equal volumes of 2x Bind buffer was added and DNA/protein precipitate was pelleted at 10,000*g* for 10 min. The supernatant was transferred to a fresh tube containing 150 μl of a 50% slurry of poly-U Sepharose and incubated at room temperature on a rotating wheel for 30 min. The beads were collected by centrifugation at 250g for 2 min. The beads were washed 3 times with 1x Wash buffer. Messenger RNA was liberated from the beads by the addition of 50 μl of distilled water and incubation at 70°C for 10 min followed by removal of the beads by centrifugation at 10,000*g* for 2 min. If subsequent enzymatic reactions were to be performed on the mRNA sample Sarcosyl was omitted from the Wash buffer.

2.4 Northern Blot. Purified mRNA was prepared as described above and subjected to electrophoresis through 0.7% agarose gels containing 7.5% formaldehyde, 1x MOPS buffer for 4 hours at 150V in 1x MOPS running buffer. After electrophoresis gels were washed for 15 min in distilled water then mRNA transferred to GeneScreen nylon membranes by capillary action with 2x SSC. The transferred mRNA was then immobilized to the membranes by a single 150 kJ dose of UV-C irradiation and efficient transfer visualized by UV light. Blots were pre-hybridized for 20 min at 65°C with Hybridization buffer then hybridized with the appropriate probes overnight at 65°C in a rotating hybridization oven. Then washed until background had decreased to acceptable levels with 0.1x SSC / 0.1% SDS at the appropriated temperature (65°C).

2.5 Differential hybridization screening. Randomly primed cDNA's were prepared by reverse transcription of purified mRNA samples using Superscript Reverse Transcriptase (GIBCO/BRL) in the following reaction. Five hundred nanograms of mRNA was added to 5 μl of 5x Superscript buffer, 500 μM dNTPs, 25 pmol pdN_6, 5 U RNasin, 10 U Superscript reverse transcriptase and the final volume adjusted to 25 μl with distilled water. The reaction was then allowed to proceed at 45°C for 30 min then at 55°C for 30 min before termination by incubation at 70°C for 15 min. PCR fragments of conserved PTPase catalytic domains from PTPases upregulated in response to IFNγ were generated by touch-down PCR using degenerate oligonucleotides Deg #1 (DFW) [5'-CTCAGTCGACCTT T/C TGG C/A G I ATG G/A T I TGG GA A/G C], GXGXXG [5'-CTCAGTCGACCC I A C/T I CC I GC A/G CT G/A CAGTG], and Deg #2 (QYWP)

[5'-CTCAGTCGACCAA A/G TG T/C G C/A I CA A/G TA T/C TGGCC] using cDNAs generated from mRNAs purified from RAW264.7 cells stimulated with 500 U/ml murine IFNγ. PCR fragments were agarose gel purified and sub-cloned blunt-ended into EcoRV digested pSSBS. Positive clones were selected on the basis of blue/white selection using X-gal (100 μg/ml) and IPTG (2 mM) within the bacterial culture plates. Positive clones were confirmed with a Sal I restriction digest liberating the 350 bp insert. DNA from positive clones was prepared and equal amounts immobilized on Hybond-N nylon membranes by slot blotting. A PCR probe was prepared from cDNAs generated from unstimulated mRNA samples using identical conditions as described previously with the addition of 75 μCi of [α^{32}P] dCTP (3000 Ci/mmole). Slot blots were hybridized with the PCR probe overnight at 65°C in Southern hybridization buffer. Slot blots were then washed at 65°C in 0.1x SSC / 0.1%SDS for 30 min and exposed to X-ray film at -80°C. Upregulated PTPase messages were identified on the basis of the *absence* of a hybridization signal due to under representation of the PTPase mRNA in the PCR probe prepared from the unstimulated sample. Clones representing candidates for upregulation were sequenced manually using the chain termination method (Sanger *et al.*, 1977).

2.6 Cloning of PTPε intracellular domains. The cDNA encoding the intracellular domains of PTPε were generated by PCR using 5' and 3' oligonucleotide primers: [5'-CTCGGATCCCCCATGAGGAAGCAGAGGAAAGCTGTGGTC] and [5'-GAGGGATCCAATTGCGGCCGCTCATTTGAAATTAGCATAATCAGA] as described in the published sequence (Krueger et al., 1990) synthesized on a Applied

Biosystems DNA Synthesizer (model 391). Messenger RNA was prepared from HL-60 cells as described earlier. Complementary DNA strands were generated by reverse transcription by the addition of the reaction mixture (5 µl 5x Superscript buffer, 500µM dNTPs, 25 pmol pdN_6, 5 U RNAsin, 10 U Superscript Reverse transcriptase final volume 25 µl) to 1.0 µg of purified mRNA in distilled water. Reactions were carried out at 45°C for 30 min followed by incubation at 55°C for 30 min. Five microlitres of the reverse transcriptase reactions were then subjected to touch-down PCR amplification using oligonucleotides described earlier under the following reaction conditions (10 µl 10x Taq buffer, 200 µM dNTPs, 1.5 mM $MgCl_2$, 1 µM 5' primer, 1 µM 3' primer, 1 U Taq DNA polymerase final volume adjusted to 100 µl). Full-length cDNAs were purified by agarose gel electrophoresis then digested with BamHI and MunI restriction enzymes restriction sites for these enzymes were included within the 5' primer, and 3' primer, respectively. Digested DNA fragments were gel purified and directionally sub-cloned into the BamHI, EcoRI digested pGEX-2T expression vector utilizing the fact that MunI and EcoRI share compatible ends.

2.7 Recombinant expression of PTPε, PTPα, and CD45 intracellular domains. The pGEX-2T-PTPε, pGET-2T-tag-PTPα, pGEX-2T-tag-CD45 prokaryotic expression vectors were transformed into competent XL-1 blue bacteria. 50 ml overnight cultures were grown in 100 µg/ml ampicillin/Luria broth and added to 1 litre of the same culture medium and grown to an OD_{600} of 0.6 at 37°C in the absence of IPTG. Recombinant PTPε, PTPα, and CD45 were induced with the addition of 0.1 mM IPTG and cultures

grown in the presence of IPTG for 6 hours at 23°C. Bacteria were pelleted by centrifugation at 5,000*g* for 15 min at 4°C. The bacterial pellets were resuspended in 10 ml of Buffer A and lysed by sonication with 3x 30 second pulses on ice. The bacterial extracts were then subjected to ultracentrifugation at 100,000*g* for 30 min at 4°C and the supernatants stored at -80°C prior to further purification.

2.8 PTPase purification. The bacterial extracts were added to 1.0 ml of a 50% glutathione Sepharose slurry and incubated at 4°C for 1 hour. The beads were washed 4 times with Buffer A and once with Buffer B before cleavage in 1.0 ml of Buffer B containing 50 µl of thrombin (400 µg/ml). Glycerol was added to 50% (v/v) final concentration before storage at -80°C. Protein concentration was determined by SDS-PAGE and coomassie staining in the presence of BSA standards. Protein concentrations were adjusted to 50 µg/ml before storage.

2.9 Production of PTP mutant cDNA's. Mutant PTPε cDNA's were generated by overlap extension PCR (Ho *et al.*, 1989) using oligonucleotide pairs M13 reverse primer + mC1>Aa [5'-ACCCACGCCCGCGCTAGCGTGAACCACAATGGG], M13(-20) primer + mC1>As [5'-CCCATTGTGGTTCACGCTAGCGCGGGCGTGGGT] to amplify PTPεC334A fragments; M13 reverse primer + mC2>Aa [5'-CCCTGCTCCCGCCGTAGCGTGCACGGTGATGGG], M13(-20) primer + mC2>As [5'-CCCATCACCGTGACAGCTAGCGCGGGAGCAGGG] to amplify PTPεC629A

fragments; M13 reverse primer + mPPIPa [5'-CACGGGCATGGGGGGGAACTTCTTGGG], M13(-20) primer + mPPIPs [5'-CCCAAGAAGTTCCCCCCCATCCCCGTG] to amplify PTPεF112P fragments from the full-length cDNA in the pBluescript derivative pSSBS (REF). Amplification was carried out under the following reaction conditions (5 μl 10x Vent Buffer, 200 μM dNTP's and 4 U of Vent DNA polymerase the final volume adjusted to 50 μl) using touch-down PCR (2 cycles of 96°C for 45 sec, annealing at 65°C for 1 min, 73°C for 1 min, 2 cycles annealing at 64°C, 2 cycles annealing at 63°C, 2 cycles annealing at 62°C, 2 cycles annealing at 61°C, 2 cycles annealing at 60°C, 2 cycles annealing at 59°C, 2 cycles annealing at 57°C) and PCR fragments purified by gel electrophoresis in a 1.0% agarose gel and resuspended in 20 μl of distilled water. Full-length cDNA's carrying mutations were generated from the PCR fragments by extension of the overlap contained within the synthetic oligonucleotides with a second round of touch-down PCR using 1.0 μl of each agarose gel purified PCR fragments and M13 reverse + M13(-20) primers. Full-length cDNA's were gel-purified and digested with Not I then sub-cloned into pSSBS for sequence analysis. Mutated PTPε cDNAs were then shuttled into the Not I site of the CMV promoter based episomal expression vector pBCMGSneo (Karasuyama and Melchers, 1988).

2.10 Antibodies. The anti-GRB2 monoclonal antibody was from Transduction Laboratories. The anti-GRB2 polyclonal antibody and the SRC2 antiserum specific the C-terminal peptide sequence 509-533 of Src and conserved sequences of Fyn and Yes

was from Santa Cruz Biotechnology. The anti-phosphotyrosine monoclonal antibody (4G10) as well as the anti-src monoclonal (GD11) were obtained from Upstate Biotechnology Inc. The FITC labeled goat anti-rabbit IgG $F(ab')_2$ antibody, and TRITC labeled Goat anti-Mouse IgG $F(ab')_2$ antibody were obtained from Caltag. The rabbit polyclonal antibody PTPε15ic was raised against a PTPε-unique 12-residue peptide derived from the intercatalytic region sequence of human PTPε 413-424 (TMHGTTTHFDKI), and PTPε16d2 was similarly raised against a peptide corresponding to a second PTPε-unique sequence 555-587 (IKNDTLSEAISIRDFLVTLNQPQARQEEQVRVV) within the C-terminal catalytic domain (Krueger *et al.*, 1990). Both peptides were coupled with N-terminal cysteine-linked keyhole limpet hemocyanin and anti-sera generated by repeated immunization of New Zealand white rabbits. Anti-sera were purified by peptide affinity column chromatography. Columns prepared by conjugation of synthetic peptide to thiol Sepharose and anti-sera eluted with 0.1 M glycine pH 2.5.

2.11 Cell culture and transfection. HL-60, 293, and Jurkat cell lines were obtained from the American Type Culture Collection. RAMOS, WEHI 231, and 2PK3 B-cell lines were provided by M. Gold (University of British Columbia). AKR1.G.1.26 , BWT200+ and T28 murine T-cell lines were provided by P. Johnson (University of British Columbia). HL-60 cells were maintained in RPMI (StemCell Technologies) supplemented with 10% fetal bovine serum (Hyclone), 2 mM L-glutamine, 2 mM sodium pyruvate, 50 U/ml penicillin G, 50 mg/ml streptomycin. PMA was added to cells at a

final concentration of 16 nM for various times as indicated. Culture medium containing undifferentiated and dead cells was discarded after 48 h. Adherent, PMA-differentiated HL-60 cells (designated here as HL-60/mac cells) were washed and allowed to recover for 24 h prior to further treatment. For pervanadate stimulation, cells were exposed to a freshly-prepared mixture of hydrogen peroxide and vanadate with final concentrations being 1 mM and 0.1 mM, respectively. Murine peritoneal exudate cells, obtained by peritoneal lavage of Balb/c mice 3 d after intra-peritoneal thioglycollate administration, were purified by adherence to plastic tissue culture dishes for 2 h at 37 °C. A cDNA encoding the transmembrane form of PTPε (Krueger *et al.*, 1990), generously provided by A. Schmidt (Merck, West Point, PA), was inserted into a human cytomegalovirus immediate-early gene promoter-based eukaryotic expression vector for transient expression in 293 cells. Lipofectamine (GIBCO/BRL) was used for transient as well as stable transfections. For transfections 6-well plates were coated with 20 mg/ml bovine fibronectin in PBS overnight at 4 °C then washed twice with PBS prior to the cells being plated. Cells were seeded at 2.0 x 10^5 cells/well on to the fibronectin-treated plates the day before transfection. The following day, 2.5 μg of DNA in 100 μl of serum free media (SFM) (Optimem, GIBCO/BRL) was combined with 15 μl of lipofectamine in 100 μl SFM. The DNA/lipofectamine transfection cocktail was incubated for 30 min. HEK293 cells were carefully washed once with SFM to remove any serum then the transfection cocktail with the addition of 800 μl SFM was layered onto the cells. After 5-7 hours at 37 °C the transfection was terminated by the addition of 2 ml of 10% serum-containing media. The transfected cells were allowed to recover 24 hours prior to lysis and analysis. Stable transfectants were obtained by dilution cloning. After gentle typsinization and

dilution to 40 ml of serum containing media, supplemented with 600 μg/ml G418. Cells were then seeded onto four 96-well dishes at 100 μl/well and selected for a period of 10 days with the addition of 100 μl of G418 containing complete media after 5 days. The final concentration of G418 used was 600 μg/ml. In previous experiments this concentration was determined to kill G418 sensitive cells within 7 days.

2.12 Immunoprecipitation and immunoblotting. Cells were lysed in TX100 lysis buffer or RIPA buffer and incubated on ice for 10 min. Insoluble material was pelleted by centrifugation 10,000 x *g* for 10 min and lysates were adjusted to a protein concentration of 1.0 mg/ml using the BCA Test kit (Pierce), then pre-cleared with Gammabind G Sepharose (Pharmacia). Lysates were then incubated for 1 h on ice with 1.0 μg PTPε15ic anti-sera. Immune complexes were collected with 10 μL of Gammabind G sepharose for 1 h at 4 °C on a rotating wheel, and washed 5 times with lysis buffer. Immunoprecipitates were boiled for 10 min in sample buffer and separated using 10% SDS-PAGE before transfer to Duralose (Stratagene) or Immobilon-P membranes (Millipore). Membranes were blocked with 5% (w/v) bovine serum albumin in TBST (20 mM Tris-HCl pH 7.5, 150 mM NaCl, 0.05% Tween-20) at room temperature for 1 h, and incubated with 0.2 μg/ml of polyclonal antiserum (in TBST and 5% bovine serum albumin) for 1 h. Following incubation with the secondary antibody, blots were visualized via an Enhanced Chemiluminescence (ECL) system (Amersham). Cells were also scraped into hypotonic lysis buffer (25 mM Tris-HCl pH 7.5, 2 mM EDTA, 1 mM EGTA, 1 mM Na_3VO_4, 250 mM sucrose, with protease inhibitors),

followed by cell lysis on ice with 20 strokes of a glass dounce homogenizer. Nuclei and large debris were removed by centrifugation at 800 x *g* for 15 min. The particulate material was obtained by centrifugation at 100,000 x *g* for 1 h; the supernatant was the cytosolic fraction.

2.13 Immunoflourescence. Cells were grown on coverslips coated overnight with bovine fibronectin at 20 μg/ml. After washing with PBS the cells were fixed with 3.0% paraformaldehyde in PBS for 10 min. at room temperature. Coverslips were washed with PBS then cells permeablized with 0.2% Triton X-100 in PBS. After washing, the cells were blocked with 2.5% BSA in PBS and then stained with PTPε15ic polyclonal antibody at 0.5 μg/ml for 1 hour. After extensive washing the cells were stained with FITC labeled goat anti-rabbit IgG $F(ab')_2$ at 1/250. Coverslips were mounted and photographed with a CCD camera, mounted to a Carl Zeiss immunoflourescence microscope, using a standard FITC filter set.

2.14 Surface Biotinylation. HEK 293 cells maintained in log phase growth were cultured to ~80% confluency on T175 culture flasks. Cells were transferred to ice and washed 3 times with ice cold HBS (Hepes Buffered Saline) [20 mM Hepes pH 7.4, 150 mM NaCl]. Ten millilitres of Biotinylation buffer [HBS + 0.2 mM NHS-LC-Biotin] was incubated with the washed cells for 1 hour on ice. Biotinylation buffer was removed and cells washed 2x with HBS and remaining active NHS-LC-biotin was neutralized by incubation

with three changes of TBS (Tris Buffered Saline) [20 mM Tris-NH_2 pH 7.4, 150 mM NaCl] 15 minutes each. Cells were then lysed with the addition of TX100 lysis buffer and scraped. Cellular debris was removed by centrifugation and cleared lysates stored at –80 °C.

2.15 Malachite green solution preparation. One volume of 4.2% (w/v) ammonium molybdate in 4N HCl was added to 3 volumes of 0.045% (w/v) malachite green. This solution was stirred for a minimum of 30 min before filtering through a 0.22 μm filter. The filtered solution was stored for up to 6 months at 4°C. Tween-20 (0.01% v/v) was added to an aliquot of filtered malachite green solution prior to use.

2.16 Inorganic phosphate standard curve. Standards were prepared from KH_2PO_4 that had been desiccated at 80°C for 5 hours. Appropriately diluted inorganic phosphate standards in a volume of 25 μl were delivered to half volume wells of a 96 well microtitre plate, followed by the addition of 50 μl of the malachite green working solution. After a 15 min incubation at room temperature the optical density of each well was measured at 620 nm.

2.17 Phosphotyrosine containing peptides. Phosphotyrosine containing peptides were synthesized using solid-phase methods with *t*-butyloxyl carbonyl (*t*-boc) and alpha-

protected amino acids, with the appropriated side chain protection, as described (Clark-Lewis et al., 1991). Phosphopeptides were synthesized with *t*-boc Tyr PO_4 $(Bzl)_2OH$. After chain assembly, the peptides were deprotected via triflouromethane sulfonic acid (TFMSA). Each 100 mg of peptide resin was stripped with 100 µl thioanisole, 50 µl ethandithiol and 1 ml of triflouroacetic acid (TFA). 100 µl of TFMSA was added and allowed to react for 2 hours at room temperature. The peptide was precipitated with diethyl ether, washed, and then dissolved in 6 M guanidine HCl, pH 8.5. For purification this mixture was loaded directly onto reverse phase HPLC (Clark-Lewis et al. 1991). The mass of each peptide was confirmed using ion-spray mass spectroscopy on a model AP1 III triple quadrupole mass spectrometer (SCIEX, Thronhill, Ont.,) with a liquid delivery interface. The amino acid composition was comfirmed by amino acid analysis.

2.18 Phosphatase Assays. PTPε was immunoprecipitated from varying quantities of cell lysate protein using 1 µg of polyclonal antibody, as described above but with omission of PTPase inhibitors, followed by two washes with PTP buffer (50 mM NaCl, 50 mM KOAc pH 6.0, 0.2 mM dithiothreitol). Otherwise recombinant PTPε was used. In certain instances during determination of pH optima 50 mM Mes pH6.5-8.0 and 50 mM Tris-HCl pH8.0-9.5 were used. PTPase reactions were carried out (Harder *et al.*, 1994) using the following phosphopeptide substrates, synthesized as previously described (Dechert *et al.*, 1994): *src*^{Y527} (TSTEPQpYQPGENL), *hck*^{Y501} (TATESQpYQQQP), PDGF-R^{Y1021} (NEGDNDpYIIPLPD), IFNγ-Rα^{Y440} (APTSFGpYDKPHVL), STAT91^{Y701} (GPKGTGpYIKTELI). Reactions were initiated by the addition of 30 µL

of PTP buffer containing 200 μM of synthetic phosphopeptide. Inorganic phosphate liberated was quantitated by the addition of 60 μl of malachite green solution then incubated for 15 min at room temperature before optical density measurement at 620 nm.

2.19 Liquid Chromatography/Mass Spectroscopic analysis. Instrumentation used and LC-ESI-MS analyses was a modification of those described elsewhere (Hess *et al.*, 1993). Following SDS-PAGE purification and Coomassie blue staining/destaining, protein bands were excised and partially dried. Following complete pulverization of the gel, proteins were digested *in situ* at 37 °C, 16 h in 50 mM ammonium bicarbonate pH 8.3 with either 12.5 μg/μl trypsin (Promega) or chymotrypsin (Sigma). Sample volume was reduced to 10-20 μL in a Speedvac concentrator before loading onto a 320 μm (internal diameter) x 15 cm long C18 reverse phase HPLC column (Micro-Tech Scientific). The column was connected via a Rheodyne sample injection valve to the gradient pump outlet of a Michrom Ultrafast Microprotein Analyzer HPLC system (BioResources Inc.). The downstream end of the HPLC column was connected to the ESI interface of a PE-Sciex API-III triple quadrupole mass spectrometer (MS) by a 50 cm long x 50 μm internal diameter x 150 μm outside diameter fused silica capillary (Polymicro Technologies). The chromatography mobile phases were (phase A): 0.05% TFA and 2% acetonitrile, and (phase B): 0.045% TFA, 80% acetonitrile. Tuning and calibration of the MS was performed either with polypropylene glycol or myoglobin. The quadrupole was scanned from m/z 300 to 2000 at 2.9 s/scan. All mass spectra data were 'background subtracted'.

2.20 Kinase assays. Src was immunoprecipitated from 500 μg of cell lysate with 2 μg of anti-src monoclonal antibody GD11 as described in section 2.12. Immunoprecipitates were washed 5 times with RIPA buffer followed by a single wash with Kinase buffer (20 mM PIPES [piperazine-*N*, *N*-bis 2-ethanesulfonic acid] pH 7.2, 10 mM $MgCl_2$, 5 mM $MnCl_2$). Kinase assays were initiated with the addition of 10 μCi [γ ^{32}P] ATP (3000 Ci/mmole) and terminated after 10 minutes at 25 °C by the addition of 1/5 vol. of 5x SDS-PAGE sample loading buffer. Reactions were boiled for 5 minutes then proteins separated via SDS-PAGE. After electrophoresis gels were dried X-ray films exposed.

Chapter 3

The Screen for PTPases Regulated by IFNγ and PTPε Expression in Cells of the Monocyte/Macrophage Lineage

3.1 Differential hybridization Screening System

To investigate PTPase expression in macrophage cells under pro-inflammatory conditions, the mouse macrophage cell line RAW 264.7 was used as a source of messenger RNA (mRNA) for a differential hybridization PCR screening system. The RAW 264.7 cell line was originally produced from thioglycolate elicited Balb/c peritoneal macrophages, after transformation by infection with the Ableson Murine Maloney leukemia virus (Raschke *et al.*, 1978). Originally derived from near fully differentiated macrophages, this line exhibits many of the functions associated with true monocyte/macrophage cells while retaining the ability to divide, a cellular function lost in terminally differentiated macrophages. Macrophage functions, including adherence to

the substratum, active phagocytosis, production of TNFα and IL-1 in response to LPS and IFNγ and all of the well known macrophage cell surface markers including CD14, CD16 (FcγRIII), CD32 (FcγRII), CD64 (FcγRI), and the CD11b/CD18 complex previously known as Mac-1 or Complement-3 receptor (CR3) are all expressed by RAW264.7 cells. These features imply that gene regulation, in response to pro-inflammatory cytokines, will closely mimic that observed in *ex vivo* primary cells, making RAW 264.7 cells an ideal model cell type for studying PTPase gene regulation in cells of the monocyte/macrophage lineage.

The approach taken was to prepare mRNA from RAW 264.7 cells with or without exposure to murine IFNγ for a period of 24 hours (figure 3.1.1). Messenger RNAs from stimulated RAW 264.7 cells were used as templates to prepare random primed cDNAs. Random priming was used instead of poly-A priming so as not to bias cDNA production towards the 3 prime end in the event that mRNA quality varied from batch to batch. The cDNA reactions were then used as substrates for the PCR of PTPase catalytic domains using the degenerate oligonucleotides deg 1 and GXG specific for highly conserved nucleotide sequences within the PTPase catalytic domain (figure 3.1.2) (as described in Materials and Methods). The oligonucleotide sequences were chosen by compilation of all known PTPase catalytic domains at the time, including both membrane proximal and distal catalytic domains in the case of dual domain PTPs. Figure 3.1.2 shows the resulting PTP catalytic domain alignment. At nucleotide sequence sites where the occurrence of more than 2 nucleotides was probable, the nucleoside analog Inosine (I) was

incorporated because of its ability to hydrogen bond in a stable manner with both purines and pyrimidines. The ability to base pair freely with both types of nucleotides

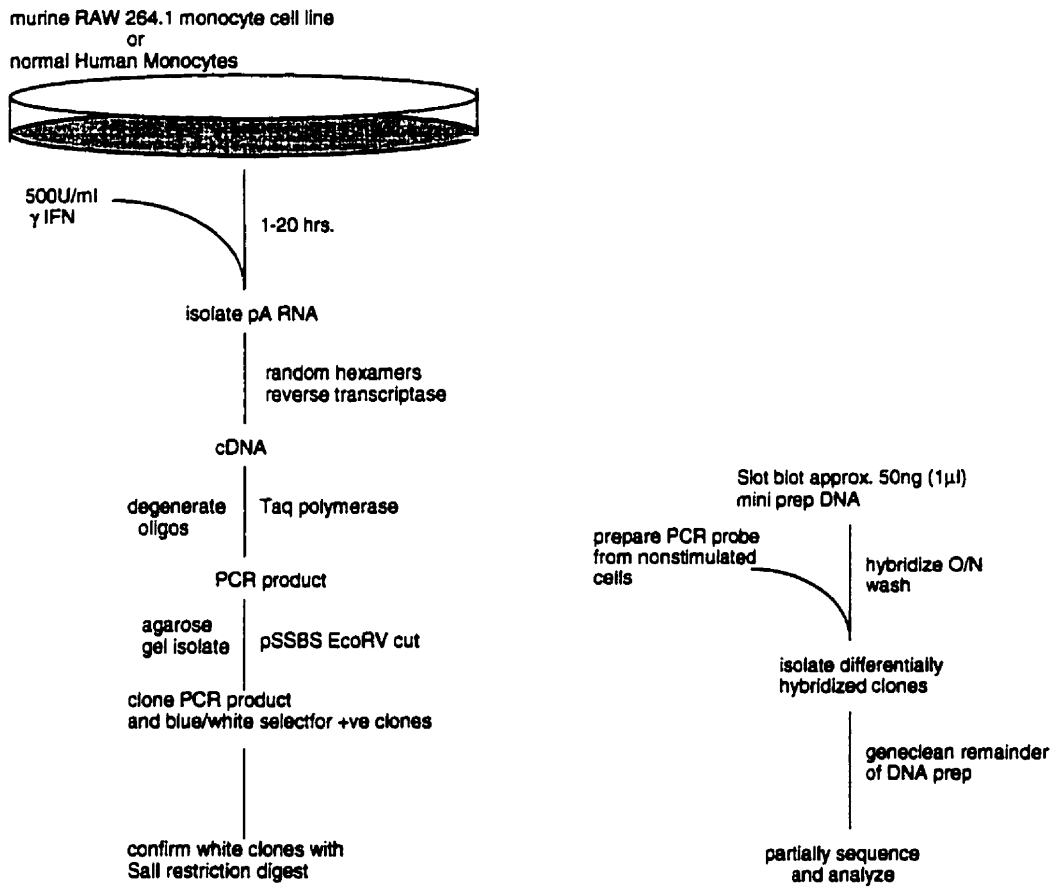

Figure 3.1.1 Differential hybridization screening

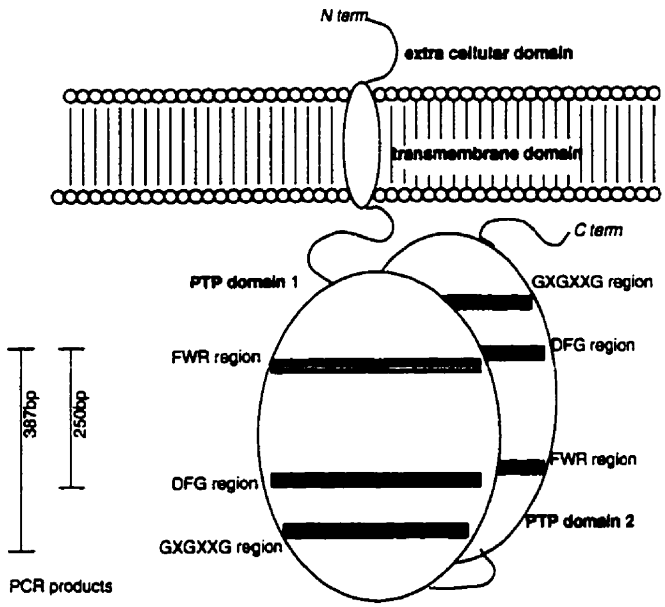

Figure 3.1.2 Degenerate oligonucleotide selection

effectively decreases the degeneracy of the oligonucleotide while allowing the maximum number of permutations for annealing.

The expected size of the PCR product was ~350 base pairs upon agarose gel electrophoresis (figure 3.1.3a). Amplification fragments this size were purified using the Pharmacia Sephaglass band prep kit and cloned into the EcoRV site of the pUC based plasmid pSSBS (figure 3.1.3b). The plasmid pSSBS is identical to the pBluescript II KS vector with the addition of a second SalI site at the expense of a XbaI site. The SalI sites in pSSBS flank the EcoRV site to allow efficient excision of PCR fragments.

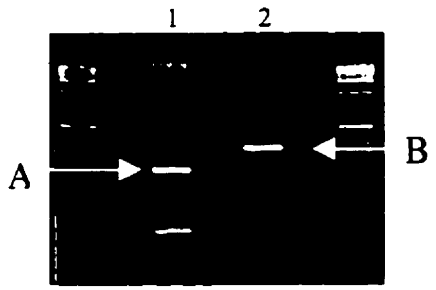

Figure 3.1.3a Degenerate primer PCR products. Photograph of ethidium bromide stained 5% agarose gels. Lane 1 PCR products were derived from deg#1, deg#2 degenerate oligo-nucleotides. Arrow A indicates the 250 bp PCR fragment for subcloning. Lane 2 PCR products were derived from deg#1, deg#3 degenerate oligo-nucleotides. Arrow B indicates the 387 bp PCR fragment for subcloning into the pBluescript derived plasmid, pSSBS.

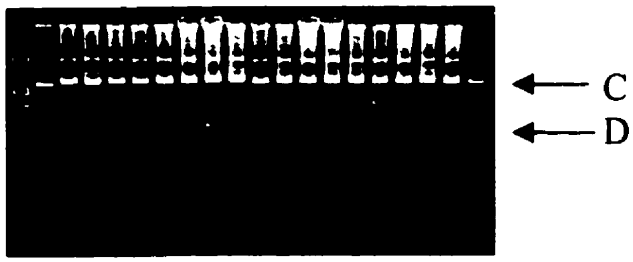

Figure 3.1.3b Cloning of PCR fragments into pSSBS. Photograph of ethidium bromide stained 1% agarose gels containing SalI digests of DNA preperations from pSSBS. PCR fragment ligations. Arrow C indicates the linearized parent plasmid. Arrow D indicates the 287 bp PCR fragment liberated from the plasmid.

One hundred nanograms of each clone was immobilized onto nylon membranes and subjected to hybridization with a [α^{32}P]-dCTP labeled PCR probe prepared from cDNA reverse transcribed from an unstimulated mRNA sample. After extensive high stringency washing candidate upregulated PTPase cDNAs were chosen by an under represented signal on autoradiography (figure 3.1.4).

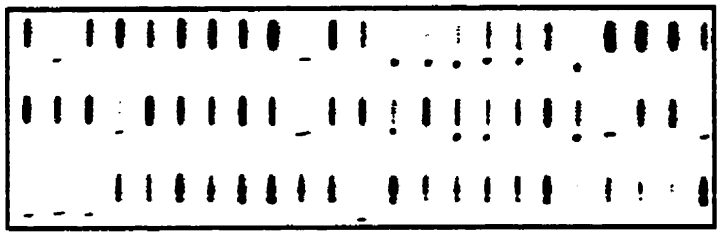

Figure 3.1.4 Autoradiograph of PTPase PCR fragments. Autoradiograph of slot blotted plasmids containing PTPase PCR fragments from stimulated RAW 264.7 cells. Blots were probed with ^{32}PαdCTP labeled PCR reactions using mRNA purified from non-stimulated cells. After hybridization with ^{32}P labeled probes blots were washed with high stringency. Dashes indicate mRNA species corresponding to this plasmid is not present in non-stimulated RAW 264.7 cells. Dots indicate the possibility of low abundance messages.

Candidate clones were manually sequenced using T3 and T7 sequencing primers. Approximately 250 base pairs of nucleic acid sequences were obtained from each clone. Sequence analysis of the candidate PTPases was carried out on a Sparc Unix workstation using Blast or Fasta sequence similarity analysis programs with global matching, a ktup of 4, and no gaps. Sequence searches were carried out against the rodent nucleotide database within Genbank.

Screening in this manner, using IFNγ stimulation varying from 6 hours to 24 hours, of 173 clones isolated 12 clones were designated as putatively regulated PTPases. Sequence analysis of the 12 candidate clones provided only 4 distinct PTPases cDNAs, 3

transmembrane PTPases and one cytosolic. PTPα, CD45, PTP1B and PTPε were identified as candidate mRNAs for induction in mouse macrophages in response to IFNγ and highlighted for further investigation.

Each of these PTPs identified in our search had been previously cloned and characterized. PTPα is a widely expressed transmembrane PTPase possessing two tandem catalytic domains and is characterized by a small heavily glycosylated extra-cellular domain. Recent reports implicate PTPα in regulation of $pp60^{c\text{-}src}$ activity and in control of neurite out-growth and neuronal differentiation (den Hertog *et al.*, 1993). CD45, also known as leukocyte common antigen (LCA), is a well-known leukocyte cell surface marker (Thomas 1989). Characterized by highly regulated exon splicing to produce several variants with distinct extra-cellular domains, CD45 has also been shown to play a role in the regulation of src family kinases (Mustelin *et al.*, 1989, 1990, 1992, Trowbridge *et al.*, 1991, Ostergaard *et al.*, 1990). The PTPase activity of CD45 has been shown essential in the activation of p56lck during antigen receptor stimulation in T lymphocytes and p53/56lyn in the case of B-lymphocytes (Weiss 1993, Ales-Martinez *et al.*, 1991). Unlike the two previous candidates, PTP1B is a non-transmembrane PTPase (Tonks *et al.*, 1989). This PTPase appears to be activated by proteolytic cleavage at its C-terminal tail, which anchors the PTPase to the endoplasmic reticulum (Frangioni *et al.*, 1993). While its function remains unclear, PTP1B has been implicated in insulin receptor signaling, EGF receptor signalling as well as intra-ER tyrosine kinase dephosphorylation and regulation (Lammers *et al.*, 1997, Milarski *et al.*, 1993). PTPε, the last of the four PTPases identified, shares very high sequence homology with PTPα (~85%) and is also

characterized by a small extra-cellular domain however PTPε's extra-cellular domain shows no sequence similarity with that of PTPα. Although little is known of the function of PTPε, recent reports have implicated PTPε in cellular adhesion and/or insulin receptor signaling (Lammers *et al.*, 1997). Due to the paucity of information regarding the function of PTPε, in addition to its homology with PTPα which may afford re-use of certain existing reagents, PTPε was chosen for further analysis as an upregulated PTPase in the macrophage cell line.

3.2 Northern Blot Analysis of PTPε Expression.

For further analysis of PTPε expression, the human monocyte cell line HL-60 was included as a representative human cell line with macrophage/monocyte characteristics. Developed in 1979 in the laboratory of R.C. Gallo at NIH, HL-60 was derived from a patient with leukemia (Collins *et al.*, 1978). A growth factor independent cell line with myeloid characteristics, HL-60 is capable of differentiation in response to a number of agents. As a result, HL-60 cells have been induced to differentiate towards a variety of hemopoietic cell lineages. DMSO, and retinoic acid cause granulocyte-like differentiation. Vitamin D3 and IFNγ cause monocyte differentiation, while treatment with phorbol-esters for 48 hours causes adherence to plastic, cessation of proliferation, and an increase in the following: complement receptors, Fc receptors, lysozyme activity, phagocytosis, microbicidal activity, src family kinase expression. These characteristics and others identify phorbol ester-differentiated HL-60 cells as macrophage-like cells,

possibly making these a human counterpart for RAW 264.7 cells. In addition, HL-60 affords the opportunity to study PTPε expression during the process of macrophage/monocyte differentiation.

To observe PTPε mRNA expression in the two representative cell lines, oligonucleotides corresponding to the 5 prime membrane proximal area of human PTPε (ptpe15) and to the 3 prime region of human PTPε (ptpe25) were used to PCR amplify the cytosolic portion of human PTPε. Complementary DNA reverse transcribed from HL-60 mRNA was used as a substrate in the PCR reactions and purified DNA fragments were used as DNA probes as well as subcloned into the prokaryotic expression vector pGEX-2T.

Messenger RNA purified from RAW 264.7 cells and HL-60 cells after treatment with various stimuli was subjected to Northern blot analysis with human PTPε probes. Figure 3.2.1 reveals that PTPε mRNA level is induced in HL-60 cells only after stimulation with a few key pro-inflammatory stimuli. Lipopolysaccaride (LPS) (figure 3.2.1a) and IFNγ (figure 3.2.1b) both induce ~6.5 kb, ~2.1 kb and ~1.8 kb PTPε messages in HL-60. The presence of three hybridizing transcripts was unexpected since only a single ~8 kilobase message had been previously reported for PTPε (Krueger et al. 1990). However, similar transcript heterogeneity was observed in MEL cells treated with various stimuli (Kume *et al.*, 1994). In addition, evidence of as many as four different transcripts was obtained from analysis of various mouse mammary tumor lines (Elson and Leder, 1995a). Since high stringency conditions were used during hybridization and subsequent washings, the possibility of a cross-reacting PTPase message, while not eliminated, is

unlikely. The most probable explanation for the number of messages observed is alternative splicing of a single primary transcript. The presence of alternative transcripts is a common feature of transmembrane PTPases.

Figure 3.2.1 shows a representative northern blot from four independent experiments. The induction of PTPε message followed similar kinetics regardless of whether LPS or IFNγ was used as the stimulus. While PTPε mRNA was detectable in control unstimulated cells, an increase in levels was not detectable until at least 3 hours had elapsed (figure 3.2.1). Induction of PTPε message generally reached maximal levels after approximately 20 hours of stimulation (figure

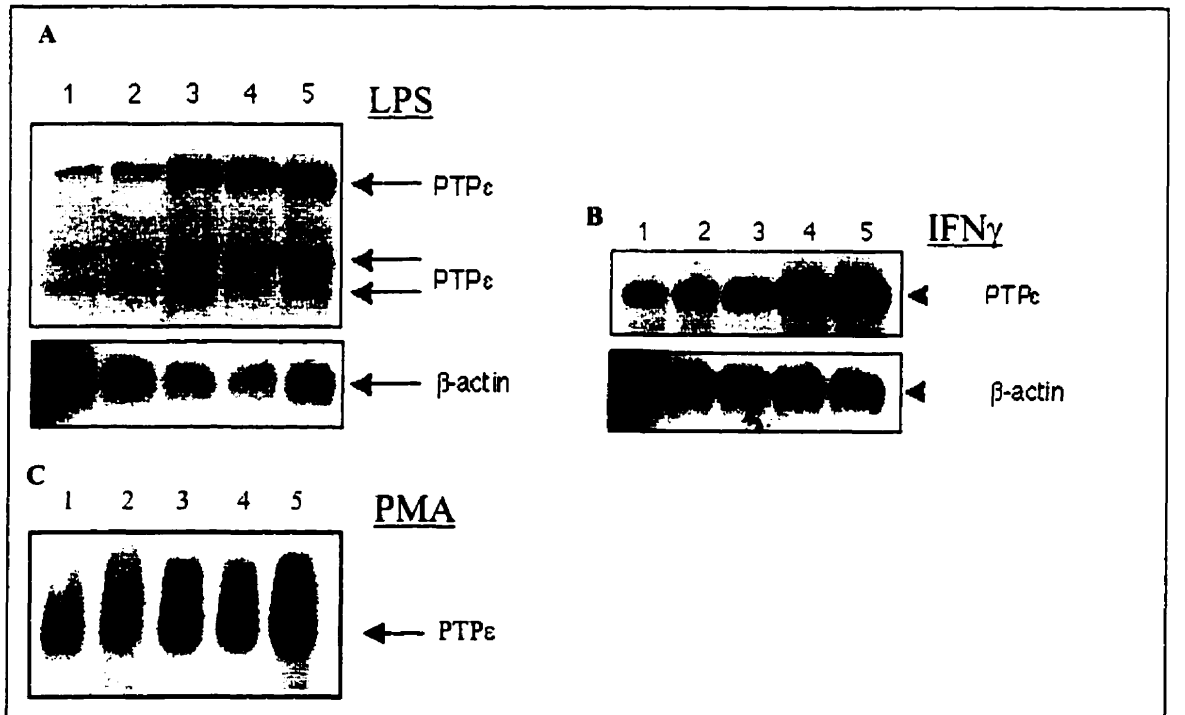

Figure 3.2.1. PTPε message levels in response to, LPS (a) and IFNγ (b) Phorbol esters (c). PTPε message levels observed by Northern blot analysis in response to 1.0 μg/ml LPS (A), 100 U/ml IFNγ (B), or 16 nM PMA (C). Lane 1, unstimulated control; lane 2, 1 hour exposure; lane 3, 3 hour exposure; lane 4, 6 hour exposure; lane 5, 20 hour exposure. Lower panel represents human β-actin re-probe of the blot above.

3.2.1) with densitometric analysis revealing a 16-fold (+/- 0.4) increase in message levels (figure 3.2.1). While the mechanism responsible for PTPε induction in response to LPS and IFNγ remains to be elucidated, figure 3.2.2 shows a similar induction of PTPε message in response to ortho-Vanadate, a powerful PTPase inhibitor.

To assess PTPε expression at the message level in response to other pro-inflammatory stimuli a panel of hemopoietic growth factors, as well as chemotactic cytokines (chemokines) were used to treat HL-60 cells in a time course from 1 hour to 20 hours. Figure 3.2.3 shows the PTPε mRNA expression profiles from these experiments, using GM-CSF, IL-1, MCP-1 as the pro-inflammatory stimuli. Interestingly,

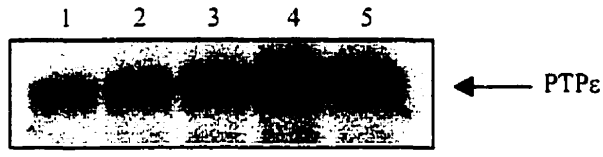

Figure 3.2.2 Expression of PTPε mRNA in response to Vanadate. MRNA isolated from HL-60 cells in response to 50 μM Vanadate. (Lane 1) control unstimulated cells. (Lane 2) cells stimulated for 1 hour, (Lane 3) 3 hour stimulation, (Lane 4) 6 hour stimulation, (Lane 5) 20 hour stimulation.

of the stimuli tested only MCP-1 elicited a modest induction of PTPε messenger RNA. The mRNA expression levels appear to show a gradual increase in response to LPS and IFNγ, as well as phorbol esters.

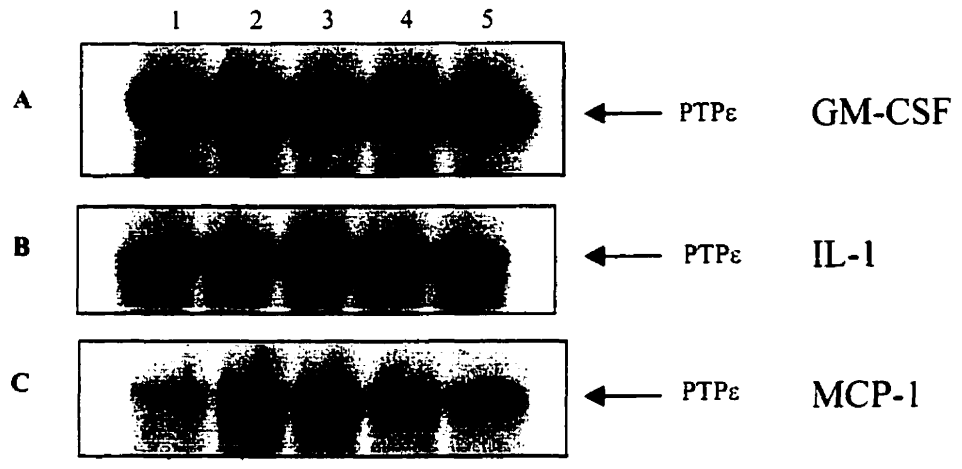

Figure 3.2.3. Expression of PTPε mRNA in response to Cytokine stimulation. MRNA isolated from control unstimulated HL-60 cells (Lane 1). (Lane 2) cells stimulated for 1 hour, (Lane 3) 3 hour stimulation, (Lane 4) 6 hour stimulation, (Lane 5) 20 hour stimulation. With 200 ng/ml GM-CSF (*panel A*), 40 U/ml IL-1α (*panel B*), 200 ng/ml MCP-1 (*panel C*).

3.3 Expression of PTPε protein in hemopoietic cells

To study the product of the PTPε gene, three rabbit polyclonal antibodies were generated against synthetic peptides corresponding to regions within PTPε unique to the PTPase. PTPεEC polyclonal antisera was generated against the synthetic peptide sequence PTPε 21-44 (RGNETTADSNETTTSGPPDPGASQ). This sequence

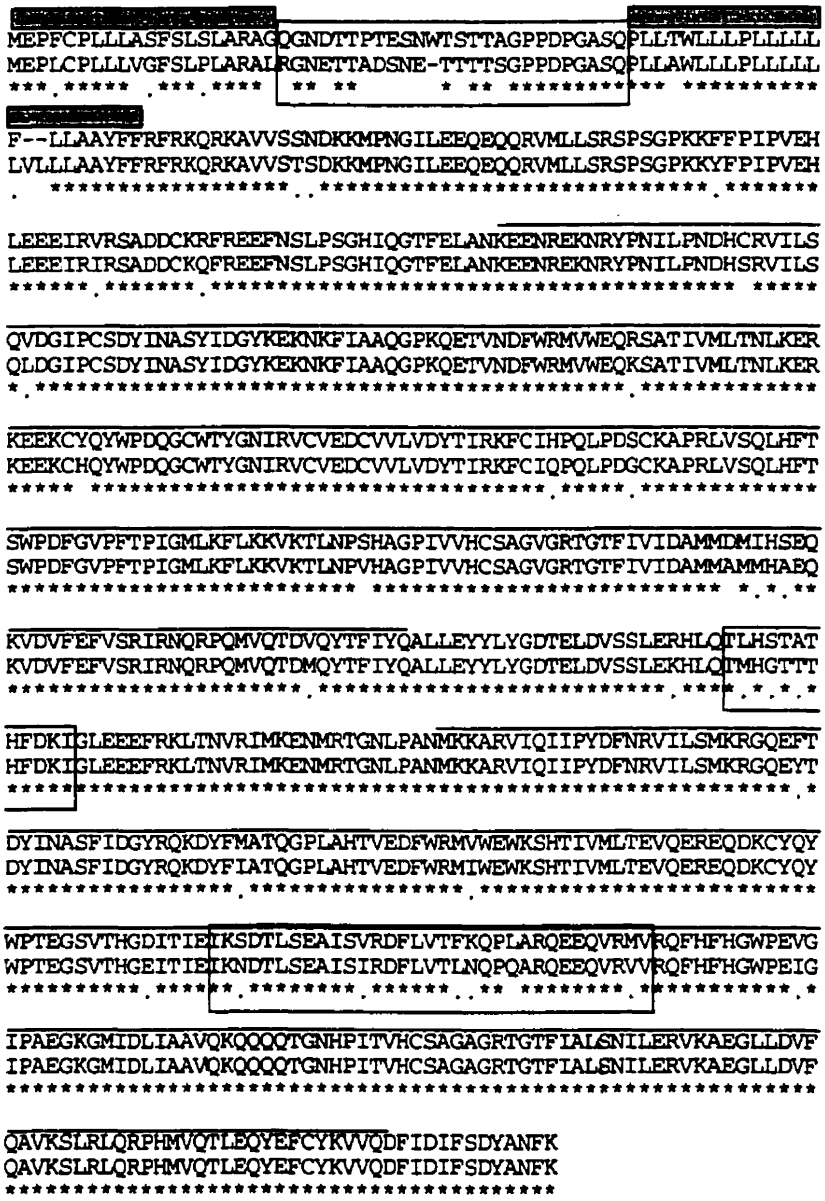

Figure 3.3.1 Regions of antibody peptide selection in PTPε The polypeptide sequences of murine PTPε above and human PTPε below. Identical amino acids are indicated with a star, homologous substitutions with a dot. The regions highlighted in gray indicate the putative signal peptide and tranmembrane domian. The first catalytic domain and second tandem catalytic domain are indicated by horizontal line. Boxed regions denote areas used as templates for synthesis of immunogens for polv clonal antibodies.

PTPε15ic was generated against the amino acid sequence PTPε 413-424 (TMHGTTTHFDKI) which is found with the intervening region between the tandem catalytic domains (figure 3.3.1). PTPε16d2 was raised against the oligo-peptide PTPε 555-587 (IKNDTLSEAISIRDFLVTLNQPQARQEEQVRVV) and is found within the C-terminal catalytic domain of PTPε (figure 3.3.1). The sequence PTPε 555-587 along with those peptides used for the previously described antibodies also exhibit little sequence homology with PTPα.

Crude antiserum was purified by column chromatography using the immunizing peptide linked to thiol-Sepharose beads as the affinity purification resin. The resulting polyclonal antibodies were tested for specificity and affinity towards PTPε and PTPα by immunoblotting samples of the recombinant proteins (expression of rPTPε and rPTPα is described elsewhere). The antibodies were also tested for their ability to immunoprecipitate PTPε and PTPα by immunoprecipitation from crude bacterial lysates expressing recombinant PTPε and PTPα GST fusion proteins. Figure 3.3.2 summarizes the results of the antibody characterization. Lanes 1, 3 ,5 and 7 in the upper panel indicate that PTPε15ic, PTPε16ic and anti-LRP (the PTPα specific antisera) are all able to immunoblot for PTPε. Indeed, PTPε15ic appears to be the best antibody for immunoblotting with PTPε16ic exhibiting a somewhat lower signal. Lanes 2, 4, 6, and 8 provide internal controls since these lanes contain the ~60kDa GST-PTPεD2 fusion protein which migrates at a lower molecular weight than the larger GST-PTPε fusion protein. The lower panel of figure 3.3.2 indicates that all antisera tested except for anti-LRP150 (a PTPα specific antibody) are capable of immunoprecipitating GST-PTPε

fusion protein from bacterial cells overexpressing the fusion protein. Thus, for subsequent boosts, purifications and all further studies PTPε15ic and PTPε16d2 were used for protein characterization since, both PTPε15ic and PTPε16d2 immunoprecipitated and immunoblotted recombinant PTPε but not PTPα. This implied that the reagents displayed high reacitivity towards PTPε and therefore it is fair to say specific for PTPε and unlikely to react with other PTPs. These results confirm that experiments performed with PTPε15ic and PTPε16d2 should not produce ambiguous results due to cross-reactivity with PTPα.

As previously reported, treatment of HL-60 cells with PMA resulted in cells having a monocyte-like appearance (Collins *et al.*, 1987). Thus, within ~24 h of PMA-exposure significant morphological changes were seen including vacuole formation and adhesion to tissue culture plastic of cells with a monocytoid appearance. After 2 to 3 days, maximum attachment of cells was observed and was accompanied by minimal cell death. Continuous exposure was not required for phorbol ester-mediated differentiation of HL-60 cells. Thus, after 2 days of stimulation, adherent cells were washed and cultivated in PMA-free media for a final 24 h to obtain HL-60/mac cells.

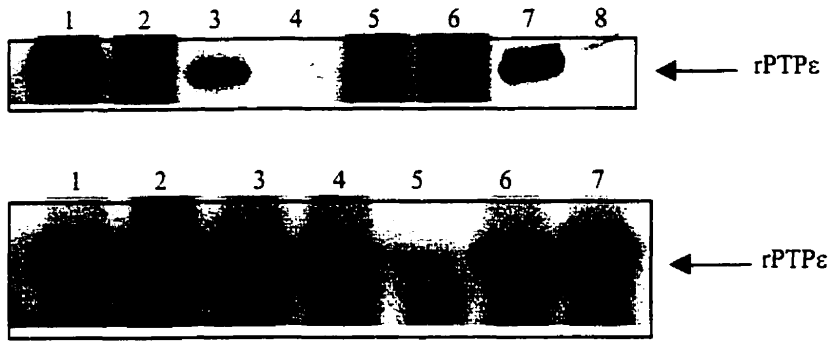

Figure 3.3.2 Testing of PTPε specific antibodies with recombinant PTPε. *Upper Panel* Lysates prepared from bacteria expressing GST-PTPε (lanes 1, 3, 5, 7) GST-PTPεD2 (lanes 2, 4, 6, 8) were western blotted with the following polyclonal antisera PTPε15ic (lanes 1 and 2), PTPε16ic (lanes 3 and 4), PTPε17ic (lanes 5 and 6), anti-LRP (anti-PTPα) (lanes 7 and 8). *Lower Panel* Lysates prepared from bacteria expressing GST-PTPε were subject to immunoprecipitation with 2.5 μg of the following antisera PTPε14ic (lane 1), PTPε15ic (lane 2), PTPε16ic (lane 3), PTPε17ic (lane 4), anti-LRP150 (lane 5), anti-LRP (lane 6), anti-LRPD2 (lane 7). Immunopreciptitates were then western blotted with PTPε15ic anti –PTPε polyclonal antibody.

Figure 3.3.3 illustrates the relative levels of PTPε15ic antibody-reactive proteins in PMA-stimulated HL-60 total cell lysates harvested at various time points as shown. The antibody detected a single major protein, migrating as a doublet, of approximately 72/74 kDa and a third cross-reacting protein migrating at ~85 kD. The signal corresponding to the p72/74 protein was present at low levels until approximately 20 hours post-PMA exposure of HL-60 cells. Once present, the level of p72/74 in the HL-60 cells appeared to remain stable for up to 72 hours in culture (data not shown). The expression of p72/74 appears to correlate well with the mRNA expression patterns observed in the phorbol ester stimulation, figure 3.2.2. However, p72/74 expression does not correlate well with mRNA expression patterns in the LPS and IFNγ stimulation (figure 3.2.1). This discrepancy in mRNA expression patterns was addressed in section 3.2. However, it appears the hypothesis for mRNA expression may be extended to

describe protein expression especially in the face observations that induction of message by LPS and IFNγ doesn't result in protein translation in HL-60 cells as described in figure 3.3.4. These results further suggest that while they are able to rapidly induce mRNA expression and translation, LPS and IFNγ are only capable of delivering a partial signal, which results in increased message but a block at the translation level. It is interesting that while PMA induction of PTPε results in mRNA expression at 3 hours, expression of PTPε protein (p72/74) is not observed until 20 hours of exposure. This time point coincides with morphological changes in HL-60 cells that are commensurate with adherence to the substratum. It might be speculated that mRNA upregulation and a second signal, such as adherence to the substratum is required for p72/74 expression.

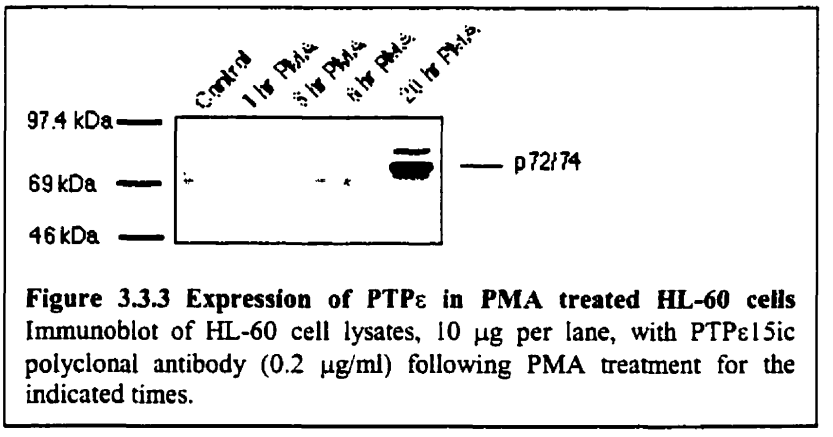

Figure 3.3.3 Expression of PTPε in PMA treated HL-60 cells Immunoblot of HL-60 cell lysates, 10 μg per lane, with PTPε15ic polyclonal antibody (0.2 μg/ml) following PMA treatment for the indicated times.

To compare the SDS-PAGE migration characteristics of the oberved p72/74 with the previously cloned cDNA for PTPε the pBCMGSneo eukaryotic expression vector

was used to transfect HEK293 cells with a PTPε cDNA encoding a predicted ~80 kDa transmembrane form of this phosphatase (Krueger *et al.*, 1990). The human cytomegalovirus immediate-early gene promoter was used to drive expression of a ~100 kDa protein, that was recognized by the PTPε16d2 antibodies by immunoprecipitation (figure 3.3.4) as well as immunoblotting (Fig 3.3.4, lanes 1 through 8). This polypeptide species correlated well with the molecular weight of the putative full-length transmembrane isoform of PTPε. Recognition of both p72/74 and p100/110 by both PTPε15ic polyclonal antibody (figure 3.3.4, lanes 3 and 4) and antibody PTPε16d2 (figure 3.3.4, lanes 7 and 8) confirmed the specificity of the antibody reagents for PTPε polypeptides. These observations also indicated that both PTPε specific epitopes are contained within the novel p72/74 species suggesting this polypeptide is an isoform of transmembrane PTPε. The PTPε16d2 antibodies appeared to be of lower affinity than the PTPε15ic antibodies owing to their weaker ability to immunoprecipitate p72/74 and p100/110 (figure 3.3.4 lanes 7 and 8). The difference between the predicted (~80 kDa) and observed (100 kDa) molecular weights for the transmembrane form of PTPε may have been due to glycosylation (Elson and Leder, 1995a) as a diffuse band, indicative of heterogeneous glycosylation, migrating at approximately 110 kDa was also observed.

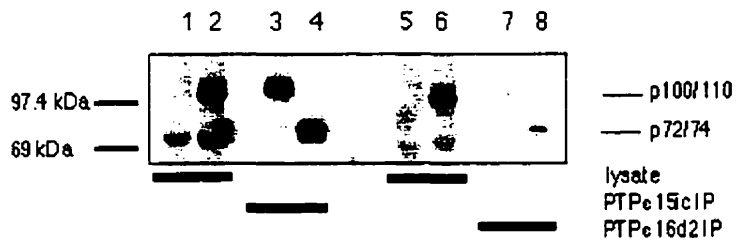

Figure 3.3.4, Expression of PTPε. Lysates obtained from control 293 cells (lane 1 and 5), and from 293 cells transfected with a cDNA encoding the transmembrane form of PTPε (lane 2 and 6). Lysates obtained from HL-60/mac cells (lanes 4 and 8) and from 293 cells transfected with the transmembrane form of PTPε (lanes 3 and 7) were immunoprecipitated with PTPε15ic antibodies (lanes 3 and 4) or with PTPε16d2 antibodies (lanes 7 and 8) and immunoblotted with PTPε16d2 antibodies. Lanes 1 through 4 were blotted with PTPε15ic. Lanes 5 through 8 were blotted with PTPε16d2.

An increase in the level of p72/74 was also seen in immunoprecipitations with PTPε15ic antibodies from detergent-soluble lysates of PMA-treated, as compared to untreated, HL-60 cells (figure 3.3.5). By densitometry this corresponded to a ~16-fold increase in p72/74-specific signal on the film. In contrast to the results obtained using PMA, differentiation of HL-60 cells with DMSO resulted in only slight upregulation of PTPε (figure 3.3.6). As can also be seen in figure 3.3.5, p72/74 was also detected in the Jurkat T-lymphocyte cell line, and in thioglycollate-elicited peritoneal-exudate derived cells.

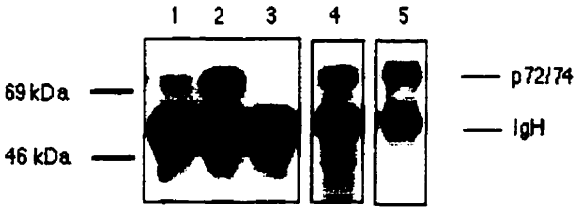

Figure 3.3.5, PTPε expression in hemopoietic cells. PTPε was immunoprecipitated from HL-60/mac cells (lanes 1 and 2) with PTPε15ic (2.0 μg) antibodies or normal rabbit serum control (lane 3), Jurkat cells (lane 4) or mouse thioglycollate-elicited peritoneal-exudate adherent cells (lane 5). PTPε was immunoblotted with PTPε15ic antibodies (0.2 μg/ml).

Detection of p72/74 in peritoneal macrophages as well as the Jurkat T cell line indicated that PTPε expression was not limited to hemopoietic cell lines, or to macrophages. However, in DMSO-mediated differentiation of HL-60 cells, which resulted in granulocytic differentiation, only a weak upregulation of p72/74 was observed indicating that while p72/74PTPε is expressed in a variety of hemopoietic cells and cell lines, its expression may not be ubiquitous in hemopoietic cells.

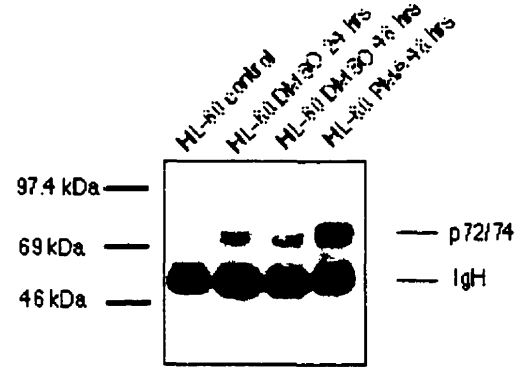

Figure 3.3.6, PTPε expression during Granulocytic differentiation of HL-60 cells. PTPε15ic immunoprecipitates from untreated (lane 1), dimethyl sulfoxide-treated (Me_2SO) (lanes 2 and 3), or PMA-treated Triton X-100 solublized HL-60 cells (lane 4), were immunoblotted with the PTPε15ic antibody.

3.4 p72/74 possesses PTPase activity

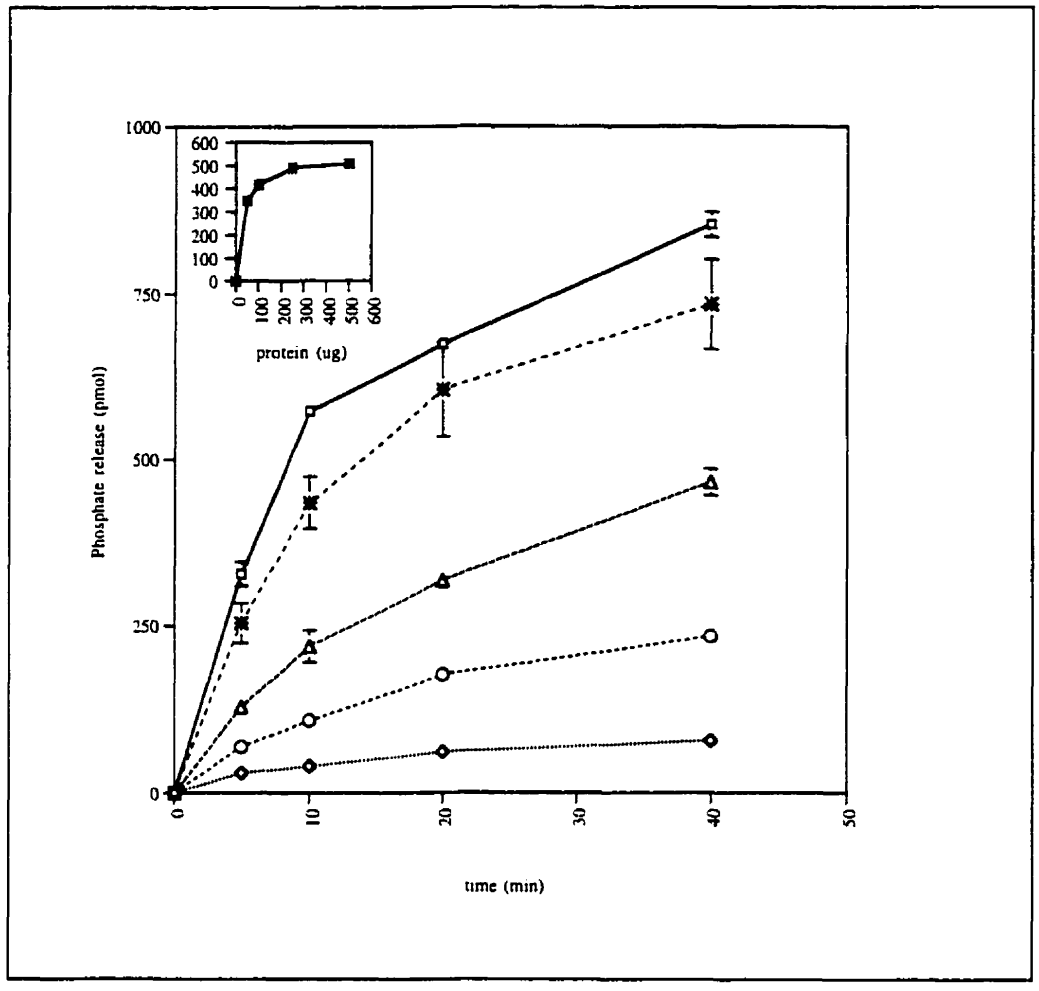

Fig. 3.4.1 **Phosphatase activity of immunoprecipitated p72/74.** Inorganic phosphate release, quantitated by the Malachite green method, was plotted as a function of time in PTPase assays carried out using 200 μM synthetic phosphopeptides with p72/74 protein obtained by immunoprecipitation of HL-60/mac lysates with PTPε15ic antibodies. All measurements were background subtracted using immunoprecipitation PTPase reactions in the absence of PTPε15ic. (o) IFNγ-Rα^{Y440}, (Δ) *hck*^{Y501}, (✳) *src*^{Y527}, (◊) STAT91^{Y701}, (❑) PDGF-R^{Y1021}. Inset shows calibration of phosphate release from the PDGF-R^{Y1021} phosphopeptide using p72/74 immunoprecipitated from HL-60/mac cells using 1.0 μg of PTPε15ic and increasing amounts of cell lysate.

	k_m	V_{max}	V_{max}/k_m
PDGFR-Y^{1021}	197 +/- 9	265 +/-12	1.3
Src-Y^{527}	288 +/- 15	589 +/-30	2
Hck-Y^{501}	293 +/- 4	455 +/-16	1.6
STAT-Y^{701}	882 +/- 34	77 +/-13	0.09
IFNγR-Y-440	-	-	-

Figure 3.4.2 Kinetic analysis of p72/74PTPε. PTPε was immunoprecipitated from HL-60/mac cells lysates using PTPε15ic polyclonal antibody. Immunoprecipitates were subjected to PTP assays as described in sections 2.12 and 2.18 (pg 25, pg 28). K_m and V_{max} values obtained are comparable to those observed with recombinant PTPε.

As can be seen in figure 3.4.1, PTPε15ic immunoprecipitated material contains an active PTPase. The inset of figure 3.4.1 shows the increasing activity immunoprecipitated with PTPε15ic antibody using increasing amount of HL-60 crude protein lysate. From these results it was concluded that p72/74 was a PTPase. Experiments outlined in section 3.3 indicated that p72/74 was detectable by two different antibodies both specific for PTPε provided convincing evidence that p72/74 was likely the only PTPase immunoprecipitated using PTPε15ic antibodies and was indeed a PTPε isoform. Further experiments in section 3.5 however provide confirmation of this statement.

A survey of the following synthetic peptide substrates: IFNγ-Rα^{Y440}, *hck*^{Y501}, *src*^{Y527}, STAT91^{Y701}, and PDGF-R^{Y1021}, indicated that PDGF-R^{Y1021} was the best substrate, *in vitro,* of the substrates tested, with STAT91^{Y701} being the least favoured substrate. Figure 3.4.2 shows the kinetic parameters for the time course presented in figure 3.4.1, obtained from three independent experiments. The results of these analyses

indicate that p72/74 also exhibits some degree of substrate specificity, a finding that potentially sheds some light on p72/74 function. It appeared that p72/74 displayed similar kinetic parameters to that observed with recombinant PTPε. The synthetic substrates appeared similar in their preference by PTPε. In general, though, the k_m values obtained with p72/74 were higher than those observed with recombinant PTPε. This may be due to the method of preparation of the immunoprecipitated material. In chapter 4 this data will be incorporated into a more in-depth analysis of the enzyme characteristics of PTPε utilizing recombinant PTPε in conjunction with immunoprecipitated material.

3.5 Liquid Chromatography/Mass Spectrometric analysis of p74

Peptide	*Location*	*Molecular Predicted*	*Mass Observed*
VDVFEFVSR	361-369	1097.56	1097.0
VIQIIPYDFNR	457-467	1377.75	1376.5
NDTLSEAISIR	557-567	1218.63	1218.0
DFLVTLNQPQAR	568-579	1401.75	1402.5
TGTFIALSNILER	637-649	1434.80	1433.5
AEGLLDVFQAVK	652-663	1289.71	1289.5

Table 3.5.1, Liquid Chromatography/Mass Spectroscopic analysis of p74 tryptic peptides. The sequences and molecular masses of p74-derived tryptic peptides are shown. Peptides whose fragmentation patterns revealed identifying sequence information are shown in bold lettering. Those not in bold displayed corresponding peptide masses in PTPε. Sequence coordinates for the peptides were according to Krueger *et al.* (1990).

As the molecular weight of PTPε, predicted from the cDNA (Krueger *et al.*, 1990) in the absence of glycosylation was ~80 kDa, it was critical to characterize the p72/74 protein further before it was considered to be a PTPε isoform. Thus, following PMA treatment, detergent-soluble lysates of large-scale HL-60/mac cell preparations were subjected to immunoprecipitation with PTPε15ic. After SDS-PAGE, Coomassie staining demonstrated the 72/74 kDa was a protein doublet (data not shown). To determine the nature of the p74 species, LC/MS analysis was performed on the more abundant ~74 kDa gel band. LC-ESI-MS analysis revealed several peptide fragments in both the trypsin and chymotrypsin digested samples. The measured masses of several of the peptides matched predicted fragment masses derived from the PTPε sequence (Table 3.5.1). In addition, the mass spectra of three peptides generated fragmentation patterns corresponding to the predicted internal amino acid sequence of PTPε (Table 3.5.1). Peptides corresponding to the predicted extracellular domain of the mature PTPε protein (Krueger *et al.*, 1990), however, were not identified.

3.6 Expression of the cDNA encoding non-transmembrane PTPε

With the cloning and sequencing of a PTPε cDNA which lacked the transmembrane and extracellular domain (Elson and Leder 1995a) from the monocyte/macrophage cell line HL-60, many questions were answered as to the origin and nature of the smaller PTPε isoform. However, the question arises as to how the 72/74 kDa doublet is generated. Post-translational modifications, such as phosphorylation or proteolysis, may account for the doublet, however, one of the four messages observed by

Northern blotting may give rise to one of the polypeptides, in which case the cDNA cloned by Elson and Leder likely corresponds to one of the species in the 72/74 doublet. To determine the origin of the p72/74 doublet, the PTPε cytosolic cDNA under the control of the EF-1α promoter was transiently transfected using the eukaryotic expression vector pcDEF3, into HEK 293 cells by lipofection. Expression of PTPε was observed by immunoprecipitation and immunoblotting with anti-PTPε polyclonal antibodies. As shown in figure 3.6.1, using PTPε immunoprecipitated from HL-60 lysates as a control (lane 1) as well as immunoprecipitates (lane 3) only the 74 kDa band of the p72/74 doublet was observed upon transfection with the cytosolic PTPε cDNA (lane 2). This was true for both hemopoietic and non-hemopoietic cell lines as the same results were obtained when non-transmembrane PTPε was transfected in to BaF/3 as well as Jurkat

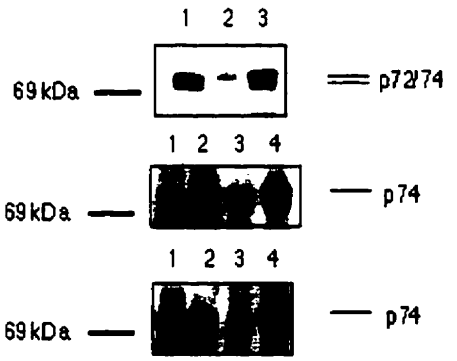

Figure 3.6.1, Expression of non-transmembrane isoform of PTPε. (Top panel) PTPε15ic polyclonal antibody immunoblots of PMA-treated HL-60 cell lysate (lane 1), PTPε15ic immunoprecipitates from 293 cells transiently transfected with non-transmembrane PTPε (lane 2), PTPε15ic immunoprecipitates from PMA-treated HL-60 cells (lane 3). (Middle panel) PTPε15ic immunoblots of Jurkat cells transiently transfected with; control vector, 10 μg of protein lysate (lane 1), non-transmembrane PTPε cDNA, 10 μg of protein lysate (lane 2), control vector, PTPε immunoprecipitated with PTPε15ic antibody (lane 3), non-transmembrane PTPε cDNA, PTPε immunoprecipitated with PTPε15ic polyclonal antibody (lane 4). (Bottom panel) PTPε15ic immunoblots of BaF/3 cells transiently transfected with; control vector, 10 μg of protein lysate (lane 1), non-transmembrane PTPε cDNA, 10 μg of protein lysate (lane 2), control vector, PTPε immunoprecipitated with PTPε15ic antibody (lane 3), non-transmembrane PTPε cDNA, PTPε immunoprecipitated with PTPε15ic polyclonal antibody (lane 4).

cells lines (figure 3.6.1).

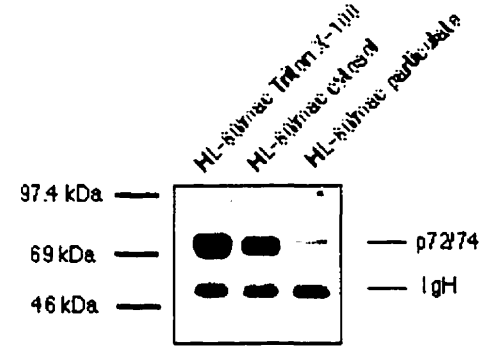

Figure 3.6.2, PTPε sub-cellular localization. PTPε15ic immunoprecipitates from Triton X-100 solublized PMA-treated HL-60 cells (lane 1), crude cytosol (lane 2) or crude particulate (lane 3) protein immunoprecipitates were immunoblotted with PTPε15ic antibodies.

To determine the sub-cellular localization of the p72/74 doublet, membrane and cytosolic fractions were prepared from HL-60/mac cells. Anti-PTPε immunoprecipitates using 1.0μg of PTPε15ic antibody were then compared from 1.0 mg of detergent soluble lysate, 500 μg of cytosolic fraction and 500 μg of the crude membrane fraction. As shown in figure 3.6.2 the majority of p72/74 was found in the cytosolic fraction of the HL-60/mac cells (lane 2). Densitometric analysis revealed that ~94% of the p72/74 signal was within the cytosolic fraction, with only ~6% detected within the particulate fraction. Figure 3.6.2 , lane 3 also shows that of the two isoforms observed, p72/74, only the p74

isoform could be detected within the particulate fraction. This suggests the p72/74 isoforms can be differentially localized.

3.7 Phosphorylation of PTPε

Examples of enzyme regulation by post-translational modifications are common. Protease cleavage, glycosylation and phosphorylation are just a few methods employed by biological systems to regulate enzymes. A number of PTPases have been reported to become phosphorylated on serine, threonine, and tyrosine residue and to be regulated by these modifications (Flint *et al.*, 1993, Bouchard *et al.*, 1994, Stein-Garlach *et al.*, 1995). Indeed, PTPε's closest relative, PTPα, has been shown to be phosphorylated on tyrosine as well as serine and threonine residues, the latter reported to be PKC dependent (Su *et al.*, 1994, Hunter *et al.*, 1995). In light of these observations, phosphorylation of PTPε was examined in resting HL-60 cells as well as in response to pervanadate stimulation.

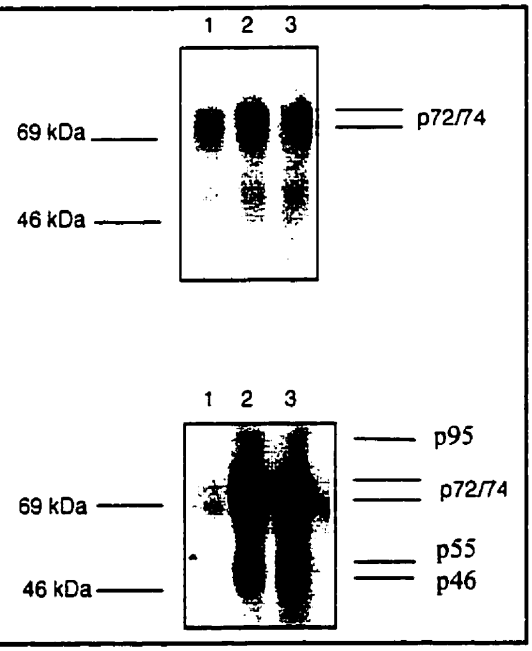

Figure 3.7.1 Phosphorylation of PTPε in HL-60/mac cells. PTPε was immunoprecipitated, using PTPε15ic polyclonal antibody, from PMA differentiated HL-60 cells after labeling with ^{32}P for 4 hours. (Top Panel) 18 hour exposure. Unstimulated cells (lane 1), cells stimulated with pervanadate for 1minute (lane 2), cells stimulated with pervanadate for 15 minutes (lane 3). (Bottom Panel) Blot in top panel immunoblotted with anti-phosphotyrosine monoclonal antibody.

3.7.1 Pervanadate induced tyrosine phosphorylation of PTPε

As illustrated by PTPα and the SH2 domain containing PTPases, PTPases may themselves be regulated by tyrosine phosphorylation events (Sun and Tonks, 1994). To induce the tyrosine phosphorylation of p72/74, the PTPase-inhibiting/PTK-activating agent pervanadate was employed (Heffetz *et al.*, 1990; Secrist *et al.*, 1993; Posner *et al.*, 1994). ^{32}P labelling of HL-60/mac cells revealed that p72/74 was phosphorylated at low levels in resting cells but upon pervanadate stimulation the amount of ^{32}P labelled p72/74 increased ~8 fold. The anti-phosphotyrosine specific monoclonal antibody 4G10 was used for immunoblotting of gel-separated proteins. Triton X-100 solublized cell lysates showed a dramatic increase in phosphotyrosine in response to pervanadate stimulation (Figure 3.7.1 (*lower panel*), lanes 1 and 2). Phosphotyrosine was not detectable within p72/74 immunoprecipitates obtained from resting HL-60/mac cells (Figure 3.7.1 (*lower panel*), lane 1). However, following 15 min exposure to 0.1mM pervanadate, a number of phosphotyrosine containing proteins were observed, including p72/74 (Fig. 3.7.1 (*lower panel*), lane 3). The p72/74-associated proteins were of approximate molecular weights 46 kDa, 55 kDa, 80 kDa and 95 kDa.

To determine the nature of the p72/74 associating proteins in pervanadate-stimulated HL-60/mac cells, immunoprecipitates were examined for the presence of a number of different molecules known to be commonly involved in signal transduction processes. Thus, based on estimated molecular weights of phosphoproteins observed to be associated with p72/74 immunoprecipitated from pervanadate-stimulated cells (figure 3.7.2), antibodies against the following proteins were evaluated: *csk*, *hck*, *lyn*, Shc, SH-PTP2, STAT91, *syk*, *vav*. However none of the tested proeins appeared to co-

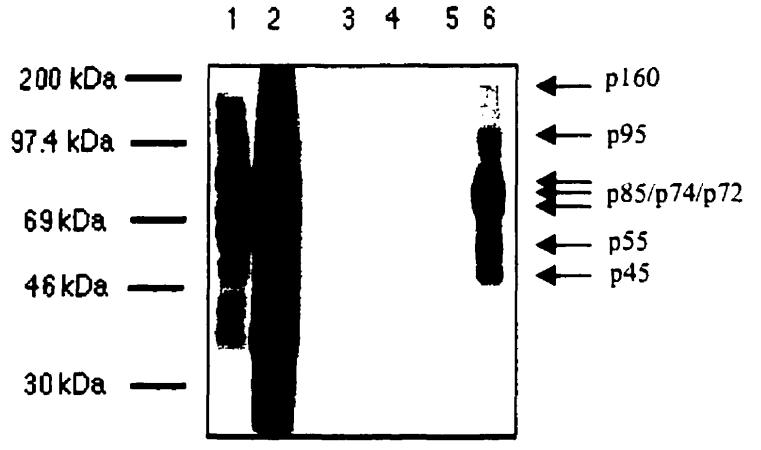

Figure 3.7.2, Effects of pervanadate on p72/74 phosphotyrosine content in HL-60/mac cells. Anti-phosphotyrosine monoclonal antibody immunoblots of unstimulated (lane 1) and pervanadate stimulated (lane 2) HL-60/mac cell lysates. As well as p72/74 (PTPε15ic) immunoprecipitates from unstimulated and pervanadate stimulated HL-60/mac cells, or normal rabbit serum immunoprecipitates from unstimulated (lane 3) and pervanadate stimulated (lane 4) HL-60/mac cells. PTPε15ic immunoprecipitate from unstimulated HL-50/mac cells (lane 5) and pervanadate stimulated HL-60/mac cells (lane 6)

immunoprecipitate with p72/74

The results of the pervanadate stimulation of HL-60/mac cells led to efforts aimed at identifying the phosphotyrosine-containing proteins observed within p72/74-containing

immune complexes. Proteins having molecular weights of approximately 45 kDa, 55 kDa, 80 kDa, 95 kDa and 150 kDa were found associated with p72/74 from pervanadate-stimulated HL-60/mac cells. The identity of these proteins is unknown. It is important to note that pervanadate stimulation, is known to have reciprocal effects on PTPases and PTKs, and can potentially lead to protein-tyrosine phosphorylation events within diverse intracellular signaling molecules (Heffetz *et al.*, 1990; Secrist *et al.*, 1993; Posner *et al.*, 1994).

3.8 Association of small adapter proteins with PTPε

As GRB2 was reported to associate with tyrosine phosphorylated PTPα (Su *et al.*, 1994; denHertog *et al.*, 1994), anti-GRB2 antibodies were used to assess whether the small SH2 and SH3 domain containing adaptor protein was present in a complex with PTPε. Use of the various antibodies revealed that GRB2 was present, although at low levels, and primarily within the p72/74 immunoprecipitates obtained from pervanadate stimulated HL-60/mac cells indicating an inducible association with PTPε (Figure 3.8.1). A trace signal corresponding to GRB2 was detectable in p72/74 immunoprecipitates from unstimulated HL-60/mac cells. This indicated that PTPε was may be phosphorylated on tyrosine 676 of the DYANFK GRB2 binding motif previously identified in PTPα. Additionally, this observation revealed that PTPε is not constitutively associated with GRB2 and is thus not constitutively phosphorylated at this site.

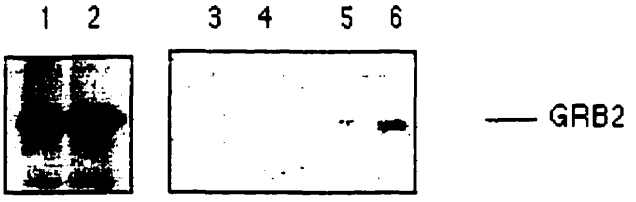

Figure 3.8.1 Association of GRB2 with p72/74 in HL-60 cells after pervanadate stimulation. Anti-GRB2 immunoblots of p72/74 immunoprecipitates from unstimulated or 0.1mM pervanadate stimulated HL-60/mac cells for 10 minutes. Lane 1 and 2 contained 15 μg of the Triton X-100 soluble protein fraction from unstimulated (lane 1) and stimulated (lane 2) HL-60/mac cells. Normal rabbit serum immunoprecipitates of unstimulated (lane 3) and stimulated (lane 4) HL-60/mac cell lysates as well as PTPε15ic immunoprecipitates from unstimulated (lane 5) and stimulated (lane 6) HL-60/mac cell lysates.

GRB2 was identified as an associating protein in p72/74-containing complexes following pervanadate stimulation of the HL-60 cells. This finding was consistent with the previous observations showing that GRB2 associated with the PTPε-like molecule, PTPα (Su *et al.*, 1994), via the phosphorylation of PTPα residue Y789 (den Hertog *et al.*, 1994). Sos, however, was not detected in the PTPα-GRB2 complexes, raising questions about the functional significance of this association (den Hertog *et al.*, 1994). The sequences in the vicinity of Y789, FSDYANFK, are identical to those surrounding PTPε Y676, making this an obvious candidate site for GRB2 association with PTPε. Further investigation either through *in vitro* mutatgenesis of this putative GRB2 binding site or through cDNA truncation analysis would identify the region of the PTPase responsible for the association.

3.9 Summary

Using PCR mediated differential hybridization PTPε was identified as a candidate PTPase mRNA upregulated by pro-inflammatory stimuli. Northern blotting analysis confirmed that the message for this PTPase was induced by a limited number of stimuli in cells of the monocyte/macrophage lineage. With the development of highly specific polyclonal antibodies, PTPε was observed as a 72/74 kDa doublet. p72/74PTPε was found to possess PTPase activity *in vitro*, predominantly within the cytosol, and its expression was observed to be regulated during cellular differentiation. Further characterization of PTPε indicated that the PTPase was phosphorylated and phosphotyrosine could be induced *in vivo* using pervanadate. Tyrosine phosphorylation was found to induce the association of the small adapter protein GRB2 with PTPε in pervanadate treated cells. However, the stoichiometry of the association appears low to the weak signals obtained The observations provided here and others point to a novel isoform of the previously described transmembrane PTPε PTPase. Indeed, recent observations published by Elson and Leder, 1997 characterize the nucleic acid sequence of the novel isoform, as shown if figure 3.9.1. Studies in chapter 5 provide a more in-depth characterization of transmembrane PTPε, as well as the novel p72/74 isoform.

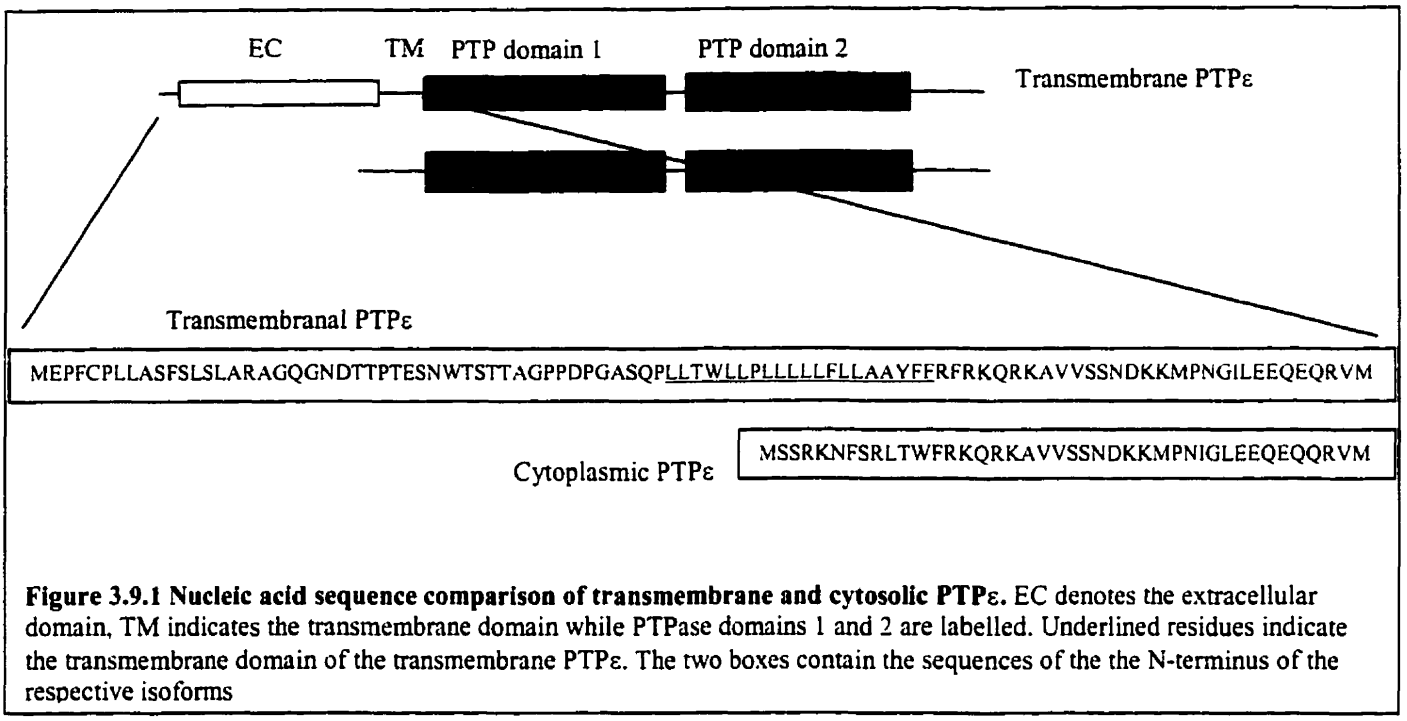

Figure 3.9.1 Nucleic acid sequence comparison of transmembrane and cytosolic PTPε. EC denotes the extracellular domain, TM indicates the transmembrane domain while PTPase domains 1 and 2 are labelled. Underlined residues indicate the transmembrane domain of the transmembrane PTPε. The two boxes contain the sequences of the the N-terminus of the respective isoforms

Chapter 4

Bacterial Expression and in vitro substrate specificity of PTPε and Substrate specificity of native PTPε

4.1 Bacterial expression of PTPases

Bacterial expression of proteins is a powerful tool for obtaining large quantities of relatively pure recombinant material. Using the glutathione S-transferase fusion protein expression system, large quantities of different PTPases were purified for further use in comparison and characterization (Smith and Johnson 1988). cDNA fragments encoding the cytosolic region containing the catalytic domains, were cloned into the pGEX-2T expression vector (figure 4.1.1). The pGEX expression system consists of a prokaryotic expression vector containing the *tac* promoter under the control of the *lacI* repressor which is also encoded on the expression vector. The glutathione S-transferase gene is thus under the control of this expression unit and contains at its C-terminus a thrombin

cleavage site followed by restriction endonuclease sites for in frame cloning of the cDNA of interest and 3 stop codons (Smith and Johnson 1988). Expression of the gene of interest involves transformation of E. coli bacteria with the pGEX expression vector containing the cDNA. Expansion of the cultures is followed by de-repression of the translation unit with the addition of the galactose analog IPTG to the cultures for up to 24 hours. The bacteria are then harvested and the PTPases purified from crude lysates by affinity column chromatography using glutathione Sepharose affinity matrix. The PTPase polypeptide sequences are liberated by batch thrombin digestion of the affinity matrix coupled to the fusion protein. Using this purification scheme approximately 500 μg/L CD45 and PTPα active catalytic domains were expressed to homogeneity as determined by Coomassie stained SDS-PAGE gels (data not shown) and stored at -80°C in 50% glycerol for future use.

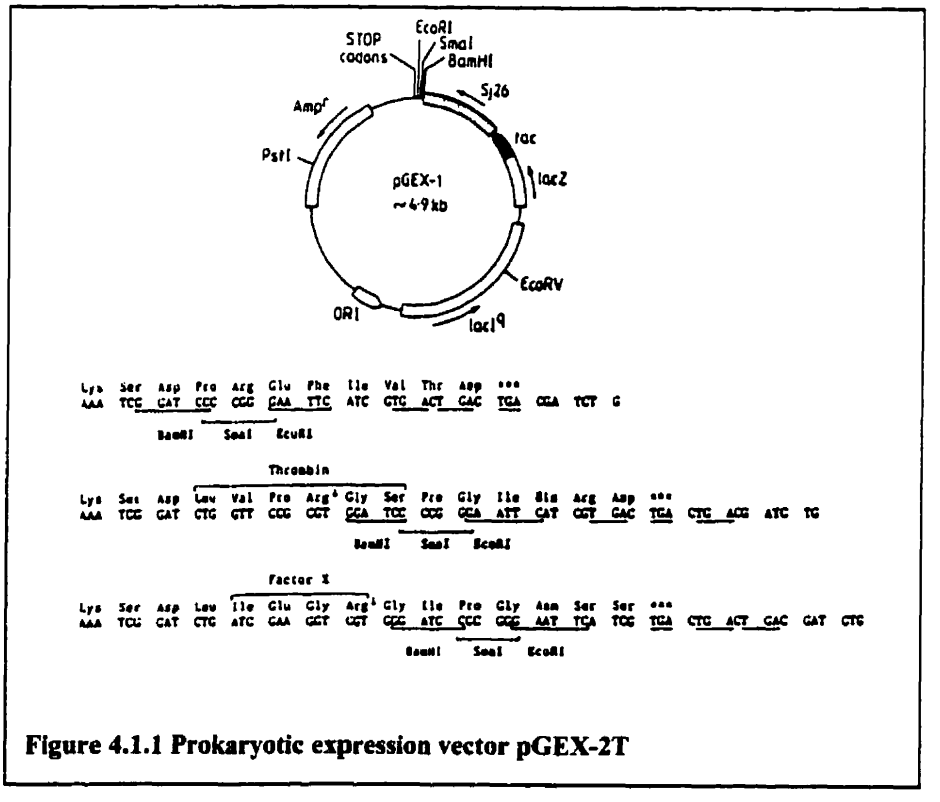

Figure 4.1.1 Prokaryotic expression vector pGEX-2T

4.2 Bacterial expression of the cytosolic region of PTPε

For bacterial expression of the catalytic domains of PTPε, mRNA was purified from HL-60 cells as described previously. A cDNA pool was prepared from the mRNA using MuMLV reverse transcriptase and random hexamer oligo-nucleotides as primers. The resulting cDNA reaction was used as the substrate in PCR amplifications using the synthetic oligo-nucleotides ptpe15 and ptpe3 and Vent DNA polymerase. Ptpe15 contains the restriction endonuclease site BamHI, preceded by the sequence CTC and followed by the complementary PTPε sequences 5'-CTCGGATCCCCCATGAGGAAGCAGAGGAAAGCTGTGGTC-3'. This strategy yielded a PCR fragment containing a 5' end that when cleaved with BamHI and ligated into pGEX-2T provided a continuous open reading frame that extended into PTPε coding sequences originating from the most N-terminal cytosolic amino acid proximal to the transmembrane domain (figure 4.2.1).

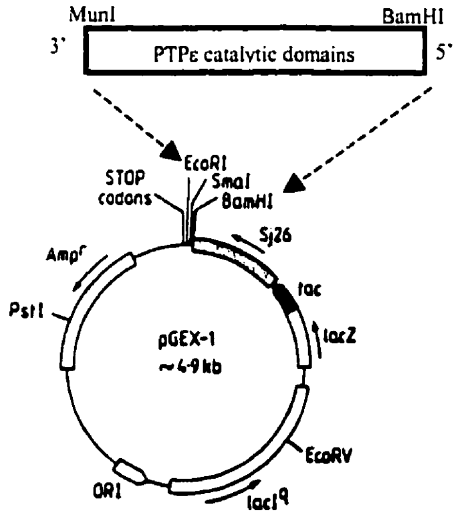

Figure 4.2.1 Construction of pGEX.2T-PTPε

The preceding sequences CTC were included to extend the 5' region of the BamHI site to facilitate efficient digestion with the restriction endonuclease. Ptpe3 contains the restriction endonuclease sites NotI, MunI and BamHI, preceded by the sequence CTC and followed by the complementary PTPε sequence 5'-GAGGGATCCAATTGCGGCCGCTCATTTGAAATTAGCATAATCAGA-3'. PCR amplification with this primer yielded a PCR fragment containing full length PTPε and the native PTPε stop codon.

4.3 Purification of PTPases

To generate sufficient quantities of recombinant PTPε for kinetic analysis large scale expression and purification of PTPα, CD45 and PTPε was carried out as described in chapter 2. pGEX2T expression vectors containing PTPα, CD45 or PTPε were introduced in to XL-1Blue *E. coli* bacteria. Cultures were initiated and bacterial pellets harvested from one liter cultures in log phase growth after 4 hours stimulation with one millimolar final concentration of IPTG at 23°C. Crude lysates were prepared by sonicating pellets resuspended in TX100 lysis buffer A and insoluble material removed by centrifugation at 100,000 x *g*. Fusion proteins were purified by affinity column chromatography using glutathione Sepharose beads. Recombinant PTPase catalytic domains were released by limited thrombin digestion and stored in glycerol. Recombinant PTPases used in the following experiments were estimated to be greater

than 95% pure by SDS-PAGE electrophoresis and coomassie or silver staining (figure 4.3.1). Approximately 350 μg/L of recombinant PTPε was expressed using this scheme.

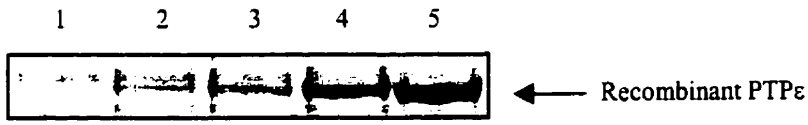

Figure 4.3.1 SDS-PAGE analysis of recombinant PTPε. Approximately 1μg of GST-PTPε was subjected to thrombin cleavage with increasing amounts of thrombin. (Lane 1) 0 ng, (lane 2) 50 ng thrombin, (lane 3) 100 ng thrombin, (lane 4) 200 ng thrombin, (lane 5) 500 ng thrombin, for 20 minutes at 23 degrees Celcius.

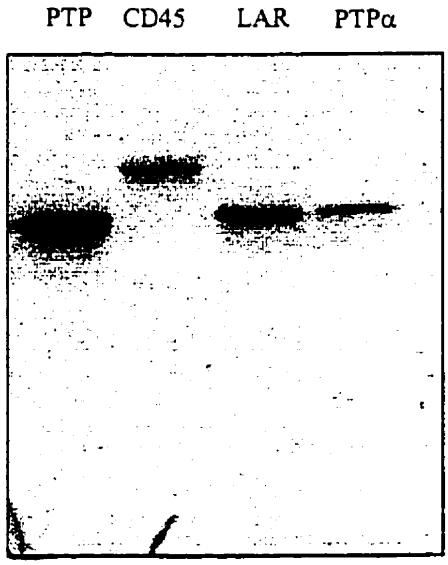

Figure 4.3.2 SDS-PAGE analysis of purified recombinant PTPases. After affinity purification with Glutathione-Sepharose and thrombin cleavage (as described in sections 2.7 and 2.8). Approximately 1μg of eluted proteins were analyzed on a 10% SDS-PAGE gel for purity.

4.4 Synthetic substrate preparation

In vitro substrate analysis was carried out using six, 13 residue oligopeptides. The oligopeptides were synthesized containing phosphotyrosine residues corresponding to sites of *in vivo* phosphorylation centrally within the peptide. Since little information exists with respect to the essential features of phosphorylation sites, it was felt that while 13 residue phosphopeptides may not retain the three-dimensional conformation of phosphorylation sites, the flanking six amino acids would maintain the primary sequence while minimizing non-specific secondary structures. The aim of these experiments was to shed some light on the possible *in vivo* substrates of PTPε, define a theoretical optimum substrate from the characteristics of a number of suitable *in vitro* substrates, as well as to compare the substrate specificity of PTPε with that of LAR and CD45.

The six peptides synthesized and employed in this study were: the C-terminal region of the protein tyrosine kinase *src*; this peptide contains the negatively regulating tyrosyl residue Tyr 527; peptides corresponding to phosphorylation sites within the β-chain of the PDGF receptor, Tyr 1021, Tyr 1009 and Tyr 857. Upon growth factor mediated dimerization the intrinsic tyrosine kinase activity of the PDGF-R results in phosphorylation of these residues providing docking sites for a number of signaling proteins including PI-3 kinase, SHP2 and PLCγ (Koch *et al.*, 1991, Cantley *et al.*, 1991); peptides corresponding to three phosphorylation sites within the cytosolic region of the CSF1 receptor, Tyr 699 and Tyr 708 in a similar fashion to that described in the case of the PDGF-R the intrinsic kinase acitivity of the CSF1-R results in phosphorylation of

these tyrosyl residues which may play a role in CSF1 signal transduction (van der Geer and Hunter *et al.*, 1990, Reedijk *et al.*, 1992).

4.5 In vitro characterization and substrate specificity of PTPε

To quantify free phosphate produced in the PTPase reactions, the modified malachite green colorimetric assay was used. In the presence of inorganic phosphate the color of malachite green changes from orange to dark green. This phosphate detection system had been previously used in the detection of inorganic phosphate in the analysis of calcineurin (Lanzetta *et al.*, 1979). With modifications, most importantly the addition of 0.01% Tween 20, the sensitivity of the assay was increased to detect inorganic phosphate with a sensitivity of 300 pmol. In addition, the reaction can be carried out in a microtitre plate (Harder *et al.*, 1994).

Before substrate preferences and enzyme comparisons could be carried out, a buffer analysis and pH profile of PTPε was completed. Figure 4.5.1 shows the results of the pH optimization, where PTPε had a pH optima of 5.6 using KOAc buffered reaction conditions (50mM NaCl, 50mM KOAc pH 6.0, 0.2mM DTT). The apparent low pH optima, compared to physiological conditions where pH is 7, is probably due to the requirments within the catalytic site where the catalytically essential cysteine residue prefers its R group as an anion ($-S^-$) vs. the protonated form (-SH). *In situ,* associated

proteins may serve to lower the local pH mimicking the pH optima experimentally determined.

Using the reaction conditions developed in earlier experiments, a substrate preference analysis was carried out using PTPε, with PTPα and CD45 included for a comparative analysis of substrate preference between related PTPases. PTPase reactions were carried out in a standard KOAc buffered PTPase assay cocktail at pH6.0 (50mM KOAc pH6.0, 50mM NaCl, 0.2mM DTT). For pH ranges 4 to 6.5 KOAc was the buffer of choice, for ranges 6.5 to 8.0 Mes buffer was used and for ranges 8.0 and above Tris-HCl was used. In the case of PTPα and CD45, pH 6.5 and pH 7.0 was used, as these were the observed pH optima in these experiments and confirmed in the literature (data not shown). The pH of 6.0 was chosen for PTPε, instead of the experimentally determined 5.6, since all substrates were prepared in a mildly acidic buffer to ensure their solubility. With the addition of the substrate the final reaction pH approaches the optimum.

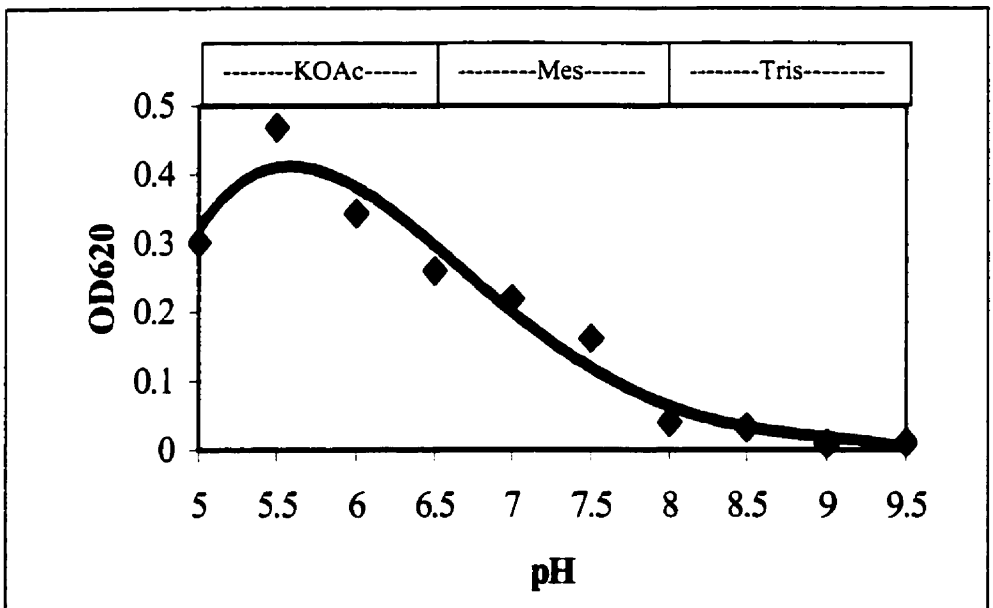

Figure 4.5.1 pH optimum of PTPε using PDGF-R^{Y1021}

Tabulated in figure 4.5.2 are the results of the *in vitro* analysis. In comparison to LAR and CD45, PTPε showed overall lower affinity for all synthetic substrates tested. The K_m value of 224 μM for src^{Y527} is similar to that of PDGF-R^{Y1009}, 250 μM for PTPε. LAR had K_m values of 159 μM and 91 μM respectively for src^{Y527} and PDGF-R^{Y1009}. CD45 had K_m values of 101 μM for src^{Y527} and 107 μM for PDGF-R^{Y1009}. Those substrates which appeared to be the prefered substrates for LAR and CD45, were also those synthetic peptides with the highest activities for PTPε.

	PTPε			LAR			CD45		
Substrate	k_m [a]	V_{max} [b]	V_{max}/k_m	k_m	V_{max}	V_{max}/k_m	k_m	V_{max}	V_{max}/k_m
Src^{Y527}	224 +/-15	534 +/-17	2.4	159 +/-6	290 +/-11	1.8	101 +/-8	897 +/-7	8.9
PDGF-R^{Y1021}	147 +/-4	615 +/-9	4.2	77 +/-3	961 +/-7	12.5	260 +/-11	843 +-11	3.2
PDGF-R^{Y1009}	250 +/-7	625 +/-4	2.5	91 +/-9	891 +/-11	9.8	107 +/-13	888 +/-3	8.3
PDGF-R^{Y857}	NC	NC	-	124 +/-14	865 +/-3	6.9	115 +/-19	403 +/-7	3.6
CSF1-R^{Y699}	NC	NC	-	NC	NC	-	193 +/-22	119 +/-24	0.6
CSF1-R^{Y708}	1275 +/-34	187 +/-26	0.2	239 +/-14	177 +/-16	0.7	188 +/-19	65 +/-6	0.4

Table 4.5.2 Kinetic analysis of PTPε, PTPα and CD45

a-μM
b-μmole/min/mg
NC-Not computed

4.6 Comparison of substrate preference of recombinant vs. native PTPε

While kinetic measurements made with recombinant enzymes are easily performed and reliable, comparison studies were also carried out using native enzyme immunoprecipitated from differentiated HL-60 cells. These studies were carried out to determine whether post-translational modifications such as serine, threonine or tyrosine phosphorylation might modify the substrate specificity or enzyme activity of PTPε.

HL-60 cells were allowed to differentiate towards the monocyte/macrophage lineage with PMA for 48 hours, then they were allowed a 24 hour recovery period in the absence of PMA. The recovery period was to permit PKC levels to return to normal, since prolonged PMA exposure results in down-regulation of PKC (Hsu *et al.*, 1998). HL-60/mac protein lysates were prepared in TX100 lysis buffer with the omission of orth-vanadate and in the presence of 1.0 mM DTT to prevent oxidation of the essential cysteine residue within the active site. To quantify the specific activity of immunoprecipitating antibody PTPε was immunoprecipitated from various amounts of protein using 1 μg of PTPε15ic antibody and PTPase assays carried out using PDGFR pY^{1021} as the substrate. A standard curve was obtained from this experiment and the point at which anti-PTPε antibodies immunoprecipitate saturating amounts of PTPase activity was determined. The arbitrary number of 12.0 units of PTPε PTPase activity was made equivalent to the amount of phosphate released from the amount of protein immunoprecipitated with 1 μg of PTPε15ic antibody, using saturating quantities of

protein lysate. These results provided a basis for the substrate specificity analysis using native PTPε immunoprecipitated from 100 μg of HL-60/mac cell lysate.

Figure 3.4.1 on page 50 shows the results of the specificity analysis using a small panel of synthetic phosphopeptides consisting of *src*^{Y527} (TSTEPQpYQPGENL), *hck*^{Y501} (TATESQpYQQQP), PDGF-R^{Y1021} (NEGDNDpYIIPLPD), IFNγ-Rα^{Y440} (APTSFGpYDKPHVL), STAT91^{Y701} (GPKGTGpYIKTELI). It is clear that native PTPε exhibits some substrate specificity since PDGF-R^{Y1021} and the *src* family members *src*^{Y527}, *hck*^{Y501} appear to be superior substrates *in vitro* in comparison to the IFNγ–Rα^{Y440} and STAT91^{Y701}.

Recombinant PTPε prepared as described earlier was subjected to substrate specificity analysis similar to that undertaken with native PTPε. Five nanograms of rPTPε was used in enzyme assays carried in 96 well plate format using standard PTPε PTPase assay buffer (50mM NaCl, 50mM KOAc pH6.0, 0.2mM DTT). Liberated free phosphate was measured by the addition of 2 volumes of malachite green reagent (MG reagent) which also terminated the enzyme activity. Analysis was carried out within the linear portion of the MG reagent response curve and spectrophotometer measurements at 620nm converted to free phosphate concentration by calibration of the curve with standards of known phosphate concentration. Table 4.5.3 shows in tabular form the k_m and V_{max} values obtained from the analysis. The substrate preferences of the recombinant enzyme appear to mirror the preferences of the endogenous enzyme shown in figure 3.4.1.

Substrate	K_m (μM)	V_{max}	V_{max}/k_m
PDGF-R^{Y1021}	147 +/-4	615 +/-9	4.2
src^{Y527}	224 +/-15	534 +/-17	2.4
hck^{Y501}	532 +/-7	446 +/-11	0.8
Stat91^{Y701}	1275 +/-27	187 +/-13	0.14
IFNγ-R^{Y440}	-	-	-

Table 4.5.3 *In vitro* substrate analysis of recombinant PTPε

The V_{max}/k_m values indicate that PDGF-R^{Y1021} (4.2) of this small panel of substrates is the most preferred with the *src* peptide (2.4) also showing characteristics of a resonable. The nature of the observed k_m values and the V_{max} values indicate that PTPε in general shows no striking substrate preference. The IFNγ-R^{Y440} substrate was included, however no kinetic parameter could be calculated due to the poor nature of substrate turn-over in those reactions.

Native p72/74PTPε appears to exhibit activity towards a broad range of synthetic substrates. PDGF-R^{Y1021} appears to be the best substrate of the panel of 5 substrates tested with *src*^{Y527}, *hck*^{Y501}, Stat91^{Y701}, IFNγ-R^{Y440} following in descending order.

4.7 Summary

In vitro analysis of recombinant PTPε revealed a pH optima of 5.6. While capable of liberating inorganic phophate from all substrates tested, PTPε did exhibit some degree of substrate specificity, especially when compared to other recombinant PTPases such as CD45 and PTPα (the two PTPases used for comparison in this study). While PTPε appeared to prefer the same substrates as other transmembrane PTPases, the order of preference and general catalytic activity towards the substrates suggested that it might have a specific profile of substrate specificities. The results obtained in the *in vitro* analysis may be useful in providing clues with respect to the direction of characterization to be taken in the following *in vivo* analysis described in more detail in chapter 5. From the small number of peptides sampled *Src* is a plausible candidate for an *in vivo* substrate when compared to the kinetic parameters of IFNγ-R^{Y440} or $STAT91^{Y770}$ peptides.

Chapter 5

Over-expression of transmembrane and non-transmembrane PTPε in mammalian cells and the role of a putative SH3 binding motif in PTPα/PTPε family of PTPases

5.1 Expression of PTPε in HEK 293 cells

Over-expression of genes is a commonly used method of characterizing the protein products of specific genes. A number of well described model systems exist for studying proteins of interest in mammalian cell lines including CHO cells, PC12 cells, A431 cells, NIH3T3 cells and BaF/3 cells. The HEK 293 human embryonal kidney cell line was chosen for the ease with which foreign genes may be introduced and for the presence of the adenovirus E1a protein which efficiently activates transcription from

CMV-based expression vectors. Preliminary experiments had revealed that PTPε was not expressed in this cell line, and that only moderate levels of PTPα were present.

To drive expression of PTPε in HEK 293 cells, the murine cDNA encoding full length transmembrane PTPε was cloned into the eukaryotic expression vector pBCMGSneo. pBCMGSneo accomplishes gene expression through the Cytomegalovirus (CMV) promoter and confers resistance to cytotoxic compound G418 by also containing the neo^r cassette (figure 5.1.1). In addition pBCMGSneo contains ~69% of the Bovine Papilloma Virus which posses the necessary sequences to maintain extra-chromosomal replication of the vector. The potential to maintain many copies of the gene of interest within the transfected cell results in increased expression.

Since the discovery of the catalytically essential cysteine residue within the active site of the PTPases (Charbonneau *et al.,* 1989), its modification, by *in vitro* mutagenesis to either a serine or alanine residue results in the abolition of detectable PTPase activity. Figure 5.1.2 illustrates the crystal structure of PTP1B. Since the 1^{st} catalytic domain of tandem catalytic domain PTPases show high sequence identity with PTP1B, the crystal structure

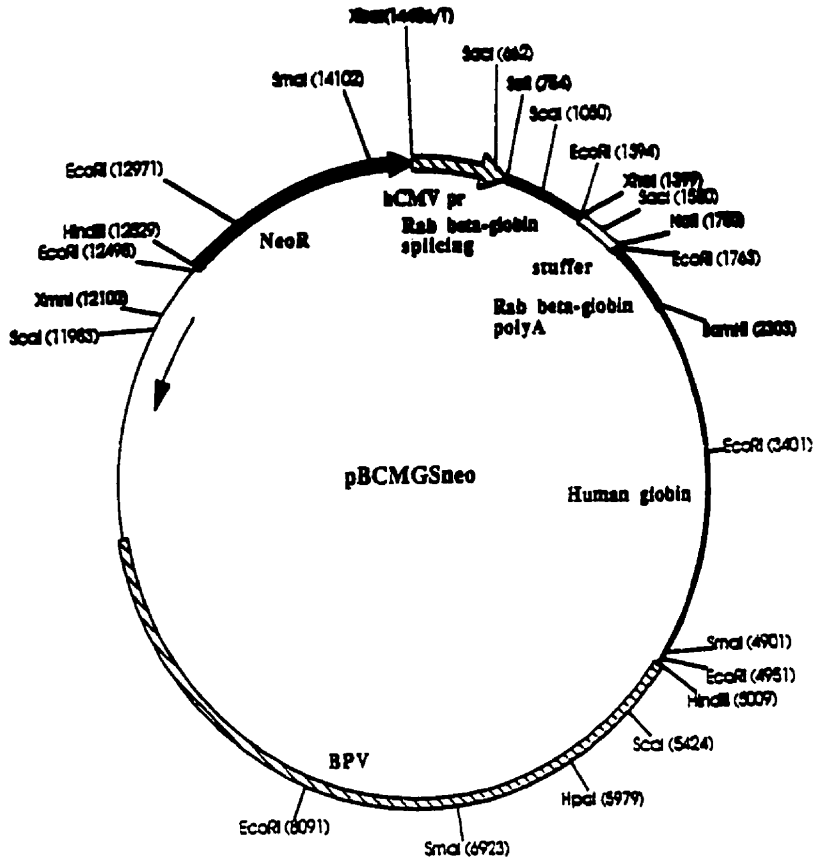

Figure 5.1.1 The pBCMGSneo-PTPε expression vector. After XhoI NotI digestion to remove the stuffer fragment, various PTPε cDNA's were cloned in to the linearized vector.

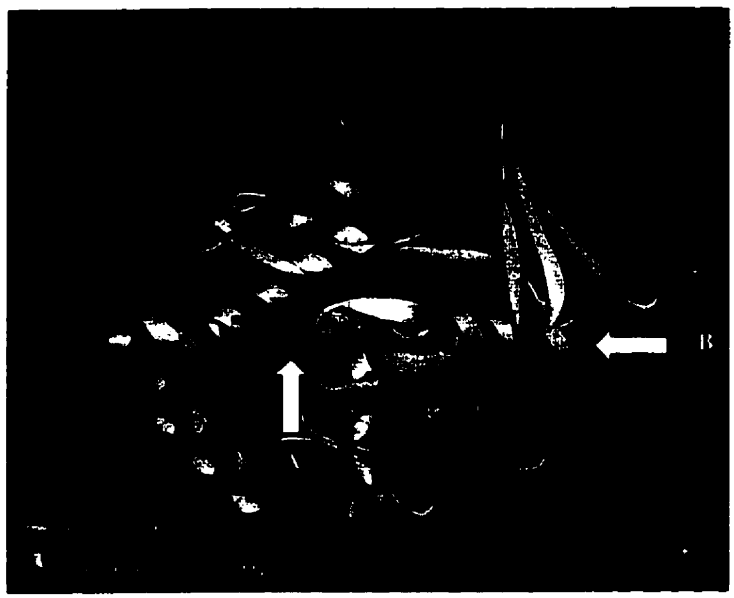

Figure 5.1.2 Crystal structure of Human PTP1B. Arrow B indicates the location of the central helix and arrow A illustrates the active site. The enzyme was crystalized in the presence of Tungstate. The ion can be seen covalently bound to the active site cysteine (*arrow A*). ( )

of PTP1B is analogous to the first catalytic domain of PTPα and other dual catalytic domain transmembrane PTPases. The crystal structure of PTP1B can then be seen as a template for other catalytic domains. As is evident in figure 5.1.2, the aforementioned cysteine residue (*arrow A*) is located at the end of the central helix (*arrow B*) within the substrate pocket of the enzyme. Catalytically inactive forms of PTPases, generated by alanine or serine substitutions of the cysteine residue have been a useful tool in uncovering their roles in biological signal transduction pathways (Pannifer *et al.*, 1998, Jai *et al.*, 1995). Recent evidence indicates that these mutants, to varying degrees, trap substrates within the active site of the PTPase domain (Pannifer *et al.*, 1998). This is achieved because residues within the pocket of the active site serve to stabilize π electron distribution of the aromatic ring as well as charge distribution of the highly polarized phosphate group. Enzyme-substrate interactions provide sufficient electrostatic interactions for substrate binding in spite of the absent covalent phosphothiol ester linkage provided by the thiol anion the catalytic cysteine forms within the low pH conditions of the active site. This phenomenon may result in the sequestration of PTPase substrates. The result, inhibition of wild-type function resulting in dominant negative phenotypes or inhibition of substrate function within its pathway. This potentially culminates in a phenotype.

Figure 5.1.3 shows the strategy employed for the creation of PTPε mutants C334A, C629A, and C334A/C629A. The conversion of cysteine 334 to an alanine residue was accomplished with the use of complementary oligonucleotides C1>Aa (5'-CCCACGCCCGCGCTAGCGTGAACCACAATGGG-3') and C1>As (5'-

CCCATTGTGGTTCACGCTAGCGCGGGCGTGGGT-3') with the underlined nucleotides forming the mispaired regions resulting in the codon change. The conversion of the cysteine 629 to an alanine residue was obtained with the use of complementary oligonucleotides C2>Aa (5'- CCCTGCTCCCGCCGTAGCGTGCACGGTGATGGG-3') and C2>As (5'-CCCATCACCGTGACAGCTAGCGCGGGAGCAGGG-3'). As outlined in figures 5.1.3a and 5.1.3b, overlap extension PCR was used to create the mutant cDNAs. This method was utilized for speed, since the process requires the length of time necessary to complete two PCR amplifications, as well as accuracy because >99% of the PCR product will contain the desired mutation. Utilization of overlap extension PCR negated the need for extensive screening of clones to identify those carrying the desired mutation. Both mutagenized cDNAs were

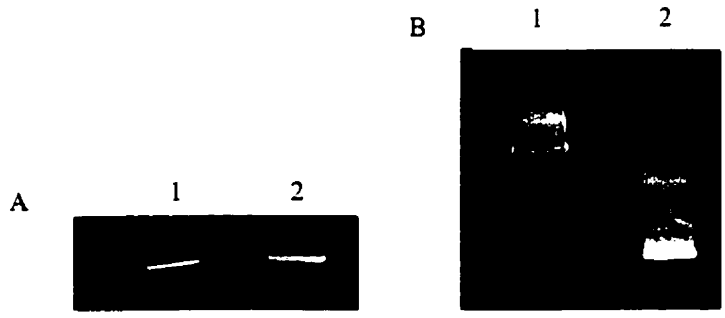

Figure 5.1.3 Overlap extension PCR mutagenesis of C334 and C629 of PTPε *(Panel A)* The 5 prime PCR fragment (lane 1) and 3 prime PCR fragment (lane 2) of the C334A overlap extention reaction. *(Panel B)* The 5 prime PCR fragment (lane 1) and 3 prime PCR fragment (lane 2) of the C629A overlap extension reaction.

sub-cloned into pSSBS for mapping and partial sequencing. The final PTPε catalytic mutant PTPεC334A/C629A, which has both domains inactivated, was constructed by

cloning the 1.7 kb StyI fragment of pSSBS-PTPεC334A into the StyI site of the purified 3.1 kb fragment of pSSBS-PTPεC629A. This simple swapping strategy exchanges the wild-type StyI fragment for the C334A mutant fragment conserving the open reading frame of the cDNA. The resulting chimeric cDNA containing both C334A and C629A mutants was mapped for integrity then shuttled into the pBCMGSneo expression vector via the NotI cloning site.

Introduction of the eukaryotic expression vectors into HEK 293 cell line was accomplished by transfection using Lipofectamine (GIBCO-BRL). Briefly, lipofection consists of the emulsification of DNA with a specialized ionic lipid resulting in the

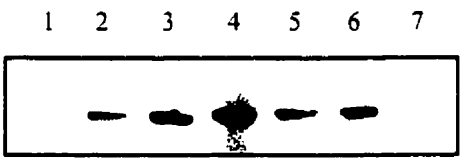

Figure 5.1.4 Transient expression of PTPε in HEK 293 cells. HEK 293 cells were transiently transfected with various amounts of wild-type PTPε expression vector. PTPε expression was analyzed by immunoprecipitation and immunoblotting with PTPε15ic. Lane 1 transfection with control vector. Lane 2 0.5 μg. Lane 3 1.0 μg. Lane 4 2.0 μg. Lane 5 5.0 μg. Lane 6 10.0 μg. Lane 7 20.0 μg.

formation of liposomes capable of delivering DNA within the cell. Preliminary experiments titrating the quantity of DNA transfected revealed that, with this cell type, target DNA can be transfected with efficiency approaching 90% when PTPε expression was determined by immunoflourescence. Transient transfection experiments revealed that

the introduction of ~2 μg of pBCMGSneo-PTPε plasmid resulted in optimal expression levels after an overnight (~18 hour) recovery period (figure 5.1.4). However, one modification in particular resulted in much greater efficiency. The introduction of a single step coating of the tissue culture plates with bovine fibronectin 20 μg/ml prior to cell seeding resulted in enhanced adhesion of the cells to the substratum. This proved to be essential since HEK 293 cells in the presence of Optimem serum free medium, which is required for efficient transfection, exhibited greatly reduced adhesion to tissue culture plates. The resulting transfections were of both higher efficiency and protein yield since 100% of the seed cells were harvested (data not shown).

Transfection of full length PTPε (pBCMGSneo-PTPε) into HEK 293 cells had no obvious effect on cell survival as compared with control vector (figure 5.1.5). Protein lysates prepared with TX100 lysis buffer were subjected to immunoprecipitation and immunoblotting with PTPε15ic polyclonal antibody. Figure 5.1.5 shows that introduction of pBCMGSneo-PTPε in to HEK 293 cells resulted in expression of a 100/110 kDa species migrating with the characteristics of a doublet. The presence of a 100/110 kDa protein with reactivity to anti-PTPε antisera indicates that immature PTPε undergoes post-translational modifications resulting in an apparent molecular weight substantially higher than the predicted 78 kDa.

Transfections of the mutant forms of PTPε were carried out using the same conditions employed for pBCMGSneo-PTPε. Introduction of pBCMGSneo-PTPεC334A, pBCMGSneo-PTPεC629A or pBCMGSneo-PTPεC334A/C629A resulted in no

detectable change in cell survival as compared to vector control. Figure 5.1.5 shows that the transfection of the various catalytic mutants of PTPε into HEK 293 cells resulted in identical migration patterns of PTPε, as observed when wild-type PTPε was introduced, indicating that the full-length protein was being expressed.

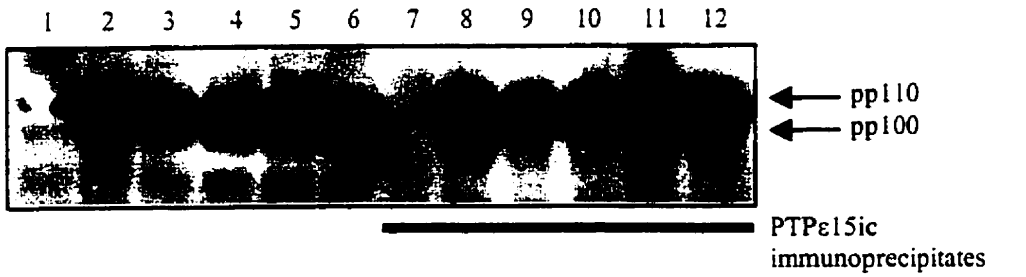

Figure 5.1.5 Expression levels of wild-type and various mutants in transfected HEK 293 cells. HEK 293 cells were transfected with empty control vector (lane 1 and 7), PTPε (lane 2 and 8), PTPεC334A (lane 3 and 9), PTPεC629A (lane 4 and 10), PTPεC334A/C629A (lane 5 and 11), PTPεF112P (lane 6 and 12) and selected for stable expression. TX100 lysates were prepared and either directly western blotted (lanes 1 through 6) or subjected to PTPε immunoprecipitation then blotted (lanes 7 through 12) with PTPε15ic polyclonal antibody.

While expression of PTPε cDNA had no effect upon cell survival, there was a noticeable difference in cell morphology in cells expressing wild-type PTPε, PTPεC334A/C629A and control vector. Figure 5.1.6 shows that cells expressing wild-type PTPε although very similar in shape to cells transfected with control vector did posses an increased number of cellular protrusions in addition these cells seemed to have a lower number of cell-cell contacts. They tended to spread out in culture and cover the entire substratum. In addition, cells expressing the wild-type construct were able to adhere to the substratum much better than control cells (data not shown). These characteristics were much more apparent when cells expressing PTPε were compared to

cells expressing PTPεC334A/C629A. Cells transfected with the dominant negative mutant of the PTPase, had very few cellular protrusions, and maintained a very high number of cell-cell contacts and were often observed to grow in clumps. Additionally cells expressing PTPεC334A/C629A did not spread out in culture and cover the entire substratum but instead grew in long cellular tracts always maintaining very tight cell-cell adhesion while not adhering to the substratum efficiently. These results indicated that PTPε may play a role in cell-cell and/or cell-substratum adhesion.

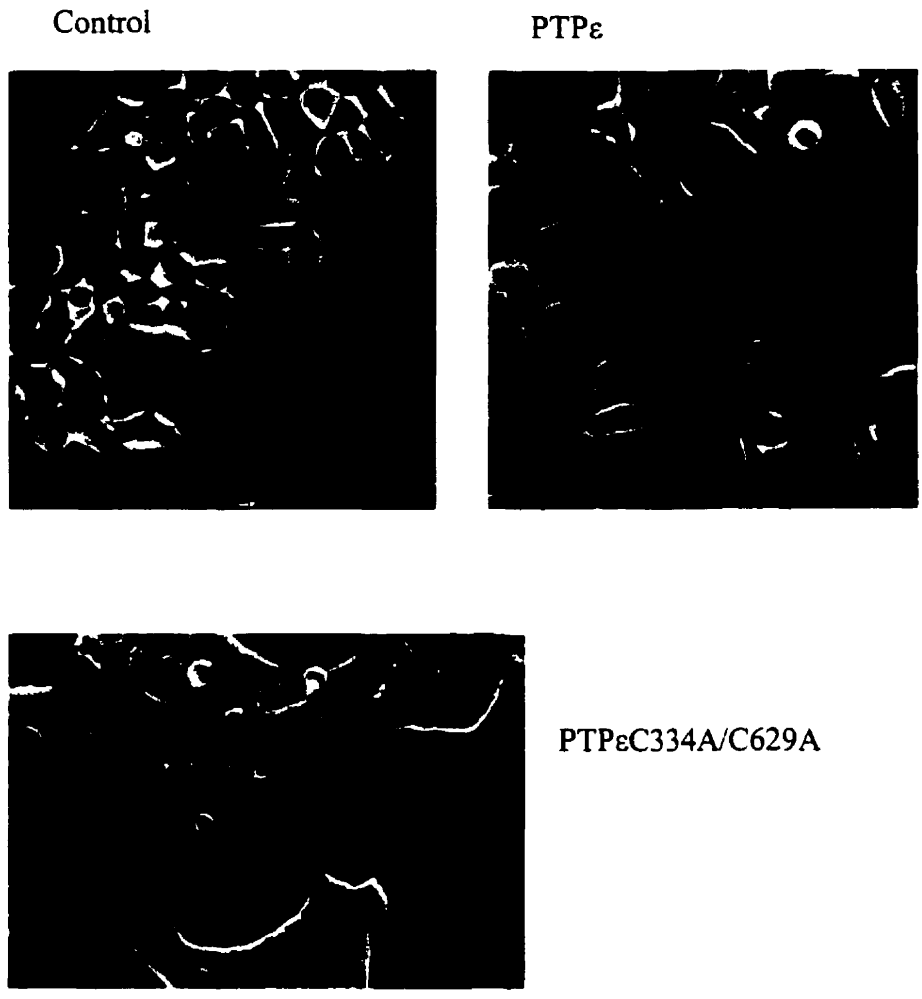

Figure 5.1.6 Morphology of cells expressing PTPε. HEK 293 cells expressing various forms of PTPε in a stable manner were seeded in culture at identical concentrations then photographed under phase contrast microscopy at 200x magnification. *Upper right panel* shows 293 cells transfected with the empty control vector. *Upper left panel* shows 293 cells transfected with wild-type PTPε. *Lower left panel* shows the morphology of 293 cells transfected with PTPεC334A/C629A

To confirm that p100/110 possessed PTPase activity, immunoprecipitations were carried out using PTPε15ic polyclonal antibodies from protein lysates of transiently transfected HEK 293 cells. The lysates were prepared in the presence of 1.0 mM DTT to maintain the active site cysteine in a reduced state ensuring preservation of PTPase

activity. Figure 5.1.7 shows PTPase activity associated with the immunoprecipitates. It can be seen that ectopically expressed PTPε was catalytically active while PTPεC334A mutant exhibited no catalytic activity. In addition, PTPεC629A was observed to be catalytically acitve while the double mutant, PTPεC334A/C629A, predictably was not (data not shown). These results indicated the first catalytic domain of PTPε was responsible for the majority of the detectable PTPase activity. The second catalytic domain either possessed little PTPase activity, had high substrate specificity and therefore unable to dephosphorylate the synthetic substrate PDGF-R^{Y1021} (NEGDNDpYIIPLPD), or the acitivity of 1st catalytic domain was required for activity.

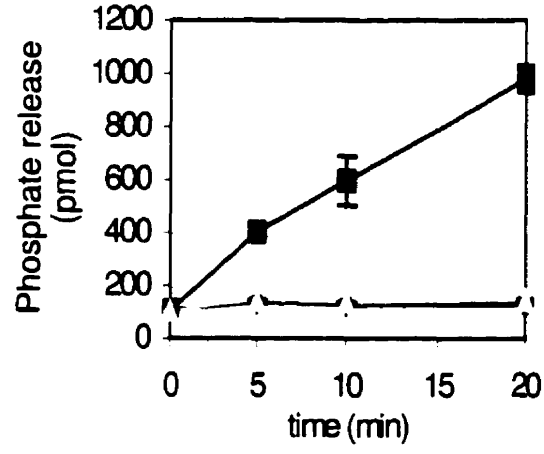

Figure 5.1.7 Protein tyrosine phosphatase activity of ectopically expressed PTPε and mutants. Whole cell lysates prepared from 293 cells exhibiting stable expression of ▲ PTPεC334A, ● Control and ■ PTPε were subjected to immunoprecipitation with PTPε15ic polyclonal antibody. Immunoprecipitates were then subjected to MG PTPase assays. OD values were converted to pmols of PO_4 using a inorganic PO_4 calibration curve.

The observation of the p100/110 doublet was of great interest since the higher molecular weight band appeared somewhat fuzzy (figure 5.1.5). This characteristic is suggestive of heterogeneous glycosylation of a pre-processed "core" protein. Due to the presence of three potential N-linked glycosylation sites and three O-linked glycosylation sites within the extracellular domain of PTPε the addition of carbohydrate moieties was the most likely explanation for the observed molecular weight. To investigate this possibility further, protein lysates were prepared from HEK 293 cells with stable expression of PTPε and PTPε immunoprecipitated with PTPε15ic. Immunoprecipitates were subjected to deglycosylation using N-glycanase which selectively removes carbohydrate moieties from N-linked sites. Figure 5.1.8 indicated that the heterogeneous p110 isoform of PTPε resulted from N-linked glycosylation as denoted by the disappearance of the p110 band with increased exposure to N-glycanase. These results also suggest that the increased molecular weight of premature p100 isoform over the predicted molecular weight is due to glycosylation at the numerous potential O-linked sites within the extracellular domain of PTPε.

Figure 5.1.8 De-glycosylation of PTPε expressed in HEK 293 cells. HEK 293 cells with stable wild-type expression of PTPε were either left untreated (lane 1), or treated with N-glycanase for 1 hour (lane 3), or 16 hour treatment (lane 4). PTPε was visualized by immunoblotting with PTPε15ic.

5.2 Phosphorylation of PTPε expressed in HEK 293 cells and total cell lysate phosphotyrosine profiles

Phosphorylation is a prevalent post-translational modification event with the ability to regulate the function of proteins. Since the over-expression of an active PTPase may indeed have a detectable impact on endogenous substrates, TX100 lysis buffer solublized lysates from HEK 293 cells over-expressing either wild type PTPε or various mutants were probed with the anti-phosphotyrosine antibody 4G10. Phosphotyrosine profiles revealed little change in the relatively abundant proteins whose phosphotyrosine content can be measured in this method.

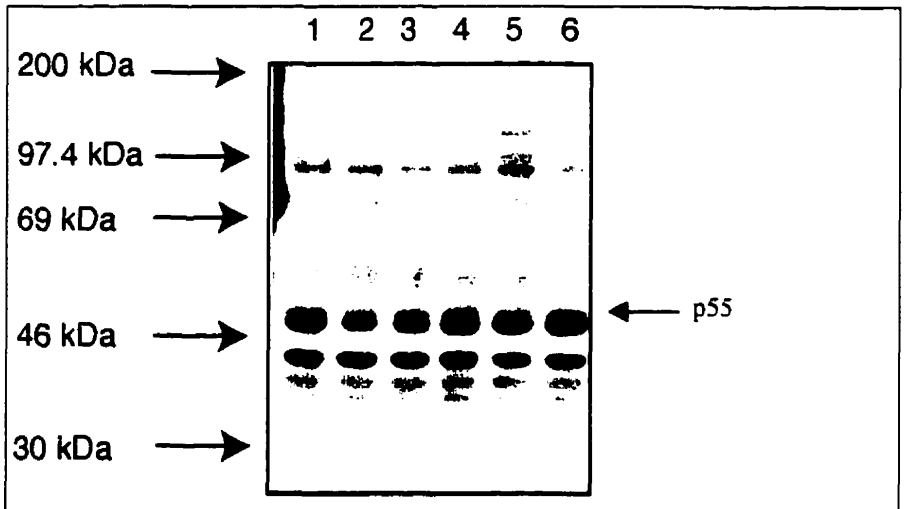

Figure 5.2.1 Phosphotyrosine profiles of HEK 293 cells expressing PTPε and mutant forms. Cell lysates from HEK 293 cells expressing either empty vector (lane 1), wild-type PTPε (lane 2), PTPεC334A (lane 3), PTPεC629A (lane 4), PTPεC334A/C629A (lane 5), or PTPεF112P (lane 6) were subjected to SDS-PAGE. Immunoblots were probed with the anti-phosphotyrosine monoclonal antibody 4G10.

The exception is a group of proteins migrating with an apparent molecular weight of approximately 55 kDa (figure 5.2.1) whose phosphotyrosine content appeared to decrease with the expression of an active PTPε membrane proximal catalytic domain. Figure 5.2.1 shows the correlation between the active catalytic domain of PTPε and pp55 tyrosine phosphorylation.

To investigate the amount of tyrosine phosphate found in PTPε, HEK 293 cells with stable expression of PTPε, PTPεC334A, PTPεC629A, or PTPεC334A/C629A protein lysates were prepared from resting cells or cells stimulated with pervanadate. The covalent binding of pervanadate to the essential cysteine within the active site of PTPases results in irreversible inhibition of PTPase activity leading to deregulated tyrosine phosphorylation of various substrates by PTK's. After immunoprecipitation, immunoblotting with anti-phosphotyrosine antibodies revealed the extent of PTPε tyrosine phosphorylation. As shown in figure 5.2.2 PTPε immunoprecipitated from cells expressing the wild-type PTPase as well as various catalytic mutants show increased amounts of phosphotyrosine in proteins of molecular weight pp40, pp55, pp85, pp100, pp110, and pp160.

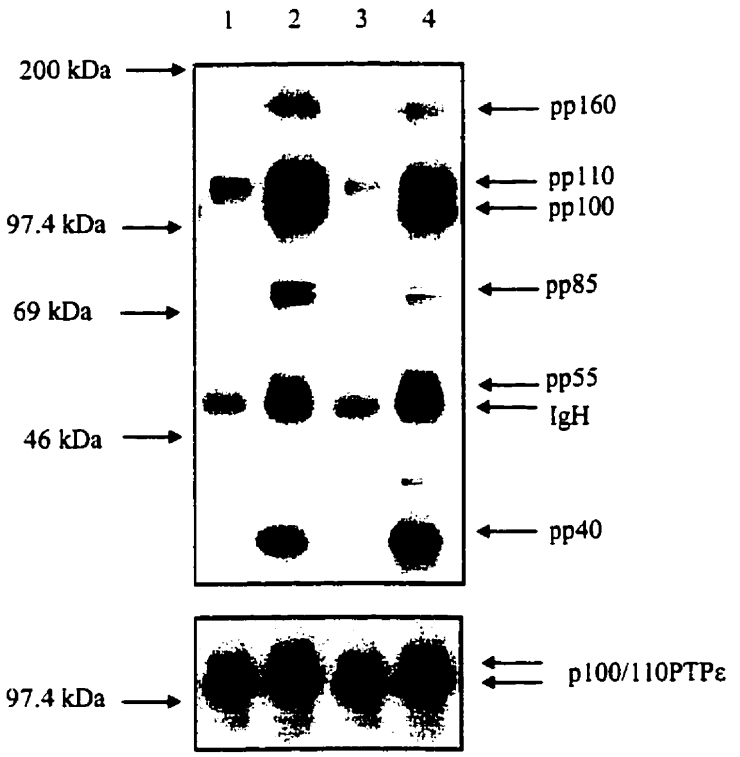

Figure 5.2.2 Pervanadate treatment of HEK 293 cells expressing PTPε cDNAs. (*Upper panel*) Cell lysates prepared from HEK 293 cells with stable expression of wild-type PTPε (lanes 1 and 2) or PTPεC334A (lanes 3 and 4) were either not stimulated (lanes 1 and 3) or stimulated (lanes 2 and 4) with 100nM pervanadate for 10 minutes. Various isoforms of PTPε were immunoprecipitated with PTPε15ic polyclonal antibodies and phosphotyrosine content determined by immunoblotting with anti-phosphotyrosine monoclonal 4G10. (*Lower panel*) the upper panel stripped and re-probed with the anti-PTPε antibody PTPε15ic.

Stripping and re-probing of immunoblots with PTPε15ic suggested that pp100/pp110 were PTPε polypeptides (figure 5.2.2 *lower panel*). The strong phosphorylation observed with pervanadate stimulation suggested that PTPε might be associated with tyrosine kinases that were normally regulated by PTPase activity. The presence of pp40, pp55, pp85, and pp160 were unexpected and suggested that PTPε may

be able to associate with a number of PTK substrates. The identities of the associated proteins observed are unknown.

GRB2 was reported to associate with tyrosine phosphorylated PTPα (Su *et al.*, 1994; den Hertog *et al.*, 1994). Anti-GRB2 antibodies were used to determine whether GRB2 would associate with PTPε in a similar fashion. PTPε was immunoprecipitated, using PTPε15ic antibody, from TX100 protein lysates of HEK 293 cells exhibiting stable expression of PTPε from the pBCMGSneo expression vector. With the use of anti-GRB2

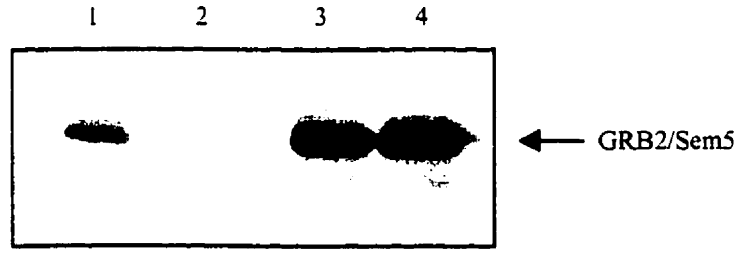

Figure 5.2.3. GRB2 association with PTPε. TX100 lysates prepared from HEK 293 cells transfected with PTPε and selected for stable expression. PTPε was immunoprecipitated with PTPε15ic and probed with anti-GRB2 antibodies. Lane 1 HEK 293 lysate. Lane 2 cells transfected with empty control vector. Lane 3 cells expressing PTPε. Lane 4 cells expressing PTPε and stimulated with 0.1μM pervanadate for 10 minutes.

monoclonal antibodies, it was determined that GRB2 was present in anti-PTPε immunoprecipitates from both resting and pervanadate stimulated PTPε expressing HEK 293 cells (figure 5.2.3).

5.3 Src family kinases

The phosphotyrosine profiles generated in figure 5.2.1 suggested that over-expression of PTPε resulted in the decrease of phosphotyrosine content of a group of proteins with an apparent molecular weight of approximately 55 kDa. In addition, reports have implicated PTPα in dephosphorylation and activation of *src* family kinases in rat embryo fibroblasts (Zheng *et al.*, 1992) and P19 cells (den Hertog *et al.*, 1993). PTPε being a close relative to PTPα already shares *in vitro* substrate specificity with PTPα as shown in chapter 4. To test whether *src* kinase family members were regulated by PTPε, $pp60^{src}$ and $pp59^{fyn}$ were immunoprecipitated from HEK 293 cells over-expressing wild-type PTPε, PTPεC334A, PTPεC629A, or PTPεC334A/C629A. The immunoprecipitates were immunoblotted with the monoclonal antibody 4G10 to assess the phosphotyrosine content of *fyn* and *src*. Figure 5.3.1 shows the results of a single representative experiment which revealed that wild-type PTPε over-expressed in HEK 293 cells resulted in an 82% +/- 7 (the results of five independent experiments) decrease in *src* phosphotyrosine levels.

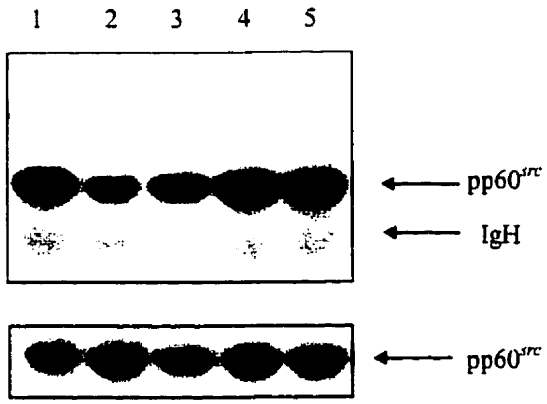

Figure 5.3.1 Phosphotyrosine content of pp60*src* in HEK 293 cells expressing wild-type PTPε or PTPε mutants. (*Upper panel*) Triton X-100 cell protein lysates were prepared from HEK 293 cells with stable expression of empty expression vector (lane 1), PTPε (lane 2), PTPεC334A (lane 3), PTPεC629A (lane 4), PTPεC334A/C629A (lane 5). $pp60^{src}$ was immunoprecipitated with anti-*src* polyclonal antibodies and *src's* phosphotyrosine content assessed with 4G10. (*Lower panel*) The immunoblot in the upper panel was stripped and reprobed with the anti-*src* monoclonal antibody GD11.

As seen in lane 2 of figure 5.3.1, *src* dephosphorylation is dependent upon PTPase activity. However, lanes 3 and 4 indicate that for efficient dephosphorylation of $pp60^{src}$ both catalytic domains of PTPε must be active. The PTPεC334A expressing cells showed a 50%+/-9 decrease in *src* tyrosine phosphorylation while the PTPεC629A expressing cells exhibited a 10%+/-5 decrease in *src* tyrosine phosphorylation. In contrast, cells expressing PTPεC334A/C629A showed at modest but reproducibile 7%+/-3 increase in *src* tyrosine phosphorylation suggesting absence of PTPε PTPase activity may enhance *src* kinase activity. These results indicate that although the membrane distal catalytic domain of PTPε may not possess detectable PTPase activity *in vitro*, it likely does play some undefined role in substrate dephosphorylation. Figure 5.3.1 (*lower panel*) shows

that a similar amount of *src* was immunoprecipitated in each case. However, it was unclear whether PTPε was capable of mediating a substantial decrease in the phosphotyrosine content of *lyn*, (figure 5.3.2 lanes 7 and 8). Figure 5.3.2 shows the observations from one of three repeated experiments which suggested that *lyn* may be a less optimal substrate than *fyn* or *src*. While PTPε was capable of decreasing the phosphotyrosine content of *src* and *fyn* by 80%+/-3 in these experiments the PTPase was capable of producing a 30%+/-13 decrease in the phosphotyrosine content of *lyn*.

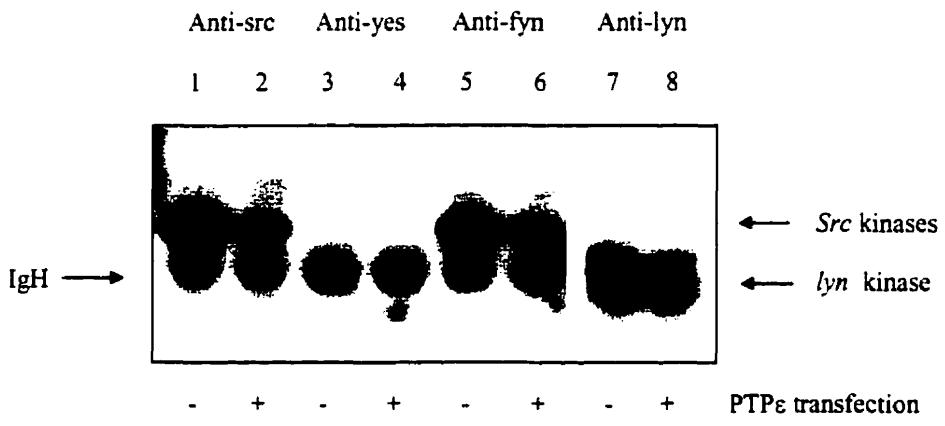

Figure 5.3.2 Decrease in phosphotyrosine content of other *src* family members in HEK 293 cells expressing PTPε. HEK 293 cells with stable expression of either empty expression vector (lanes 1, 3, 5, 7) or wild-type PTPε (lanes 2, 4, 6, 8) were subjected to immunoprecipitation with anti-src (lanes 1 and 2), anti-yes (lanes 3 and 4), anti-fyn (lanes 5 and 6) or anti-lyn (lane 7 and 8). Phosphotyrosine content of immunoprecipitated src kinases was observed with 4G10.

If PTPε is capable of directly or indirectly mediating the dephosphorylation of the C-terminal regulatory phosphotyrosine of *src* family members, then the measurable kinase activity of $pp60^{src}$ should be increased in HEK 293 cells over-expressing active

PTPε, but not in those cells expressing mutant forms of the PTPase. *Src* activity was assessed in cells expressing wild-type as well as mutant forms of PTPε by immunoprecipitating the kinase and measuring auto-phosphorylation in the presence of γ-^{32}P-ATP followed by SDS-PAGE and autoradiography. Kinase activity was measured by scanning densitometric analysis of the autoradiographs. Figure 5.3.3 shows results of one representative from four independent experiments. Figure 5.3.3 indicates that PTPε is capable of activating pp60^{src} by 2-fold (+/-0.3). Lanes 3 and 4 indicate again, that the presence of two active catalytic domains is necessary for the maximal activation of *src* kinases by PTPε. Lanes 3 and 4 reveal a smaller activation (1-fold +/-0.4) of pp60^{src} by mutants PTPεC334A and PTPεC629A respectively.

Figure 5.3.3 Activation of pp60*src* in HEK 293 cells expressing wildtype PTPε and PTPε mutants. Src immunoprecipitates were subjected to auto-kinase assays with ^{32}PγATP and phosphorylated kinase analyzed by SDS-PAGE. (lane 1) 293 cells transfected with control vector. (lane 2) 293 cells transfected with expression vector containing wild-type PTPε. (lane 3) 293 cells transfected with BCMGSneo-PTPεC334A. (lane 4) 293 cells transfected with BCMGSneo-PTPεC629A. (lane 5) 293 cells transfected with BCMGSneo-PTPεC334A/C629A.

Expression of the putative dominant negative form of PTPε (PTPεC334A/C629A), figure 5.3.3 lane 5, caused a 23%+/-8 decrease in pp60$^{c\text{-}src}$ activity as compared to control. This observation suggested that PTPε was either involved in the regulation of an upstream regulator of *src* family kinases or alternatively that PTPε is

directly responsible for modulation of *src* phosphorylation and kinase activity. If the effect of PTPε on pp60^{src} were direct, one might predict a physical association between the two proteins. To investigate this, immunoprecipitations of *c-src* were probed with anti-PTPε antibodies. Figure 5.3.4 shows that a 110 kDa protein reacting with the anti-PTPε polyclonal antibody co-immunoprecipitated with *c-src* from HEK 293 cells expressing wild-type or mutant forms of PTPε, but not when transfected with vector alone. These results suggest that the observed dephosphorylation and activation of pp60^{src} is via a direct

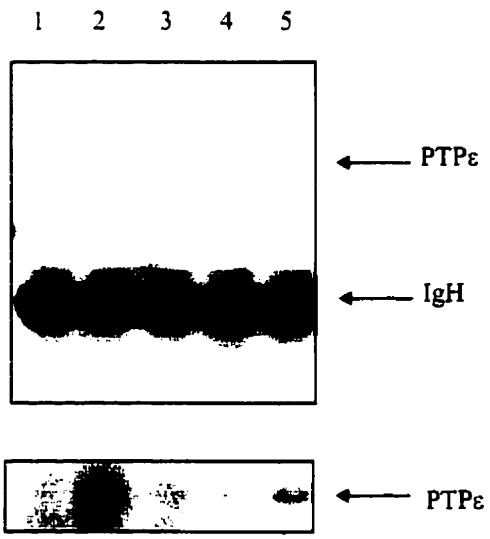

Figure 5.3.4 Co-immunoprecipitation of pp60*src* with wildtype PTPε and mutants in HEK 293 cells. HEK 293 cells transfected with various mutants of PTPε were subjected to immunoprecipitation with the anti-src monoclonal antibody GD11. (lane 1) 293 cells transfected with control vector. (lane 2) 293 cells transfected with expression vector containing wild-type PTPε. (lane 3) 293 cells transfected with BCMGSneo- PTPεC334A. (lane 4) 293 cells transfected with BCMGSneo-PTPεC629A. (lane 5) 293 cells transfected with BCMGSneo-PTPεC334A/C629A.

interaction, with *src* being an *in vivo* substrate of PTPε. It should be noted that when the reciprocal experiment was carried out, immunoprecipitating PTPε and immunoblotting with the *c-src* monoclonal antibody GD11, *c-src* could not be detected (data not shown).

5.4 CrkII phosphorylation in cells expressing transmembrane PTPε

Small adapter proteins have been shown to play an important role in intra-cellular signal transduction especially in the activation of small GTP binding proteins by recruiting their activators to signal transduction complexes at the membrane. Since earlier studies have indicated that the small adapter protein GRB2 complexed with PTPε, a limited screen was launched to uncover other members which were either regulated by PTPε or formed complexes with PTPε.

Preliminary experiments had indicated that one member of the small adapter family, CrkII, but not SHC, or Nck, appeared to show changes in its phosphotyrosine content when PTPε was over-expressed in HEK 293 cells. CrkII is a 40 kDa phosphoprotein consisting of a single SH2 domain followed by two SH3 domains. While GRB2 has not been shown to be phosphorylated on tyrosyl residues CrkII is a

phosphotyrosine containing protein. Recent studies have shown that CrkII is phosphorylated in response to a number of stimuli including EGF, insulin, IGF-I and B-cell receptor activation (Hashimoto *et al.*, 1998, Okada *et al.*, 1998, Koval *et al.*, 1998, Kiyokawa *et al.*, 1997). Figure 5.4.1 shows a representative blot of five independent experiments and as can be seen in lane 2 expression of wild-type PTPε resulted in a 92%+/-2 reduction in the phosphotyrosine content of CrkII. The diminished phosphorylation of CrkII in PTPε over-expressing HEK293 cells appears to be dependent upon the

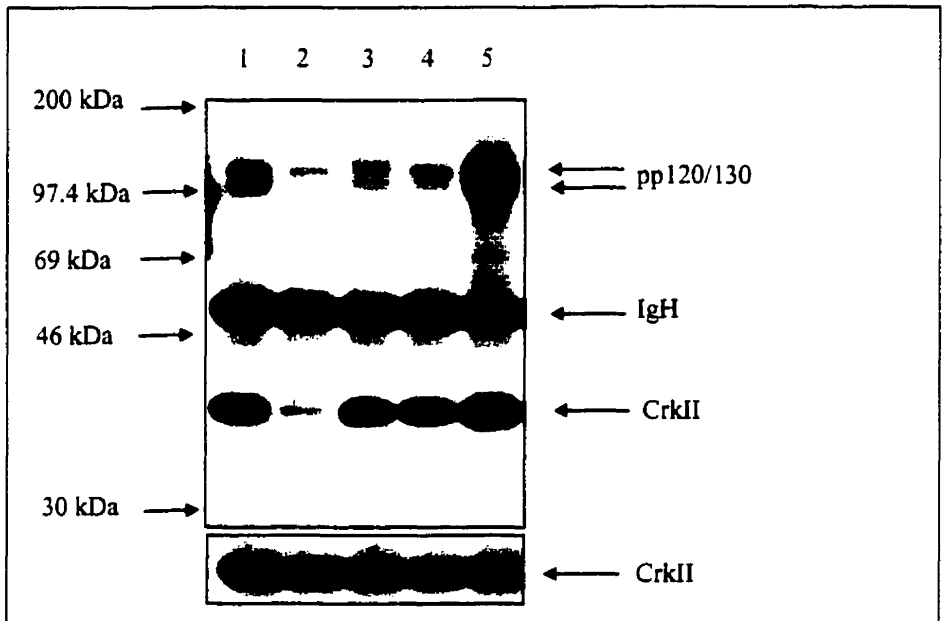

Figure 5.4.1 Modulation of CrkII phosphorylation in HEK 293 cells expressing PTPε and PTPε mutants. HEK 293 cells transfected with various mutants of PTPε were subjected to immunoprecipitation with anti-crk monoclonal antibodies.(Upper panel) (lane 1) 293 cells transfected with control vector. (lane 2) 293 cells transfected with expression vector containing wild-type PTPε. (lane 3) 293 cells transfected with BCMGSneo- PTPεC334A. (lane 4) 293 cells transfected with BCMGSneo-PTPεC629A. (lane 5) 293 cells transfected with BCMGSneo-PTPεC334A/C629A. Upper panel probed with anti-phosphotyrosine. Lower panel is the blot in upper panel stripped and reprobed with anti-crk antibodies.

presence of two active catalytic domains, as shown in figure 5.4.1 lanes 3 and 4, where CrkII tyrosine phosphorylation was essentially unchanged. The expression of the putative dominant negative mutant of PTPε may have resulted in a modest "protective" effect. The phosphotyrosine content of CrkII being increased to levels, 22%+/-9 above those of the controls in repeated experiments (figure 5.4.1 lane 5).

The arrows in figure 5.4.1 labeled p110/120 indicate the presence of high molecular weight proteins that appear to associate with CrkII. Since this immunoblot was probed with the antiphosphotyrosine antibody 4G10, this result indicated that p110 and p120 are phosphorylated on tyrosine. As can be seen in lanes 2, 3, and 4 of figure 5.4.1 the phosphotyrosine content of p110 and p120 are modulated by the presence of PTPε. To attempt to identify the associating proteins, CrkII immunoprecipitates were probed with antibodies against a number of proteins known or hypothesized to associate with CrkII, these included p130Cbl, c-Abl, Cas, and C3G (data not shown). However, none of the immunoblots were able to identify the associating proteins.

Like *src*, CrkII possesses multiple protein-protein interaction domains. To investigate whether like $pp60^{src}$, CrkII was capable of direct association with PTPε, myc tagged rat CrkII was over-expressed in HEK 293 cells already expressing wild-type PTPε and its various mutants in a stable manner. The expression vector pCAGGS-rCrkII~myc was introduced transiently into cells seeded onto fibronectin coated plates using lipofection. Figure 5.4.2 shows the expression levels of CrkII in HEK 293 expressing PTPε (lane 2), PTPεC334A (lane 3), PTPεC629A (lane 4), and PTPεC334A/C629A (lane

5) 24 hours after transfection using the anti-myc monoclonal antibody 12CA5. As can be seen, large amounts of a ~40 kDa protein reacting with anti-myc antibodies was expressed in transfected cells but not cells transfected with the empty vector. This protein is also reactive with antibodies specific for CrkII (data not shown). However, figure 5.4.5 panel B reveals that PTPε cannot be observed in 12CA5 immunoprecipitates from cells transiently over-expressing 12CA5-tagged CrkII. This observation suggested that PTPε does not form a stable association with CrkII.

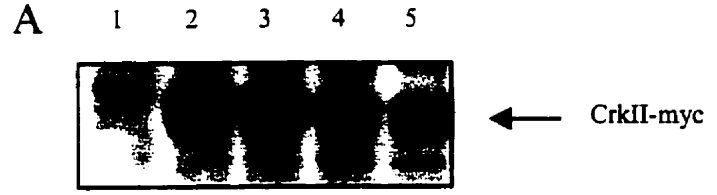

Figure 5.4.2a Over-expression of CrkII-myc with PTPε. HEK 293 cells expressing PTPε (lane 1 and lane 2), PTPεC334A (lane 3), PTPεC629A (lane 4), PTPεC334A/C629A (lane 5) were transiently transfected with either control vector (lane 1) or myc tagged CrkII (lanes 2 through 5).

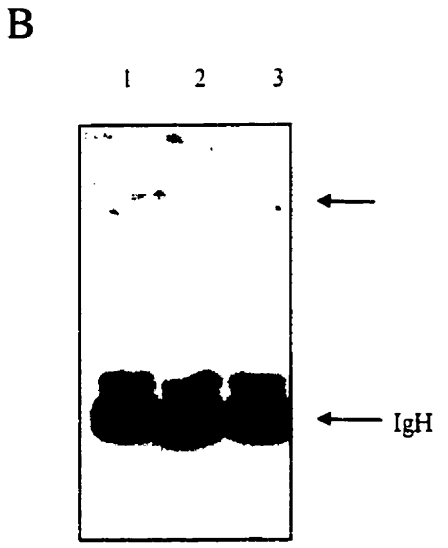

Figure 5.4.2b Association of CrkII with PTPε. HEK 293 cells expressing PTPε (lane 1), PTPεC334A/C629A (lane 2), PTPεF112P (lane 3) were transiently transfected with myc tagged CrkII. Solubilized proteins were subjected to immunoprecipitation with the 12G5 anti-myc monoclonal antibody and immunoblotted with the anti-PTPε antibody PTPε15ic.

The investigation of the effect of PTPε over-expression on HEK 293 cells suggested that this PTPase might be specific in its effects, regulating *src* family kinases and CrkII. This suggests that although PTPases in general appear to have broad substrate specificity *in vitro*, *in vivo* dephosphorylation may occur only on very specific targets, most likely governed by intracellular localization of the PTPase. This hypothesis makes investigation of the non-transmembrane isoform of PTPε of great interest since a signal

sequence, transmembrane domain, glycosylation and co-localization with membrane associated signaling molecules are precluded in the case of the non-transmembrane isoform.

Expression of the non-transmembrane isoform of PTPε (p74PTPε) was achieved in HEK 293 cells with the use of the pcDEF3 expression vector. This vector utilizes the elongation factor -1 alpha promoter (EF-1α) to obtain high level expression of PTPε as can be seen in figure 5.4.3 (*upper panel* lane 2). This figure also shows that PTPε expressed from the cDNA results in a single polypeptide migrating with an apparent molecular weight of 74 kDa. The conspicuous absence of the second species, observed in immunoprecipitates from HL60/mac cells (figure 3.3.5 lane 2), suggests that the second polypeptide may arise from a yet uncharacterized messenger RNA species. To rule out the possibility the second band of the doublet may be due to post-translational modification of the 74 kDa protein, the cDNA encoding non-transmembrane PTPε was introduced into two hemopoietic cell lines Jurkat and BaF/3. Both cell lines already express p72/74PTPε thus are capable of any post-translation modifications necessary for production of the p72 band in the p72/74 doublet. Figure 5.4.3 shows when pcDEF3-cytoPTPε is expressed in either Jurkat or BaF/3 cells an increase in the 74 kDa band of the p72/74 doublet is observed. This again suggests that the 72 kDa band of the p72/74PTPε doublet arises from an as yet uncharacterized mRNA species.

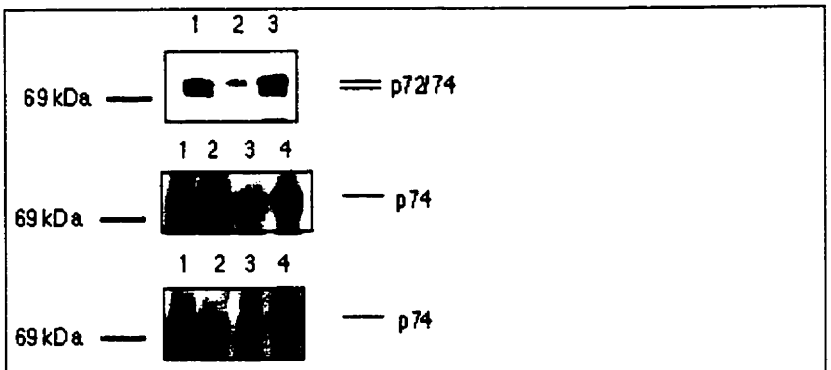

Figure 5.4.3 Transient expression of non-transmembrane PTPε in Jurkat and BaF/3 cells. (Upper panel) HL-60/mac cell lysate (lane 1) or anti-PTPε immunoprecipitation (lane 3), HEK 293 cells transiently transfected with non-transmembrane PTPε (lane 2) were immunoblotted with PTPε15ic anti-PTPε polyclonal antibody. (Middle panel) Jurkat T cell line or Baf/3 cells (Lower panel), were transiently transfected with non-transmembrane PTPε (lanes 3 and 4) cell lysate (lanes 1 and 2) and PTPε15ic immunoprecipitates were immunoblotted with anti-PTPε.

Expression of p100/110PTPε resulted in a modulation in the phosphotyrosine content of a number of signaling proteins when expressed in HEK 293 cells. To compare the impact on overall tyrosine phosphorylation of p74PTPε, anti-phosphotyrosine immunoblots were carried out on cells transiently expressing the PTPase. To assess the impact of p74PTPε on $pp60^{src}$ a demonstrated substrate of p100/110PTPε, *src* was immunoprecipitated from HEK 293 cells expressing p74PTPε and subjected to both autokinase analysis and immunoblotting with the anti-phosphotyrosine antibody 4G10. Figures 5.4.4 and figure 5.4.5 reveal that *src* autokinase activity was undiminished when p74PTPε was expressed. In addition, the phosphotyrosine content of *src* remained unchanged. The inability of p74PTPε to exhibit any effect on $pp60^{src}$ indicates that membrane localization may be essential in determining p100/110PTPε substrate preference for *src*. In addition, these results suggest that p72/74PTPε may regulate the

phosphotyrosine content of a completely different set of substrates. This observation effectively describes p72/74PTPε and p100/110PTPε as two different isoforms of the enzyme originating from a single gene. In light of these results, earlier observations describing the restricted, and mutually exclusive expression patterns of p100/110 vs p72/74 PTPε indicates a highly regulated system controlling the presence of the two very different PTPase activities. To better understand the role of p72/74PTPε its intracellular localization must be explored to determine its potential sites of action in intracellular signaling processes.

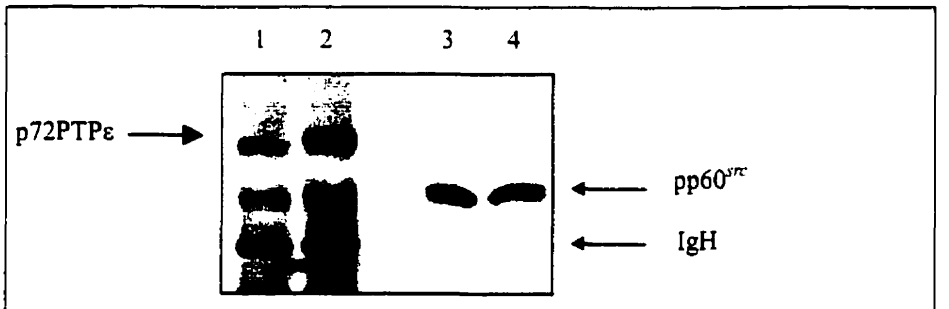

Figure 5.4.4 Phosphotyrosine content of pp60*src* in HEK 293 cells expressing non-transmembrane PTPε. HEK 293 cells were transiently transfected with non-transmembrane PTPε (lanes 2 and 4) or control vector (lanes 1 and 3). pp60^{src} was immunoprecipitated (lanes 3 and 4) anti-src polyclonal antibodies and immunoblotted with the anti-phosphotyrosine monoclonal antibody 4G10. Lanes 1 and 2 were immunoblotted with PTPε15ic.

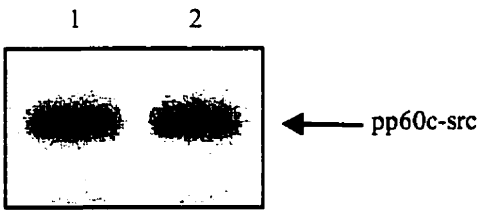

Figure 5.4.5 pp60*src* activity in HEK 293 cells expressing non-transmembrane PTPε. HEK 293 cells were transiently transfected with non-transmembrane PTPε (lanes 2) or control vector (lanes 1). $pp60^{src}$ was immunoprecipitated with anti-src polyclonal antibodies and immunoprecipitates were subjected to auto-kinase assays with $^{32}P\gamma ATP$. The phosphorylated kinase was analyzed by SDS-PAGE and autoradiography.

5.5 Localization of PTPε expressed in HEK 293 cells

The importance of intracellular compartmentalization in the understanding of cellular processes has grown significantly in recent years. Localization of proteins within the membrane is crucial to many processes ranging from the assembly of focal adhesions to aggregation, capping and internalization of the antigen receptor complexes of B-cells and T-cells (Holowkwa *et al.*, 1996, Hausen *et al.*, 1997, Kwan *et al.*, 1998, Kwiatkowska *et al.*, 1999). Identification of the molecular weight of PTPε found at the plasma membrane was determined by surface biotinylation, which labelled all transmembrane proteins located at the plasma membrane. Since PTPε was observed as a high molecular weight protein migrating with the characteristics of a glycoprotein this experiment was designed to shed some light on which isoform was actually found at the membrane. HEK 293 cells exhibiting stable expression of PTPε were grown to 80%

confluence then surface proteins labeled using NHS-LC-Biotin (N-Hydroxysuccinimidyl-Biotin) which labels primary amine groups with biotin allowing visualization with labelled avidin. After extensive neutralization of reactive biotin and repeated washing, TX100 lysates were prepared. To visualize the presence of PTPε at the outer membrane PTPε was immunoprecipitated using PTPε15ic antibodies and subjected to SDS-PAGE. After blotting to PVDF membranes, biotinylated PTPε was visualized by probing with horseradish peroxidase linked streptavidin and visualized with enhanced chemiluminescence. Figure 5.5.1 reveals that the majority of surface PTPε consists of a gp100 glycoform along with a small portion present as a possibly fully glycosylated gp110 form of PTPε. This result suggests that gp100 and gp110 isoforms of PTPε are both found on the surface of these cells.

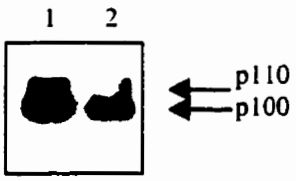

Figure 5.5.1 Surface biotinylation of HEK 293 cells expressing PTPε. HEK 293 cells expressing either wild-type PTPε (lane 1) or PTPεC334A/C629A (lane 2) were surface labeled with biotin. Cell lysates were immunoprecipitated with anti-PTPε antibodies and immunoblotted with Streptavidin linked horseradish peroxidase.

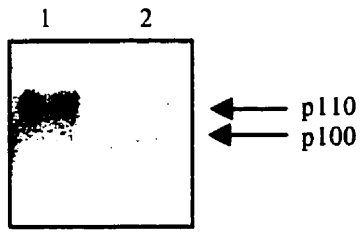

Figure 5.5.2 Phosphotyrosine content of p100/110 PTPε . The Western blot in figure 5.5.1 was stripped and reprobed with anti-phosphotyrosine monoclonal antibody 4G10. Lane 1, HEK 293 cells expressing wild-type PTPε . Lane 2 cells expressing PTPεC334A/C629A.

Interestingly, upon re-probing of this blot with anti-phosphotyrosine antibodies it appeared that only the mature gp110 was phosphorylated on tyrosine (figure 5.5.2). Indeed, transient expression experiments carried out in HEK 293 cells visualizing PTPε expression and localization by immunoflourescence revealed that PTPε was found in intracellular vesicular compartments (figure 5.5.3). Immunoblotting lysates from these cells with PTPε15ic antibodies indicated an abundance of the gp100 isoform (figure 5.1.5). These results suggested that glycosylation is potetially an important step in the biosynthesis of mature PTPε.

While surface biotinylation is a useful tool in determining whether a protein is located at the plasma membrane, and the molecular weight of the species, this technique cannot distinguish the location of the protein of interest at the inner aspect of the plasma membrane. In order to characterize the sub-cellular localization immunoflourescence is useful, cells were seeded onto fibronectin coated coverslips and, after fixation and

permeablization (with Triton X-100), stained with PTPε15ic polyclonal antibody. Immunoflourescence analysis of HEK 293 cells with stable expression of PTPε showed PTPase was concentrated at the cell surface in cell-cell junctions (figure 5.5.3). Also seen in figure 5.5.3 is the presence of intense PTPε staining in the perinuclear space and within the endoplasmic reticulum, indicating the presence of a premature form of PTPε not located at the cell surface. Interestingly, the gp110 isoform was the only form of PTPε and PTPεC334A/C629A that was phosphorylated when this mutant was over-expressed in HEK 293 cells (figure 5.5.2). This observation reiterates that not only is the gp110 isoform the mature form of PTPε in cells with stable expression of transmembrane PTPε but also in cells transiently expressing transmembrane PTPε. Figure 5.5.3 shows that transmembrane PTPε, as described earlier, was found at cell-cell junctions as well as within the perinuclear space. However, non-transmembrane PTPε, as shown in figure 5.5.3, unexpectedly exhibited the strongest immunoflourescence in the nucleus. This observation is reminiscent of the biochemical signaling of the Notch receptor. In Notch signal transduction, the receptor is cleaved by a protease at a conserved valine residue that lies close to the transmembrane domain (Schroeter *et al.*, 1998). Upon activation Notch translocates to the nucleus where interaction with the CBF1 transcription factor results in gene regulation (Jarriault *et al.*, 1995). While isoform p72/74PTPε appears to arise from a novel mRNA and not proteolytic cleavage the truncated enzyme may function in a similar manner.

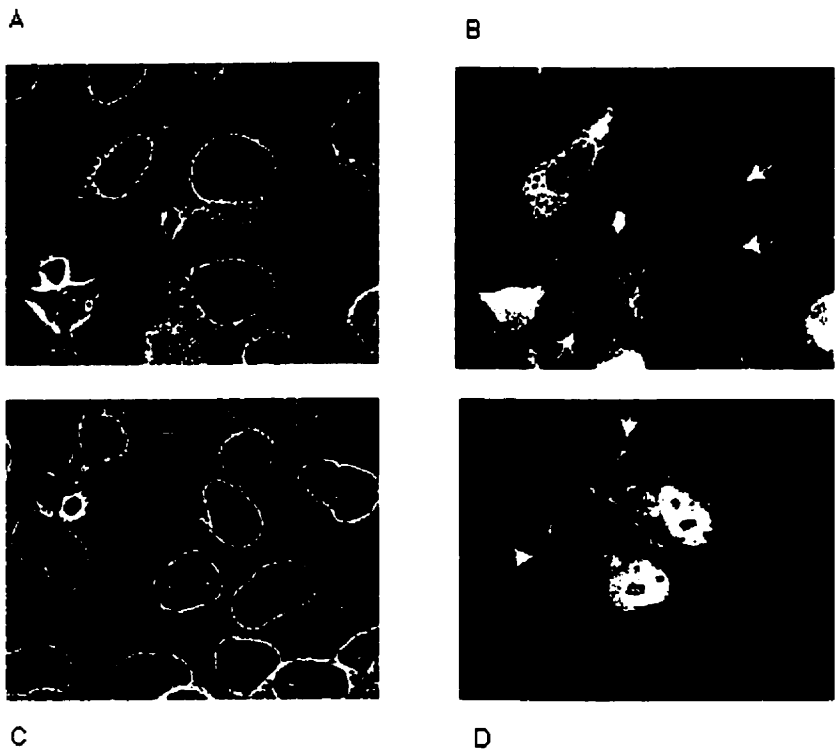

Figure 5.5.3 Immunoflourescence staining of PTPε in HEK 293 cells expressing PTPε in a stable manner. HEK 293 cells with stable expression of wild-type PTPε (panels A and B) or transient expression of non-transmembrane p74PTPε (panel C and D) were stained with PTPε15ic. PTPε sub-cellular localization was observed with FITC coupled goat anti-rabbit polyclonal antibodies and photographed under immunoflourescence. Panels A and Cshow the corresponding phase contrast photograph.

The strong immunoflourescence observed at cell-cell junctions, and at the edges of cell membranes suggested that the surface biotinylation observations described in figure 5.5.1 are valid. Immunoflourescence staining of transiently transfected HEK 293 cells with TRITC labelled phalloidin, a reageant specific for filamentous actin, revealed that non-transmembrane PTPε staining was associated with phalloidin staining filaments within the cytosol (data not shown).

Localization of an alternative spliced form of a transmembrane-cytosolic PTPase to the nucleus is a novel observation. Perhaps offering an explanation for its nuclear localization, the p72/74 sequence contains a putative bipartite nuclear localization consensus sequence within the N-terminus of the non-transmembrane isoform of PTPε (amino acids 14 to 29 RKQRKAVVSTSDKKMP). If responsible for nuclear localization this sequence is unique in that it lies within a region of the protein which is also found in the transmembrane isoform of PTPε. Thus it is likely that upon expression of the non-transmembrane isoform, due to alternative splicing or a second promoter, the signal and transmembrane domain sequences are not incorporated into the mature message, thus the nuclear localization sequence alters the distribution of the molecule. Further site directed mutagenesis experiments will be required to confirm that amino acids 14 to 29 are responsible for nuclear localization.

5.6 Significance of polyproline sequences in PTPε

Extracellular signals arriving at the membrane take the form of soluble factors, extracellular matrix components or anchored cell surface associated ligands. With the exception of G protein linked receptors where aggregation is not observed, extracellular signals then interact with receptors on the cell surface resulting in oligomerization and activation. Associated protein kinases then set in motion a cascade of phosphorylation events originating at the membrane. The resulting recruitment of signaling proteins to the site of receptor stimulation is the genesis of a complex interplay of protein-protein interactions that has only begun to be explored. With the discovery of the modular domain structure of signaling proteins, great efforts have been made to elucidate how proteins interact within signaling complexes. The list of protein interaction modules continues to grow including SH2, SH3, WW, PTB, PH, and PDZ domains, each of which maintains a specificity for a certain ligand or range of ligands with similar characteristics.

Two of these domains SH3, and WW, exhibit interesting ligand specificity. Highly specific for polyproline regions within proteins, SH3 and WW domains are able to associate with the unique left handed helix. The helix is formed by the amino acid motif PXXP, where X can be either a proline residue or a hydrophobic amino acid (Adzhubei *et al.*, 1993, Williamson 1994, Renzoni *et al.*, 1996). By careful examination of the amino acid sequences of transmembrane PTPases it was observed that certain

transmembrane PTPases possessed a polyproline motif within the membrane proximal region before the first catalytic domain of the PTPase (figure 5.6.1) (Harder, 1996).

SH3 domains or "Src homology 3 domains" were first described as regions within the *c-src* proto-oncogene that displayed significant homology with other members of the src family of protein tyrosine kinases (Sadowski *et al.*, 1986, Koch *et al.*, 1991, Pawson *et al.*, 1993, Schlessinger *et al.*, 1994). With the discovery that the SH3 domain of c-Abl had high affinities for 3BP1 and 3BP2 (Cicchetti *et al.*, 1992) polyproline sequences within proteins were shown to bind to SH3 domains. While the SH3 domain-polyproline interaction serves as a site of docking between proteins, whether this interaction plays a specific role in the regulation of enzyme activity is not completely understood. In the case of the p85 subunit of PI-3 kinase, SH3 binding is associated with enzyme activation (Pleiman *et al.*, 1994). However, in the case of c-Abl, its SH3 domain has been described to inhibit the ability of this proto-oncogene to cause transformation in cells (Jackson *et al.*, 1993). The SH3 domains of *Src* family kinases have also been shown to play a role in regulation of the kinase in cooperation with the SH2 domain through an intramolecular SH2-phosphotyrosine interaction resulting in "closing" of the active site on the kinase. Interestingly, SH3 domains appear to play a pivotal role in the formation of enzyme complexes (Okada *et al.*, 1993, Howell & Cooper, 1994, Kaplan *et al.*, 1994, Erpel *et al.*, 1995). The NADPH oxidase complex, which is involved in the production of reactive oxygen-intermediates in phagocyte activation, is one such enzyme complex, which relies upon SH3 polyproline ligand interaction (McPhail *et al.*, 1994, de Mendez *et al.*, 1996). The crystal structure of a number of SH3 domains has been solved in recent years allowing fine analysis of the mechanism of polyproline binding (Musacchio *et al.*, 1992,

Musacchio *et al.*, 1994, Lim *et al.*, 1994). Figure 5.6.2 shows the crystal structure of the Hck SH3 domain. The box highlights the binding cleft of the SH3 domain, while arrows. The ligand binding is mediated largely by hydrophobic interactions through aromatic amino acids.

PXXP containing PTPases may in fact be ligands for SH3 domain containing proteins, possibly signaling proteins. Identification of these signaling proteins could yield some insight into the signal transduction pathways regulated by transmembrane PTPases. The polyproline motifs found in certain PTPases fit the consensus for SH3 ligands and suggest the possibility that certain transmembrane PTPases may associate with other signaling molecules through an SH3-PXXP interaction. Figure 5.6.1 shows the relationship of the juxtamembrane region of a few transmembrane PTPases and SH3 binding sites of other signaling proteins. Included in the collection of PTPases that possess polyproline motifs are PTPε and PTPα. As described earlier, overexpression of PTPε was shown to result in the dephosphorylation and subsequent activation of $pp60^{src}$ (figure 5.3.1, figure 5.3.4). Overexpression of PTPα also results in dephosphorylation and activation of $pp60^{src}$ in a variety of systems (Harder 1996, den Hertog et *al.*, 1993, Zheng *et al.*, 1992). These results suggested that the polyproline region within these two PTPases may play a role in allowing a direct association of *c-src* with PTPases. This would facilitate a direct dephosphorylation event ending in the observed activation of $pp60^{src}$. However, an interesting difference was observed between the juxtamembrane sequences of PTPε and PTPα. As can be seen in figure 5.6.1, PTPα exhibits a characteristic PPLP motif. PTPα has also been demonstrated to associate with various

SH3 domains (Harder 1996). The SH3 domain of pp53/56^{lyn} showed the highest affinity, *in vitro* of those SH3 domains tested. In contrast, PTPε has the sequence FPIP, missing the critical first proline residue within the motif. In theory, the absence of the first proline residue abrogates the formation of the left-handed poly-proline helix required for efficient SH3 domain interaction. Further experiments showed that the polyproline region of PTPε is not capable of binding any of the various SH3 domains tested *in vitro* (Harder 1996). Comparison of the relative src activation observed while PTPε or PTPα was overexpressed suggested that PTPα may also be more efficient in activating pp60^{src}. The

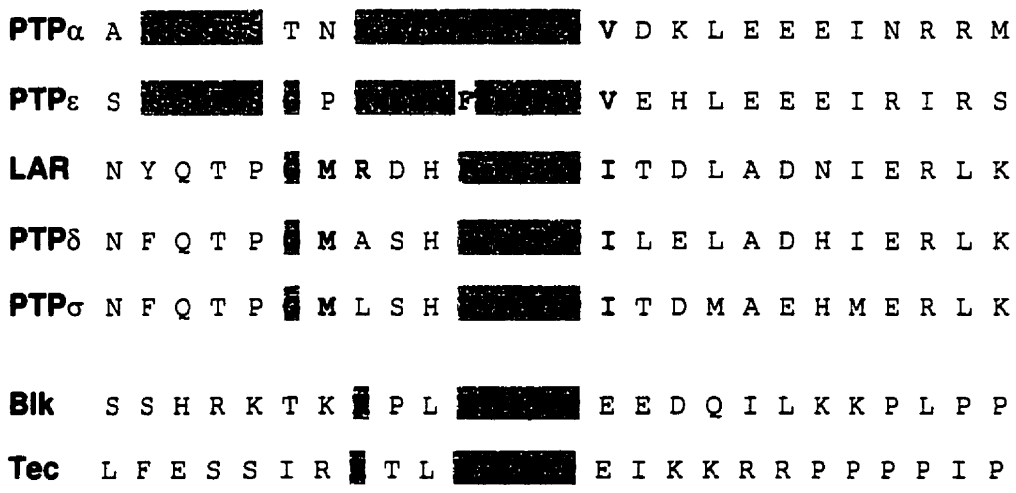

Figure 5.6.1 Alignments of membrane proximal regions of transmembrane PTPases and SH3 binding sites of other signaling molecules. Abbreviations: PTPα, protein tyrosine phosphatase alpha, PTPε protein tyrosine phosphatase epsilon, LAR, leucocyte common antigen, PTPδ, protein tyrosine phosphatase delta, PTPσ, protein tyrosine phosphatase sigma, Blk, Bruton's tyrosine kinase, Tec, tyrosine kinase expressed in hepatocellular carcinoma

question may then be asked as to whether the poly-proline region in PTPα bestows increased src dephosphorylation activity on PTPε. Furthermore, could the poly-proline

region of PTPε be modified to match that of PTPα, and if so would PTPε behave in a manner indicative of PTPα $pp60^{src}$ dephosphorylation?

To determine whether the poly-proline region within transmembrane PTPases PTPε and PTPα indeed plays a role in *c-src* dephosphorylation and activation, mutant forms of PTPε were constructed in which phenylalanine 112 (F112) was substituted with a proline residue. The resulting PTPεF112P mutant was then introduced in to the HEK 293 cell line and clones exhibiting stable expression of the mutant PTPase were examined further. The PTPεF112P mutant in effect recreates the PPIP region of the poly-proline sequence possessed by PTPα possibly restoring the putative left-handed helix formed in PTPε's close relative PTPα. The ability of PTPε to activate $pp60^{src}$ was assessed by immunoprecipitating *c-src* from cells overexpressing either wild-type PTPε or PTPεF112P mutant with the anti-src monoclonal antibody GD11. The immunoprecipitates were subjected to autokinase assay as described in materials and methods (2.20) and the phosphate incorporation assessed by SDS-PAGE and autoradiography. The rationale being PTPεF112P would be more efficient in activating *c-src* with respect to wild-type PTPε.

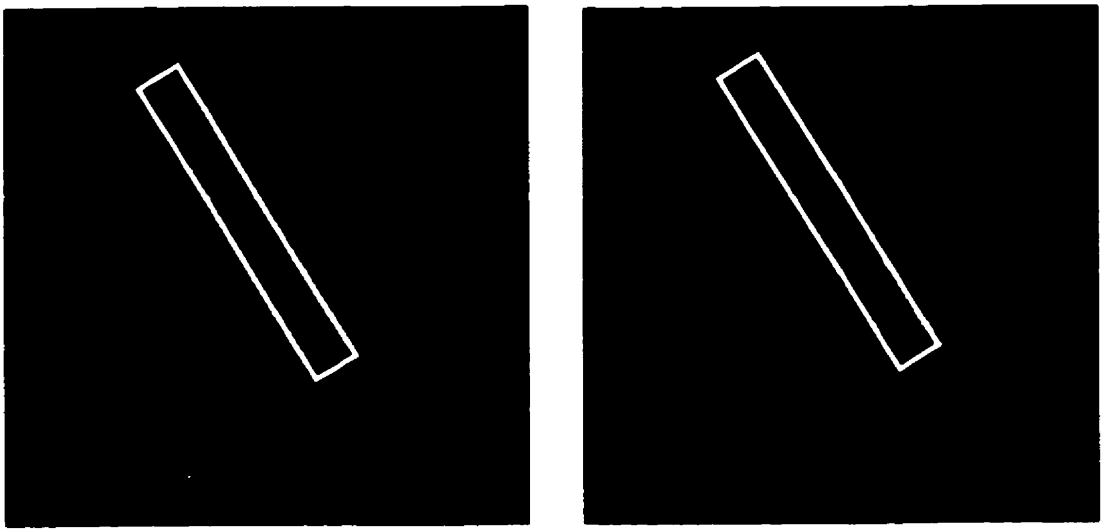

Figure 5.6.2 Space filling model (*left*), Ribbon model (*right*) of the SH3 domain of the *src* kinase family member Hck. The highlighted rectangle defines the peptide binding cleft within the SH3 domain.

5.6.1 Structural basis of F112P mutant

With the structures of both PTPα catalytic domain 1 and $pp60^{src}$ recently solved, certain predictions can be made with respect to (*i*) the structure of PTPε, (*ii*) the accessibility of the poly-proline region within the membrane proximal region of transmembrane PTPases, (iii) the structure of inactive c-src due to intramolecular folding. As can be seen in figure 5.6.3 the membrane proximal region of PTPα forms a bi-helical wedge with the poly-proline region forming the anchor points of one side of the wedge (Bilwes *et al.*, 1996). It is likely that PTPε would form a similar structure due to the very

high sequence similarity within this region in addition to conservation of side chain characteristics in areas of amino-acid substitution.

From the crystal structure of this region of PTPα, it is apparent that the poly-proline region is not buried within the protein but appears to be located on a solvent accessible surface of the protein. The crystal structure of PTPα provided evidence suggesting that the wedge formed by this region is capable of inserting into the active site of a second PTPase molecule (Bilwes *et al.*, 1996). Upon insertion, it was hypothesized that the PTPase domain would be inhibited due to displacement of potential substrates (Bilwes *et al.*, 1996). This hypothesis raises an interesting "dimerization leading to PTPase inhibition" model for transmembrane PTPases in which ligand induced dimerization would result in the PTPase in question being "turned off" (Desai *et al.*, 1993, Bilwes *et al.*, 1996). This would be the opposite of the ligand-mediated dimerization leading to activation of numerous growth factor receptor kinases and other receptors linked to kinases. The results also suggest an interesting possibility for the interaction of SH3 domains with this region, resulting in a possible conformational dissociation of the wedge from the catalytic site of the regulated PTPase, thus leading to PTPase activition. *In vitro* evidence suggested the SH3 domain of *c-src* interacted with the poly-proline region of transmembrane PTPases (*personal communication* Harder *et al.*). It is possible that the association of $pp60^{src}$ will result in dissociation of the inhibitory wedge, inducing PTPase activity. The induction of activity in turn may further activate *c-src* by dephosphorylating the C-terminal tyrosine residue. This model of PTPase-*src* interaction may describe the nature of *c-src*'s ability to constituitively co-immunoprecipitate with PTPε as well as PTPα. It may be that localization of PTPε and

PTPα to a region rich in src family kinases results in association of a fraction of the kinases with PTPε, and PTPα leading to activation of this fraction. It is conceivable that a certain level of constituitive src activity via PTPase association is maintained at the membrane at sites rich in transmembrane PTPases, especially PTPε, PTPα, and CD45. Since PTPε is localized to sites of cell-cell contact, PTPε-*src* family kinase complexes may regulate cell-cell adhesion.

Cadherin-Catenin complexes are reported to regulate cell-cell adhesion with β-catenin exhibiting exceptional *c-src* substrate characteristics *in vivo*. The morphology of HEK 293 cells expressing the dominant negative mutant of PTPε, PTPεC334A/C629A, indicated that the cell-cell vs. cell-substratum adhesion equilibrium had been altered. Cells expressing PTPεC334A/C629A in a stable fashion showed increased cell-cell adhesion and decreased cell-substratum adhesion, coinciding with a modest decrease in *c-src* tyrosine phosphorylation and activity.

5.6.2 Characterization of HEK 293 cells expressing F112P mutant

To express PTPεF112P in HEK 293 cells, the mutant cDNA was cloned into the eukaryotic vector BCMGSneo. The expression vector pBCMGSneo-PTPεF112P was then introduced into HEK 293 cells by lipofection in serum free media. Cells expressing PTPεF112P, under the control of the CMV promoter, in a stable manner were selected for in G418 at a concentration of 600 μg/ml for 7 days at limiting dilution in 96 well dishes.

Expression of PTPεF112P appeared not to be lethal since clones were readily obtained. Immunoprecipitation PTPase assays with PTPε15ic polyclonal antibodies from lysates prepared from HEK 293 cells expressing PTPεF112P showed that the mutant PTPase possessed PTPase activity (figure 5.6.4). This indicates that the F112P mutation did not alter the conformaiton of the PTPase to an extent to hinder the catalytic

Figure 5.6.3 Crystal structure of PTPα. The MP region of PTPα is shown in white, while the analogous N-terminus of PTP1B is shown in grey.

activity. Upon close observation, although HEK293 cells expressing PTPεF112P were viable, their morphological characteristics were different than control HEK293 cells and

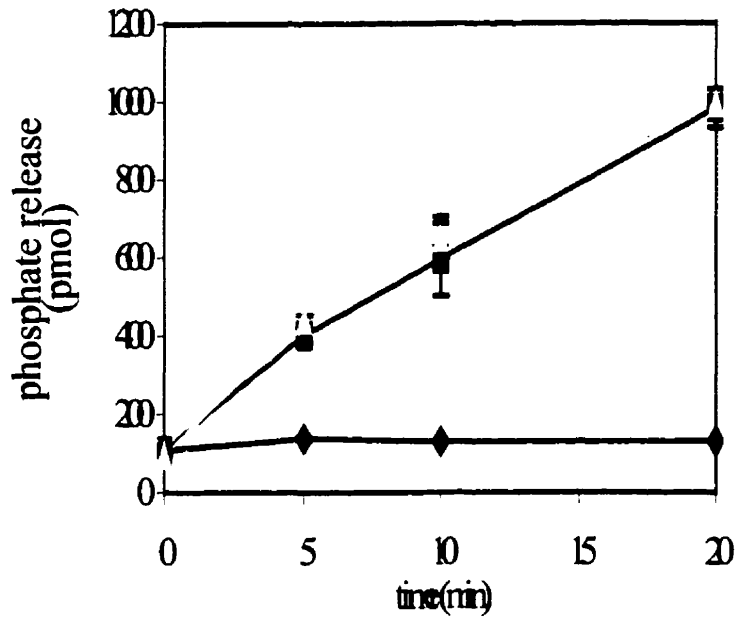

Figure 5.6.4 PTPase activity of PTPεF112P. Whole cell lysates prepared from 293 cells exhibiting stable expression of ▲ PTPεF112P, ◆ Control and ■ PTPε were subjected to immunoprecipitation with PTPε15ic polyclonal antibody. Immunoprecipitates were then subjected to MG PTPase assays. OD values were converted to pmols of PO_4 using a inorganic PO_4 calibration curve.

from 293 cells expressing wild-type PTPε. While 293 cells are adherent cells with prominent cellular processes as can be seen in figure 5.6.5, cells expressing PTPεF112P appeared to have longer, more pronounced processes as compared to those cells expressing wild-type PTPε or control cells. Although subtle, the change in cellular morphology was observed in all 293 clones expressing the F112P mutation observed. Interestingly, a report by Luttrell and Parsons also describes a similar increased prominence of cellular processes in adherent cell lines. The phenomena described was linked to an increase in *src* family kinase activity (Luttrell *et al.*, 1988).

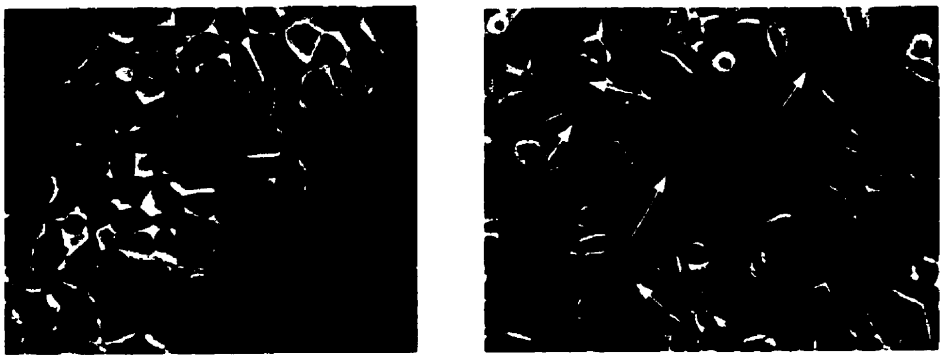

Figure 5.6.5 Cellular morphology of HEK 293 cells. Phase contrast micrographs of HEK 293 cells under normal growth conditions at 200x magnification. (*Left Panel*) Cells exhibiting stable expression of the control vector $BCMGS_{neo}$. (*Right Panel*) Cells expressing PTPεF112P. White arrows indicate spindle like cellular processes.

To determine whether the substitution of phenylalanine at position 112 for a proline residue had any impact upon the function of PTPε, immunoprecipitations of *c-src* were probed with anti-phosphotyrosine monoclonal antibody 4G10. Figure 5.6.6 reveals that *c-src* within cells expressing PTPεF112P (lane 6) possessed far less phosphotyrosine than *c-src* found in cells expressing wild-type PTPε (lane 2) or cells not expressing the PTPase (lane 1). If the dephosphorylation of *c-src* is a direct effect as suggested in section 5.6.6 this result indicates that the F112P mutation of PTPε resulted in *c-src* becoming a more prominent substrate of this PTPase. This implies that the restoration of the putative SH3 domain binding site within PTPε somehow altered the ability of PTPε to dephosphorylate *c-src*, possibly through interaction with *src*'s SH3 domain. To examine whether this phenomenon resulted in increased *c-src* activity, *src* immunoprecipitates

were assayed for autokinase activity. Figure 5.6.7 shows that PTPεF112P expression in HEK 293 cells causes not only a decrease in *c-src* phosphorylation but also a corresponding increase in *src*'s kinase activity.

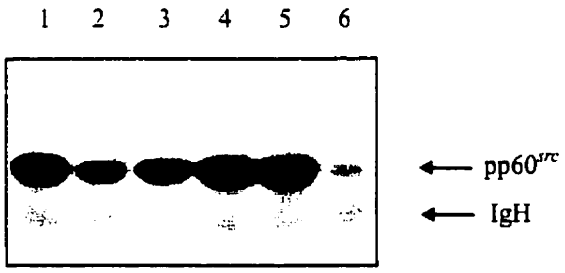

Figure 5.6.6 pp60^{src} tyrosine phosphorylation in HEK 293 cells expressing PTPεF112P mutant. HEK 293 cells transfected with various mutants of PTPε were subjected to immunoprecipitation with the anti-src monoclonal antibody GD11. (lane 1) 293 cells transfected with control vector. (lane 2) 293 cells transfected with expression vector containing wild-type PTPε. (lane 3) 293 cells transfected with BCMGSneo-PTPεC334A. (lane 4) 293 cells transfected with BCMGSneo-PTPεC629A. (lane 5) 293 cells transfected with BCMGSneo-PTPεC334A/C629A. (lane 6) HEK 293 cells transfected with BCMGSneo-PTPεF112P.

Since the C-terminal phosphorylation site is responsible for negative regulation of the family of kinases, this result suggested that, in agreement with the *in vitro* PTPase assays, that the C-terminal phosphorylation site of *src* family kinases may be an *in vivo* substrate of PTPε. The dephosphorylation of *c-src,* observed in figure 5.6.6, must also include the C-terminal regulatory phosphorylation site to bring about the increase in kinase activity observed in figure 5.6.7. It has been shown that proteins binding to the *c-src,* SH2 or SH3 domains, may also produce conformational changes that increase kinase activity. For example, binding of the *c-src* SH3 domain to a peptide fragment of the Crk-associated substrate p130^{Cas}-related protein, Sin, is sufficient to induce activation of *c-src*

(Alexandropoulos and Baltimore 1996). Similarly, binding of the human immunodeficiency virus-type 1 Nef protein to the SH3 domain of the Src family tyrosine kinase Hck increases the specific activity of the kinase in vitro (Moarefi *et al.*, 1997).

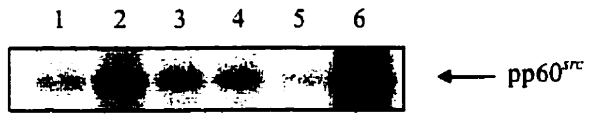

Figure 5.6.7 Activation of pp60*src* in HEK 293 cells expressing PTPεF112P mutant. RIPA buffer soluble lysates were prepared from HEK 293 cells expressing various isoforms of PTPε in a stable manner. $pp60^{src}$ was immunoprecipitated from: lane 1, cells transfected with control vector, lane 2, cells expressing wild-type PTPε, lane 3, cells expressing PTPεC334A, lane 4, cells expressing PTPεC629A, lane 5, cells expressing PTPεC334A/C629A, lane 6, cells expressing PTPεF112P, and subjected to autokinase assay.

In this context, the PTPεF112P mutant appears to have a two-fold role in the activation of *src*. First, the restoration of a putative SH3 domain may facilitate displacement of *c-src*'s SH2-SH3 domain from the C-terminal phosphotyrosine of the kinase. Secondly, this allows the PTPase to more efficiently dephosphorylate of the C-terminal phosphotyrosine of *src*, which in turn results in the kinase remaining in an active state.

In section 5.4 experiments focused upon small adaptor proteins revealed that CrkII showed decreased phosphotyrosine content in cells expressing PTPε. This result suggested that the PTPase may be directly or indirectly modulating the dephosphorylation of CrkII since the phenomenon was dependent upon the expression of

an active PTPase domain. The results observed with respect to *c-src* indicated the relationship between PTPε and CrkII should be revisited. The phosphotyrosine content of CrkII was assayed by immunoprecipitation of CrkII from cell lysates prepared from cells expressing PTPεF112P, wild-type PTPε or other mutants and immunoblotting with the anti-phosphotyrosine antibody 4G10. Figure 5.6.8 shows that indeed the F112P mutant does impact the effect of PTPε on CrkII. Lane 2 reveals that CrkII's phosphotyrosine content decreases with PTPε expression as described earlier. However, lane 6 shows that expression of PTPεF112P does not result in the dephosphorylation of CrkII as seen when wild-type PTPε is expressed.

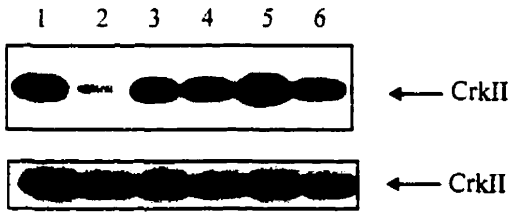

Figure 5.6.8 CrkII phosphorylation in HEK 293 cells expressing PTPεF112P. HEK 293 cells transfected with various mutants of PTPε were subjected to immunoprecipitation with anti-crk monoclonal antibodies. (Upper panel) After immunoblotting the phosphotyrosine content of CrkII was observed with 4G10 immunoblotting. (lane 1) 293 cells transfected with control vector. (lane 2) 293 cells transfected with expression vector containing wild-type PTPε. (lane 3) 293 cells transfected with BCMGSneo-PTPεC334A. (lane 4) 293 cells transfected with BCMGSneo-PTPεC629A. (lane 5) 293 cells transfected with BCMGSneo-PTPεC334A/C629A. Lower panel is the blot in the upper panel stripped and reprobed with anti-Crk antibodies.

These observations suggested that the substitution of phenylalanine residue at position 112 for a proline residue, resulted in restoration of a putative SH3 domain ligand. The substitution also altered the substrate specificity of PTPε while not disrupting, in any measurable way, PTPase activity. While a complete account of the

mechanism responsible for this phenomenon is beyond the scope of this thesis. The ability of a single amino acid substitution to significantly alter the phenotype of a PTPase warrants further study.

5.7 Summary

By utilizing cDNAs encoding both transmembrane and non-transmembrane isforms of PTPε, the different forms of this PTPase were introduced into mammalian cells. In the case of transmembrane PTPε, various mutants were characterized *in vivo*. These studies revealed that p100/110PTPε is a highly glycosylated membrane protein, found predominantly at cell-cell junctions. While p100/110PTPε was capable of associating with and modulating the phosphotyrosine content and kinase activity of the *src* family kinase members $pp60^{c\text{-}src}$ and $pp59^{fyn}$, p72/74PTPε was not. This phenomenon was probably in large part due to the localization of p72/74PTPε to the nucleus and not the plasma membrane where *src* family kinases are found. Finally, by the introduction of a proline residue at position F112, an SH3 domain-binding site was reconstituted, thus turning PTPε into a PTPα-like molecule. PTPεF112P exhibited altered substrate specificity showing increased activity towards *src* family kinases and reduced activity towards the *in vivo* substrate CrkII. These findings are summarized in figure 5.7.1.

	PTPε	PTPε C334A	PTPε C629A	PTPεC334A /C629A	PTPε F112P	P74PTPε
Morphological changes	++			+++	++	
Cytosolic						++
Nuclear						+++
Membrane associated	+++	+++	+++	+++	+++	+
Src dephosphorylation	++	+		-	+++	
Fyn dephosphorylation	++	+		-		
Lyn dephosphorylation	+					
CrkII dephosphorylation	+++	+	+	-	-	

Figure 5.7.1 Summary of *in vivo* observations with p100/110PTPε , p74PTPε and the various mutants. Plus signs indicate intensity of effect or magnitude of observation on a scale of one to three. Minus sign indicates opposing effect

Chapter 6

Discussion

The roles of protein tyrosine phosphatases in the regulation of cell growth, differentiation and cell adhesion, with a few exceptions, are still relatively poorly understood. This thesis has endeavored to shed some light on the roles of PTPases in cellular regulation by asking the question which PTPases are upregulated in cells of the monocyte/macrophage lineage in response to the pro-inflammatory stimuli IFNγ. Since cells of the monocyte/macrophage lineage play a large role in the process of inflammation, they may be a prime target system to search for novel methods of intervention for treatment of certain inflammatory diseases. A novel PCR based screening system was developed and PTPε was isolated as a candidate PTPase. The aim of this thesis then focused on the characterization of PTPε in hemopoietic and non-hemopoietic cells. This involved the production of recombinant forms of PTPε to investigate the activity and substrate specificity of PTPε in comparison to PTPα and

CD45, PTPases that share relatively high sequence similarity to PTPε. In studying both hemopoietic and non-hemopoietic cells a novel 72/74 kDa isoform of PTPε was discovered in hemopoietic cells. The analysis involved the development of novel techniques including mass spectrometric analysis of tryptic peptides and MS/MS sequencing leading to its isolation and characterization. The study of PTPε in non-hemopoietic cells required the expression of the enzyme in mammalian cells and necessitated the development of novel reagents including antibodies and mutant forms of the enzyme. PTPε expression in mammalian cells resulted in a number of insights in to the functions of PTPε in cells as well as possible *in vivo* substrates and signal transduction mechanisms of the PTPase.

6.1 Upregulation of PTPε in cells of the monocyte/macrophage lineage. Using degenerate oligonucleotides and cDNA prepared from IFNγ stimulated RAW 264.7 cells, a murine peritoneal macrophage cell line, PCR fragments of the catalytic domains of PTPases were purified. The fragments were immobilized and subjected to hybridization with labeled PCR fragments from unstimulated cells. The screen resulted in the identification of CD45, PTPα, PTP1B and PTPε as candidate PTPases. The identification of PTPε in this screen indicated this PTPase was expressed and possibly regulated in hemopoietic cells. Vanadate treatment also resulted in upregulation of PTPε message. This experiment suggested the involvement an unknown PTK in PTPε message regulation in response to LPS or IFNγ. In light of the accepted intracellular signal transduction mechanism of IFNγ it may be suggested that Jak1 and Jak3 may be the

targets of vanadate if indeed the PTPε promoter were found to possess an ISGF3/STAT1 binding site. Future studies will undoubtedly uncover the answers to these questions.

Filter hybridization analysis of mRNA purified from HL-60 cells revealed transcripts of ~6.5 kb, ~2.1 kb and ~1.8 kb hybridizing to the PTPε cDNA sequences (Seimiya *et al.*, 1995; Elson and Leder, 1995b). Similar transcript heterogeneity was observed in MEL cells treated with various stimuli (Kume *et al.*, 1994). In addition, evidence of as many as four different transcripts was obtained from analysis of various mouse mammary tumor lines (Elson and Leder, 1995a). Our study has also described the PTPε mRNA heterogeneity as well as regulation of message levels by the pro-inflammatory stimuli. The numerous PTPε-hybridizing transcripts likely arise as a result of alternative splicing of one gene, as *in situ* hybridization revealed only a single chromosomal position, 10q26, for *PTPRE* (Melhado *et al.*, 1996, Maagdenberg *et al.*, 1995)[3]. LPS and IFNγ stimulation regulated PTPε production at the post-transcriptional level in HL-60 cells. In response to IFNγ or LPS increased proteins levels were not observed, although message levels showed a 16-fold induction over a twenty hour period. In contrast to LPS, IFNγ and MCP-1 other pro-inflammatory stimuli had little effect on PTPε messenger RNA indicating that the PTPε promoter may be restricted in the stimuli that result in induction of message. This was not the case when HL-60 cells were exposed to phorbol esters where both mRNA as well as protein levels increased within 3 hours of stimulation.

While LPS and IFNγ signals originate at the plasma membrane with CD14 and the IFNγ-R respectively, PMA intercalates into the plasma membrane independent of receptor binding and activates PKC. LPS and IFNγ stimulation result in a defined intracellular signal transduction cascade, giving rise to the respective effects of the two stimuli. PMA stimulation would result in the activation of a number of different signal transduction cascades. It could be for this reason that PMA stimulation provides all the necessary signals for PTPε upregulation simultaneously, while LPS and IFNγ require a sequential signal cascade resulting in the activation of the proper kinases and transcription factors for PTPε promoter activation.

The mechanisms of mRNA induction by the various stimuli as well as the post-transcriptional regulation while an interesting phenomenon were beyond the scope of this thesis.

6.2 PTPε, PTPα and CD45. Protein tyrosine kinases have been shown to phosphorylate specific substrates *in vivo* and *in vitro* (Tan *et al.*, 1993, Milarski *et al.*, 1993, Lammers *et al.*, 1997, Ahmad *et al.*, 1997). To determine whether PTPases would display substrate specificity, recombinant PTPε, PTPα, and CD45 proteins were prepared using the pGEX prokaryotic expression system. Using a glutathione affinity matrix, the proteins were purified to greater than 95% purity as judged by SDS-PAGE. The enzymatic activities of the PTPases were examined using a panel of synthetic phosphopeptide substrates compiled from known regulatory phosphorylation sites of signaling proteins. The analysis used excess substrate and enzyme concentrations that allow less than 10% of the

substrate to be converted to the non-phosphorylated form to avoid end-product inhibition effects. In addition, reaction times were used that measure the initial rate of substrate turn over. PTPε, PTPα, CD45 and native immunoprecipitated p72/74PTPε were subjected to kinetic analysis. The plot in figure 4.3.1 revealed a parabolic curve of PTPase activity in response to increasing pH. The relatively acidic pH optima indicates that the PTPase was most efficient when an atom within the catalytic site is in a deprotonated state. The pKa of the sulfhydryl group of a cysteine residue is very close to the pH optima of PTPε suggesting that the deprotonation of the catalytically essential cysteine residue within the active site is most likely crucial for catalysis of phosphotyrosine. However, the pH optima curve of PTPε after pH 5.8 does not plateau but enters a phase of decreasing activity with increasing pH indicating that as another atom within the active site becomes protonated it is less able to participate in the catalysis of phosphotyrosine to tyrosine.

The following phosphopeptides, tyrosine 1009 an auto-phosphorylation site of the platelet-derived growth factor receptor (PDGF-R) (van der Geer *et al.*, 1994) ($PDGFR^{Y1009}$), tyrosine 1021 of the PDGFR ($PDGFR^{Y1021}$), tyrosine 527 of the c-src proto-oncogene (src^{Y527}) (Cooper and Howell, 1993), and the carboxy-terminal tyrosine of the p59/64$^{c\text{-}hck}$ *src* family PTK (Ziegler *et al.*,1987), hck^{Y501} were found to be suitable PTPε substrates for PTPε. The aforementioned substrates displayed V_{max}/k_m values of 2.5, 4.2, 2.5, 0.8. In general, PTPε showed no activity towards a number of peptides which LAR and CD45 were able to dephosphorylate with high efficiency. Those substrates which were particularly poor for PTPε, but good for LAR or CD45, include

PDGF-R^{Y857} and CSF1-R^{Y708}. These results suggested that PTPε may exhibit more restricted substrate specificity than LAR or CD45 *in vitro*, however, analysis of a larger panel of synthetic substrates would be required to validate such a determination. Peptides based on the interferon-receptor alpha-chain (IFNγ-Rα) STAT1 binding site (Farrar and Schreiber, 1993), IFNγ-Rα^{Y440}, and a phosphorylation site on STAT1 (Shuai *et al.*, 1993), STAT91^{Y701} were relatively poor substrates in the phosphatase assay. Indeed, p72/74 released only trace amounts of phosphate from the STAT91^{Y701} phosphopeptide.

While the number of different phosphopeptides used was small, there was sufficient variation between the peptide substrates that clear trends were present regarding the substrate preferences of p72/74. PDGF-R^{Y1021} appeared to be the best substrate of the panel of 5 substrates tested with *src*^{Y527}, *hck*^{Y501}, Stat91^{Y701}, IFNγ-R^{Y440} falling in the order listed. The ranking observed with the native enzyme was similar to that of the recombinant PTPε where the substrate specificity could be described with kinetic parameters. PTPε appears to prefer negatively charged residues to the amino-terminal side of the phosphotyrosine moiety, and an absence of positively charged residues at the carboxyl-terminal side. Similar results were obtained from native p72/74PTPε in immunoprecipitation PTPase experiments. . Figure 4.6.3 shows a definite preference for acidic, or residues with polar side chains containing oxygen N-terminal to the phosphotyrosine. However, non-polar, or helix breaking residues such as proline were less tolerated. The region C terminus to the phosphotyrosine residue appeared less critical with only basic residues appearing to have deleterious affects to PTPase activity. This suggests that recombinant PTPε is a suitable source of purified protein for *in vitro*

studies. Such preferences would be consistent with observations made in similar analyses of several different PTPases (Cho *et al.*, 1993; Ruzzene *et al.*, 1993; Zhang *et al.*, 1993; Harder *et al.*, 1994; Dechert *et al.*, 1994). However, additional studies employing a wider panel of substrates, and quantities of enzyme sufficient to allow kinetic analysis, will be required for a more detailed picture of the *in vitro* substrate preference of p72/74. The amount of useful information to be gained from further *in vitro* studies would likely be minimal due to the general ability of PTPases to catalyze the release of phosphate from even the poorest synthetic substrates. *In vitro* studies to date suggest that PTPases choose substrates not only by the binding preferences of the catalytic site but by other substrate binding sites located elsewhere on the molecule. However, the peptides used lack a definable secondary or tertiary structure and are unable to extend outside of the catalytic pocket of the enzyme. This may provide a partial explanation of generic nature of the synthetic substrates used as determined by the poor k_m values observed in comparison with protein kinases. It may be that protein kinases contain much of the substrate specificity information within the catalytic domain of the enzyme, possibly the substrate-binding pocket itself. In contrast the majority of PTPase substrate specificty may be determined by sequences outside of the substrate-binding pocket, possibly at adjacent sites within the catalytic domain or other sites of the protein. This may explain the very high amino acid conservation between PTPases within the catalytic site, highlighting the generic nature of the catalytic activity, whereas outside the catalytic domain PTPases diverge quite drastically.

6.3 Expression of transmembrane and non transmembrane PTPε. To characterize PTPε function, a variety of reagents were developed. These included high affinity specific polyclonal antibodies, the cDNA encoding non-transmembrane PTPε and point mutated cDNAs generated by site directed mutagenesis. The point mutated forms of the transmembrane enzyme lack the catalytically essential cysteine residue in either or both of the catalytic domains. In addition, a novel mutant was generated replacing phenyalanine 112 with a proline residue restoring a putative SH3 binding site first observed in PTPα and homologues.

Expression of the wild-type PTPε cDNA in 293 cells gave rise to a 100/110 kDa protein doublet as observed when cell lysates were immunoblotted with anti-PTPε antisera. The 100/110 kDa protein also immunoprecipitated with anti-PTPε antibodies and exhibited PTPase activity when immunoprecipitated. The migration pattern, observed by SDS-PAGE electrophoresis, of p100/110PTPε was characteristic of a protein containing significant carbohydrate structures. Indeed, the observed molecular weight of the transmembrane isoform is approximately 50 kDa greater than the predicted molecular weight deduced from the primary proteins sequence. Immunoflourescence microscopy analysis revealed that PTPε was located at the plasma membrane and in high concentration at cell-cell junctions. This cellular localization pattern suggests that PTPε may play a role in regulating the tight junctions or adherens junctions. Indeed, *src* has been shown to play a role in regulating cadherin function (Matsuyoshi *et al.*, 1992). In light of the *in vitro* substrate specificity results discussed earlier PTPε may play a role in the regulation of *src* family kinases.

The truncated cDNA proved extremely useful, giving rise to a single 74 kDa band, the p74 isoform of PTPε when expressed in mammalian cells. The absence of the 72 kDa protein observed in HL-60 cells with phorbol-ester induced differentiation, when this cDNA was expressed, indicates that the p72 isoform is probably the product of an additional messenger RNA species. This isoform was localized to the nucleus as well as associated with actin bundles within the cytosol. The subcellular localization of p74PTPε suggests that the two isoforms behave differently in cellular signal transduction. An assessment of $pp60^{c\text{-}src}$ tyrosine phosphorylation and kinase activity revealed that while expression of the transmembrane isoform resulted in dephosphorylation and increased kinase activity, when the non-transmembrane isoform was expressed there was no change in *c-src*. This observation highlights the potential complexity of PTPε function in signal transduction systems.

It was hypothesized that a single PTPε gene gives rise to similar proteins with identical catalytic domain sequences that carry out different functions and have different substrates. In the case of PTPases, cellular localization appears to be the determining factor of substrate specificity. A single PTPase may be localized to a variety of potential molecular complexes at a number sites within the cell. At any given site, there may be a completely different population of suitable substrates. This provides one explanation of why *in vitro* PTPase assays revealed very similar synthetic substrate preference profiles between different PTPases. This also suggests that not only the substrate-binding pocket determines the substrate specificity but also other sequences, and in certain instances

perhaps the entire protein plays some role in substrate recognition and association. Thus the paradigm of one enzyme, one function, one substrate may only be true for enzymes in less complex systems such as metabolic pathways. However, this may be invalid for enzymes involved in systems with high degrees of complexity, such as regulatory pathways within biological systems. Biological systems require coordinate communication between multiple pathways. High degree of cross-talk necessity to achieve the degree of regulation required for the organization a multicellular organism. This may be achieved with an economy of effort by reuse of regulatory proteins in different signal transduction systems.

6.4 PTPε signal transduction. Expression of PTPε and its mutants in eukaryotic cells gave rise to both morphological changes as well as biochemical changes. PTPε appeared to be glycosylated, which seemed to be important for the biosynthesis of the transmembrane isoform of PTPε. An initial glycosylation event gives rise to the non-heterogeneous gp100 isoform or "core protein". In a second glycosylation event the mature heterogeneous gp110 protein is produced and transported to its compartment on the cell surface. At the plasma membrane suitable upstream regulators, including PTKs and substrates, are also co-localized. It well be that glycosylation is utilized as a regulatory step controlling the amount of PTPε available at particular sites within the membrane. Indeed, immunoflourescence experiments showed intracellular vacuoles of PTPε and only the p100 isoform could be detected in transiently transfected HEK 293 cells. A possible explanation for this observation is that the intracellular machinery

responsible was not in place for the glycosylation of PTPε resulting in its transport to the cell surface.

Expression of wild type PTPε as well as its mutants resulted in six significant observable changes. First, the phosphotyrosine profile of cells expressing PTPε showed decreased phosphorylation of a number of proteins within the 40 kDa and 60 kDa ranges. Secondly, cells expressing wild-type PTPε displayed long spindle-like cellular process and a reduced number of cell-cell contacts. Thirdly, $pp60^{c\text{-}src}$ showed a decrease in tyrosine phosphorylation and a modest increase in kinase activity only in those cells expressing wild-type PTPε. Cells expressing mutant forms of PTPε where either catalytic domain was compromised, phosphorylation and kinase activity of *c-src* showed little change. However, in cells expressing the PTPεC334A/C629A mutant, where both catalytic domains were compromised, there was no detectable change in cell survival as compared to vector control. This indicated that ectopic expression of potential dominant negative forms of PTPε was not toxic to these cells. PTPε may not impinge upon any signal transduction pathways essential for cell survival. While cell survival was normal, intracellular changes were detected. *c-src* showed a modest but reproducible increase in tyrosine phosphorylation and decrease in respective kinase activity. The family of *src* protein tyrosine kinases share the same protein domain structure as well as very high sequence similarity. As shown in figure 6.1, *src* family members also share a tyrosine residue in the C-terminal region of the kinases. A key regulatory site, when phosphorylated either through auto-phosphorylation or phosphorylation by *csk* dramatically inhibits kinase activity. While all family members share this site, the amino acid sequence around this site is variable, and falls into two subfamilies. The first

subfamily contains the sequence PQYQPGENL and includes *src*, *yes*, *fyn*, and to a certain extent *fgr*. The second subfamily is defined by the sequence GQYQQQP with *lck*, *hck*, *lyn*, and (to a lesser extent) *blk* as its family members. PTPε was capable of causing a decrease in the phosphotyrosine content of *fyn* to the same extent as *src*. However, PTPε was not capable of mediating a decrease in the phosphotyrosine content of *lyn*. This observation indicated that if indeed the dephosphorylation of *src* family members is an event mediated directly by PTPε, then this PTPase may be restricted to preferencially regulating the phosphorylation of the PQYQPGENL subfamily of *src* family kinases. Co-immunoprecipitation experiments also suggested that the changes in *c-src* phosphorylation and subsequent activity might be a direct effect, revealing a stable association between $pp60^{c\text{-}src}$ and PTPε. However, when immunoprecipitating PTPε and immunoblotting for *src* an association could not be detected. A number of explanations are available to account for the inability of the reciprocal experiment to work. The poor immunoblotting efficiency of the monoclonal antibody may prohibit the approach of

src	T	S	T	E	P	Q	**Y**	Q	P	G	E	N	L
yes	T	A	T	E	P	Q	**Y**	Q	P	G	E	N	L
fyn	T	A	T	E	P	Q	**Y**	Q	P	G	E	N	L
fgr	T	S	A	E	P	Q	**Y**	Q	P	G	D	Q	T
lyn	T	A	T	E	G	Q	**Y**	Q	Q	Q	P		
hck	T	A	T	E	S	Q	**Y**	Q	Q	Q	P		
lck	T	A	T	E	G	Q	**Y**	Q	P	Q	P		
blk	T	A	T	E	P	Q	**Y**	E	L	Q	P		

Figure 6.1 Homology between C-terminal regions of *src* family members. The tyrosine residue in bold and underlined denotes the C-terminal regulatory phosphorylation site within the *src* family of protein tyrosine kinases.

immunoblotting for *c-src*. In addition, the actual contact points of the *c-src* molecule are not known, thus there is a possibility that the anti-PTPε polyclonal antibody may somehow disrupt the interaction. In any event, the functional evidence in cooperation with the detection of PTPε in *c-src* immunoprecipitates, indicate a strong likelihood that the two proteins do associate *in vivo*.

Fourthly, the small adapter protein CrkII mirrored the tyrosine phosphorylation of *c-src*. Cells transfected with wild-type PTPε showed a decrease in CrkII phosphorylation. However, cells expressing PTPεC334A, PTPεC629A, or PTPεC334A/C629A, which have either catalytic domain mutated or both, showed little change in CrkII tyrosine phosphorylation. Moreover, cells expressing PTPεC334A/C629A exhibited a modest but reproducible increase in CrkII tyrosine phosphorylation. Whether this phenomenon was a direct effect of PTPε tyrosine dephosphorylation of CrkII, or an indirect effect of PTPε expression activating an unknown signaling pathway resulting in CrkII dephosphorylation or inhibition of phosphorylation is unclear. Co-immunoprecipitation experiments indicated that PTPε and CrkII, unlike PTPε and *c-src*, did not form a stable physical association. However, those experiments did not rule out the possibility that CrkII is a physiological substrate of PTPε and the two proteins merely form a transient complex.

The significance of $pp60^{c\text{-}src}$, and CrkII dephosphorylation remains unclear. *Src* has been demonstrated to play a role in cellular adhesion (Matsuyoshi *et al.*, 1992) with the participation of PTPα possibly through the regulation of focal adhesions (Harder *et*

al., personal communication). Observations presented here describe a role for PTPε, PTPαs close relative, in cell-cell junctions. *Src* has also been shown to play a role at the sites of cellular contact through phosphorylation of E-Cadherin and β-catenin and subsequent regulation of cell-cell interactions including invasiveness of carcinoma cells while CrkII has not (Behrens *et al.*, 1993). Again the possibility exists that there are multiple pools of PTPε at the plasma membrane that have different substrates. PTPε may dephosphorylate both *c-src* and CrkII under certain physiological conditions within various pools, however, the two events are mutually exclusive since the proteins would be separated spatially and involved in different signaling pathways. At any given site, there may be a completely different population of suitable substrates.

The fifth significant difference involved expression of PTPεC334A/C629A, the mutant form of the PTPase in which both catalytic domains have had the essential cysteine residue converted to alanine, resulted in a significant morphological change. Expression of the mutant PTPase incapable of catalyzing the release of free phosphate from its substrates resulted in the mammalian cells adhering poorly to the substratum. Additionally, PTPεC334A/C629A expressing cells adhered very tightly to other cells and appeared in capable of spreading out to populate the entire culture dish. The transfected cells grew in large elongated clumps maintaining cellular contact between clumps. From these observations, it may be suggested that PTPε indeed may influence cellular adhesion. PTPε may possibly be regulating these cellular functions through dephosphorylating structural or regulatory proteins found at cell-cell junctions or cell-substratum adhesion sites. The role of PTPases in cellular adhesion is not a novel

concept, recent reports have demonstrated the role of transmembrane PTPases LAR, and RPTPβ as well as PTPζ and PTPδ in homotypic adhesion (Kypta *et al.*, 1996, Peles *et al.*, 1998). The immunoflourescence results indicating a large proportion of PTPε is localized to cell-cell contact points serves to strengthen the argument. When observed closely, cells expressing wild-type PTPε appeared to maintain very few cellular contacts compared to the parental cell line. In addition to few cellular contacts, cells expressing wild-type PTPε appeared to spread out, and populate the entire culture dish. These observations may be interpreted in a number of ways. However, the most likely interpretation places PTPε somewhere at the membrane within cell-cell adhesion complexes. In this light, active PTPε may amplify the normal signal originating from adherens junctions resulting in fewer physical cell-cell contacts yielding the same signal necessary for survival. Alternatively, hyper-expression of active PTPε may result in hypo-phosphorylation of key proteins with complexes located and cell-cell contacts resulting in the dismantling of cell-cell adhesion complexes.

Consistent with this model, the morphology of cell lines expressing PTPεC334A/C629A appears to strengthen the hypothesis, suggesting the signal emanating from cell-cell contacts, presumably through cadherin-catenin interaction, was either muted by the interfering dominant negative PTPε mutant or substrates whose phosphorylation results in dissolution of adhesion complexes were protected. Hence, the atypical cell-cell adhesion and clumping morphology may represent a cellular response to provide adequate signaling from cell-cell junctions for survival. A recent link between PTPase activity and cell-cell junction regulation through N-cadherin as well as E-

Cadherin has been reported (Burden-Gulley *et al.*, 1999, Hiscox *et al.*, 1998). Keratinocytes treated with pervanadate, exhibited a major change in cellular morphology and cadherin/catenin localization. The latter molecules were no longer observed to co-localize with the actin cytoskeleton of cells, and the amount of E-cadherin bound to the cytoskeleton decreased. A more intense phosphotyrosine labeling was apparent at the edges of the treated cells, which suggested that an increase in the phosphorylation rate of some cadherin-catenin complex proteins induced a diminished intercellular adhesion. Immunoprecipitation experiments of the E-cadherin/catenin complex from pervanadate treated keratinocytes revealed an increase in the tyrosine phosphorylation rate of E-cadherin, beta catenin and probably gamma catenin (Soler *et al.*, 1998). This report suggested an essential role for protein tyrosine phosphatase in intercellular junctions (Soler *et al.*, 1998).

The sixth and final observable difference was potentially the most interesting. Following upon observations previously made in our laboratory the polyproline region found within the juxtamembrane region of PTPε was targeted for further study. While PTPα has a primary amino acid sequence of PPLP within this region PTPε is conspicuously lacking the first proline within this motif, FPIP. Earlier work has shown that the polyproline region within PTPα was a ligand for SH3 domains. Previous work had also shown the absolute requirement for the first proline residue within this sequence for binding of conventional SH3 domains. The question then arises, why has PTPε diverged from PTPα so specifically at the polyproline motif? While this question was beyond the scope of this body of work, the ramifications of this amino acid substitution

on the signaling properties were not. To shed some light on the possible functions of this region, the phenylalanine 112 residue within PTPε was converted to a proline residue. This site directed mutant restored the polyproline motif as identified in PTPα but in the context of PTPε. When introduced into mammalian cells PTPεF112P appeared to alter the substrate specificity of PTPε *in vivo*. The PTPεF112P mutant, although fully retaining PTPase activity, did not dephosphorylate CrkII. In contrast, PTPεF112P appeared more capable of dephosphorylating $pp60^{c\text{-}src}$. The increased activity on *c-src* resulted in a dramatic increase in kinase activity, as observed by *in vitro* autokinase assays. This result suggested that the polyproline regions within PTPε, and PTPα somehow play a role in substrate determination. While many mechanisms could be postulated, two are most likely. First, the polyproline region serves as a contact point between enzyme and substrate. In the case of $pp60^{c\text{-}src}$, the polyproline region of PTPε may transiently interact with the SH3 domain in the N-terminal region of *c-src* changing the conformation of the substrate to provide access to the phosphotyrosine. By altering this region, one alters the affinity of the enzyme for the substrate leading to a shift in substrate specificity between two competing substrates. The second is, by altering a putative SH3 binding site the SH3 domain which associates with this site at the plasma membrane, is no longer able to recruit the PTPε to a specific pool where CrkII is localized. The subtle shift in PTPε distribution would result in CrkII retaining the tyrosine phosphate it would have had if PTPε were not expressed and giving the appearance that the substrate specificity of PTPε had been altered by the mutation. Either scenario may be applicable or a combination of both may be applicable. The similarities between PTPε and PTPα are striking, but the regions where amino acid identity break down are equally interesting. The respective

extracellular domains and juxtamembrane regions are the two notable regions. The less than 10% similarity of the PTPε and PTPε extracellular domains as well as the amino acid substitution at F112 in PTPε appear to mark an evolutionary fork where two very similar PTPases diverged in their intracellular functions.

To date, only the family of stress induced PTPases such as PAC-1, CL100 and MKP1 have been have been shown to be regulated by similar stimuli and localized to the nucleus. Our observations suggest that PTPε may also be included in this family of induced nuclear PTPases. However it is unlikely that nuclear PTPε regulates similar substrates as the dual specificity PTPases. Identification of the STAT (signal transducers and activators of transcription) family of tyrosine phosphorylated transcription factors, which function in a number of cytokine signal transduction pathways including the interferon signaling pathway (Fu *et al.*, 1992, David *et al.*, 1993), raises the possibility that nuclear PTPases may play active roles in regulating gene expression either through regulating the phosphorylation status of transcription factors or nuclear kinases such as c-abl. Whether this level of gene regulation is unique to PTPε remains to be seen, however, the observations described undoubtedly describe a new layer of complexity in PTPase regulation. Numerous attempts to define a role for PTPε in hemopoietic cells in response to various growth factors and cytokines yielded no change in tyrosine phosphorylation or enzyme activity. The only stimulus capable of eliciting a change in PTPε tyrosine phosphorylation was pervanadate, a stimulus currently characterized as non-physiological. Introduction of mutant isoforms of p72/74PTPε was also attempted. This

possibly would have allowed substrate trap experiments to be carried to determine the substrates of p72/74PTPε. However, poor transfection efficiencies hampered this line of investigation. In the future perhaps novel gene transfer techniques will facilitate such experiments. Further efforts must be aimed at trying to understand the physiological role of p72/74PTPε, a molecule that may represent the only protein isoform of PTPε expressed in hemopoietic cells.

During the course of this study, the expression of the transmembrane isoform of PTPε in mammalian cells indicated a role for the PTPase in the regulation of cell-cell adhesion. Immunoflourescence studies and cellular morphology form the basis for this hypothesis. While preliminary investigation revealed no change in the expression of β-catenin or cadherins, suitable reagents were not available to assess the tyrosine phosphorylation status of these key cell-cell adhesion proteins. Recent reports however, do implicate PTPases in the regulation of cell-cell adhesion through cadherin-catenin complexes (Soler *et al.*, 1998). In addition, PTPε's apparent activation of $pp60^{c\text{-}src}$ forms a tangible link to cell-cell adhesion. Expression of an active form of *src* in mammalian cells leads to hyper-phosphoryiation of β-catenin. Cadherin-catenin complexes bearing excess phosphotyrosine begin to dismantle, resulting in a loss of cell-cell adhesion (Behrens *et. al.*, 1993). This was shown by the morphology of cells expressing the dominant negative mutant of PTPε, where abnormal cell-cell adhesion was observed with a corresponding, though modest, increase in $pp60^{c\text{-}src}$ tyrosine phosphorylation and decrease in kinase activity. Interestingly, it may be that PTPε has numerous substrates at the sites of adherens junctions but the dominant phenotype is the increase in cell

adhesion, due to the modest decrease in kinase activity. While these experiments were being carried out, an effort to use homologous recombination to create homozygous null mice at the RPTPE locus was successfully completed (Pownall and Jirik, unpublished). While analysis is ongoing, preliminary experiments revealed no visible phenotype in $RPTPE^{-/-}$ mice. This finding may be interpreted in a number of ways. Due to the restricted expression pattern of PTPε as described here and by other groups, the phenotype of the PTPε knock-out may be effectively hidden since it is not yet known where PTPε function is most critical. Indeed, PTPα may in some cell types provide a level of redundancy for the loss of PTPε expression if PTPα and PTPε are concurrently expressed. This work touches upon the growing importance of the PTPase family of signal transduction enzymes and the complexity of signal transduction systems.

Chapter 7

References

Adzhubei, A.A., Sternberg, M., J. (1993). Left-handed polyproline II helices commonly occur in globular proteins. J. Mol. Biol. *229*(2), 472-93.

Ales-Martinez, J.E., Cuende, E., Martinez, C., Parkhouse, R.M., Pezzi, L., Scott, D.W. (1991). Signalling in B cells. Immunol. Today *12*(6), 201-5.

Ahmad, F., Goldstein, B.J. (1997). Functional association between the insulin receptor and the transmembrane protein-tyrosine phosphatase LAR in intact cells. J. Biol. Chem. *272*(1), 448-57.

Balsamo J, (1996). Regulated binding of PTP1B-like phosphatase to N-cadherin: control of cadherin-mediated adhesion by dephosphorylation of beta-catenin. J. Cell. Biol. *134*(3), 801-813.

Barford, D., Das, A.K., Egloff, M.P. (1998). The structure and mechanism of protein phosphatases: insights into catalysis and regulation. Annu. Rev. Biophys. Biomol. Struct. *27*, 133-64.

Bilwes, A.M., den Hertog, J., Hunter, T., Noel, J.P. (1996). Structural basis for inhibition of receptor protein-tyrosine phosphatase-alpha by dimerization. Nature *382*(6591), 555-9.

Bouchard, P., Zhao, Z., Banville, D., Dumas, F., Fischer, E.H., Shen, S.H. (1994). Phosphorylation and identification of a major tyrosine phosphorylation site in protein tyrosine phosphatase 1C. J. Biol. Chem. *269*(30), 19585-9.

Burden-Gulley, S.M., Brady-Kalnay, S.M. (1999). PTPmu regulates N-cadherin-dependent neurite outgrowth. J. Cell. Biol. *144*(6), 1323-36.

Cantley, L.C., Auger, K.R., Carpenter, C., Duckworth, B., Graziani, A., Kapeller, R., and Soltoff, S. (1991). Oncogenes and signal transduction. Cell *64*, 281-302.

Chan, A.C., Desai, D.M., Weiss, A. (1994). The role of protein tyrosine kinases and protein tyrosine phosphatases in T cell antigen receptor signal transduction. Annu. Rev. Immunol. *12*, 555-92.

Charbonneau, H., Tonks, N.K., Walsh, K.A., Fischer, E.H. (1988). The leukocyte common antigen (CD45): a putative receptor-linked protein tyrosine phosphatase. Proc. Natl. Acad. Sci. *85*(19), 7182-6.

Charbonneau, H., Tonks, N.K., Kumar, S., Diltz, C.D., Harrylock, M. (1989). Human placenta protein tyrosine phosphatase: amino acid sequence and relationship to a family of receptor-like proteins. Proc. Natl. Acad. Sci. *86*, 5252-5256.

Cho, H., Ramer, S.E., Itoh, M., Kitas, E., Bannwarth, W., Burn, P., Saito, H., Walsh, C.T. (1992). Catalytic domains of the LAR and CD45 protein tyrosin phosphatases from *E. coli* expression systems: purification and characterization of specificity and mechanism. Biochemistry *31*, 133-138.

Cicchetti, P., Mayer, B.J., Theil, G., Baltimore, D. (1992). Indentification of a protein that binds the SH3 region of Abl and is similar to Bcr and GAP-rho. Science *257*, 803-806.

Collins, S.J., Ruscetti, F.W., Gallagher, R.E., Gallo, R.C. (1978). Terminal differentiation of human promyelocytic leukemia cells induced by dimethyl sulfoxide and other polar compounds. Proc. Natl. Acad. Sci. *75*(5), 2458-62.

Collins, S.J, (1987). The HL-60 promyelocytic leukemia cell line: proliferation, differentiation, and cellular oncogene expression. Blood *70*(5), 1233-44.

Cool, D.E., Tonks, N.K., Charbonneau, H., Walsh, K.A., Fischer, E.H., Krebs, E.G. (1989). cDNA isolated from a human T-cell library encodes a member of the protein-tyrosine-phosphatase family. Proc. Natl. Acad. Sci. *86*(14), 5257-61.

Cooper, J.A., Howell, B. (1993). The When and How of Src Regulation. Cell *73*, 1051-1054.

David, M., Grimley, P.M., Finbloom, D.S., Larner, A.C. (1993). A nuclear tyrosine phosphatase downregulates interferon-induced gene expression. Mol. Cell. Biol. *13*(12), 7515-21.

Dechert, U., Adam, M., Harder, K.W., Clark-Lewis, I., Jirik, F.R. (1994). Characterization of protein tyrosine phosphatase Sh-PTP2. J. Biol. Chem. *269*, 5602-5611.

Denu, J.M., Stuckey, J.A., Saper, M.A., Dixon, J.E. (1996). Form and function in protein dephosphorylation. Cell *87*(3), 361-4.

Denu, J.M., Lohse, D.L., Vijayalakshmi, J., Saper, M.A., Dixon, J.E. (1996). Visualization of intermediate and transition-state structures in protein-tyrosine phosphatase catalysis. Proc. Natl. Acad. Sci. *93*(6), 2493-8.

Denu, J.M., Tanner, K.G. (1998). Specific and reversible inactivation of protein tyrosine phosphatases by hydrogen peroxide: evidence for a sulfenic acid intermediate and implications for redox regulation. Biochemistry, *37*(16), 5633-5642.

Desai, D.M., Sap, J., Schlessinger, J., Weiss, A. (1993). Ligand-mediated negative regulation of a chimeric transmembrane receptor tyrosine phosphatase. Cell *73*, 541-554.

Elson, A., and Leder, P. (1995a). Protein-tyrosine phosphatase ε. J. Biol. Chem. *270*, 26116-26122.

Elson, A., and Leder, P. (1995b). Identification of a cytoplasmic, phorbol ester-inducible isoform of protein tyrosine phosphatase ε. Proc. Natl. Acad. Sci. *92*, 12235-12239.

Erpel, R., Superti-Furga, G., Courtneidge, S.A. (1995). Mutational analysis of the Src SH3 domain: the same residues of the ligand binding surface are important for intra- and intermolecular interactions. EMBO J. *14*, 963-975.

Farrar, M.A., Schreiber, R.D. (1993). Annu. Rev. Immunol. *11*, 571-611.

Flint, A.J., Gebbink, M.F., Franza, B.R., Jr., Hill, D., E., Tonks, N.K. (1993). Multi-site phosphorylation of the protein tyrosine phosphatase, PTP1B: identification of cell cycle regulated and phorbol ester stimulated sites of phosphorylation. EMBO J. *12*(5), 1937-46.

Gold, M.R., DeFranco, A.L. (1994). Biochemistry of B lymphocyte activation. Adv Immunol *55*, 221-95.

Goldstein, B.J., Ahmad, F., Ding, W., Li, P.M., Zhang, W.R., (1998) Regulation of the insulin signalling pathway by cellular protein-tyrosine phosphatases. Mol. Cell. Biochem. 182(1-2), 91-9.

Guan, K.L., Butch, E. (1995). Isolation and characterization of a novel dual specific phosphatase, HVH2, which selectively dephosphorylates the mitogen-activated protein kinase. J. Biol. Chem. *270*(13), 7197-203.

Harder, K.W., Owen, P., Wong, L.H.K., Aebersold, R., Clark-Lewis, I., Jirik, F.R. (1994). Characterization and kinetic analysis of the intracellular domain of human protein tyrosine phosphatase β (HPTPβ) using synthetic phosphopeptides. Biochem. J. *298*, 395-401.

Harder, K.W. (1996). An Analysis of the Structure and Function of Protein Tyrosine Phosphatase α. Ph.D. Thesis U.B.C.

zur Hausen, J.D., Burn, P., Amrein, K.E. (1997). Co-localization of Fyn with CD3 complex, CD45 or CD28 depends on different mechanisms. Eur. J. Immunol. *27*(10), 2643-9.

Hashimoto, Y., Katayama, H., Kiyokawa, E., Ota, S., Kurata, T., Gotoh, N., Otsuka, N., Shibata, M., Matsuda, M. (1998). Phosphorylation of CrkII adaptor protein at tyrosine 221 by epidermal growth factor receptor. J. Biol. Chem. *273*(27), 17186-91.

Heffetz, D., Bushkin, I., Dror, R., Zick, Y. (1990). The insulinomimetic agents H2O2 and vanadate stimulate protein tyrosine phosphorylation in intact cells. J. Biol.Chem. *265*, 2896-2902.

Hendriks, W., Brugman, C., Schepens, J., Wieringa, B. (1994). Rapid assessment of protein-tyrosine phosphatase expression levels by RT-PCR with degenerate primers. Mol. Biol. Rep. *19*, 105-108.

den Hertog, J., Pals, C.E.G.M., Peppelenbosch, M.P., Tertoolen, L.G.J., de Laat, S.W., Kruijer, W. (1993). Peceptor protein tyrosine phosphatase α activates pp60c-src and is involved in neuronal differentiation. EMBO J. *12*, 3789-3798.

Hiscox, S., Jiang, W.G. (1998). Association of PTPmu with catenins in cancer cells: a possible role for E-cadherin. Int. J. Oncol. *13*(5), 1077-80.

Ho, S.N., Hunt, H.D., Horton, R.M., Pullen, J.K., Pease, L.R. (1989). Site-directed mutagenesis by overlap extension using the polymerase chain reaction. Gene *77*(1),51-9.

Holland, S.J., Peles, E., Pawson, T., Schlessinger, J. (1998). Cell-contact-dependent signalling in axon growth and guidance: Eph receptor tyrosine kinases and receptor protein tyrosine phosphatase beta. Curr. Opin. Neurobiol. *8*(1),117-127.

Holowka, D., Baird, B. (1996). Antigen-mediated IGE receptor aggregation and signaling: a window on cell surface structure and dynamics. Annu. Rev. Biophys. Biomol. Struct. *25*, 79-112.

Howell, B.W., Cooper, J.A. (1994). Csk Suppression of Src Involves Movement of Csk to sites of Src Activity. Mol. Cell. Biol. *14*, 5402-5411.

Hsu, S.L., Chou, Y.H., Yin, S.C., Liu, J.Y. (1998). Differential effects of phorbol ester on growth and protein kinase C isoenzyme regulation in human hepatoma Hep3B cells. Biochem. J. *333* (Pt 1), 57-64.

Hunter, T. (1995). When is a lipid kinase not a lipid kinase? When it is a protein kinase. Cell *80*, 225-236.

Ihle, J., N. (1995). Cytokine receptor signaling. Nature *377*, 591-594.

Jackson, P.K., Paskind, M., Baltimore, D. (1993). Mutation of a phenylalanine conserved in SH3-containing tyrosine kinases activates the transforming ability of c-Abl. Oncogene *7*, 1943-1956.

Jia, Z., Barford, D., Flint, A.J., Tonks, N.K. (1995). Structural basis for phosphotyrosine peptide recognition by protein tyrosine phosphatase 1B. Science *268*(5218), 1754-8.

Jirik, F.R., Janzen, N.M., Melhado, I.G., Harder, K.W. (1990). Cloning and chromosomal assignment of a widely expressed human receptor-like protein-tyrosin phosphatase. FEBS Lett. *273*, 239-242.

Kaplan, R., Morse, B., Huebner, K., Croce, C., Howk, R., Ravera, M., Ricca, G., Jaye, M., Schlessinger, J. (1990). Proc. Natl. Acad. Sci. *87*, 7000-7004.

Kaplan, K.B., Bibbines, K.B., Swedlow, J.R., Arnaud, M., Morgan, D.O., Varmus, H.E. (1994). Association of the amino-terminal half of c-Src with focal adhesions alters their properties and is regulated by phosphorylation of tyrosine 527. EMBO J. *13*, 4745-4756.

Katagiri, T., Ogimoto, M., Hasegawa, K., Mizuno, K., Yakura, H. (1995). Selective regulation of Lyn tyrosine kinase by CD45 in immature B cells. J. Biol. Chem. *270*(47), 27987-90.

Kiyokawa, E., Mochizuki, N., Kurata, T., Matsuda, M. (1997). Role of Crk oncogene product in physiologic signaling. Crit. Rev. Oncog. *8*(4), 329-42.

Koch, C.A., Anderson, D., Moran, M.F., Ellis, C., Pawson, T. (1991). SH2 and SH3 Domains: Elements That Control Interactions of Cytoplasmic Signaling Proteins. Science *252*, 668-674.

Koval, A.P., Karas, M., Zick, Y., LeRoith, D. (1998). Interplay of the proto-oncogene proteins CrkL and CrkII in insulin-like growth factor-I receptor-mediated signal transduction. J. Biol. Chem. 273(24), 14780-7.

Kreuger, N.X., Streuli, M., and Saito, H. (1990). Structural diversity and evolution of human receptor-like protein tyrosine phosphatases.
EMBO J. *9*, 3241-3252.

Krypta, R.M., *et al* (1996). Association between a transmembrane protein tyrosine phosphatase and the cadherin-catenin complex.
J. Cell. Biol.*134*(6), 1519-1529.

Kume, T., Tsuneizumi, K., Watanabe, T., Thomas, M.L., Oishi, M. (1994). Induction of specific protein tyrosine phosphatase transcripts during differentiation of mouse erythroleukemia cells. J. Biol. Chem. *269*, 4709-4712.

Kwan Lim, G.E., McNeill, L., Whitley, K., Becker, D.L., Zamoyska, R. (1998). Co-capping studies reveal CD8/TCR interactions after capping CD8 beta polypeptides and intracellular associations of CD8 with p56(lck). Eur. J. Immunol. *28*(2), 745-54.

Kwiatkowska, K., Sobota, A. (1999). Tyrosine phosphorylation/dephosphorylation controls capping of Fcgamma receptor II in U937 cells. Cell. Motil. Cytoskeleton *42*(4), 298-314.

Lammers, R., Moller, N.P., Ullrich, A. (1997). The transmembrane protein tyrosine phosphatase alpha dephosphorylates the insulin receptor in intact cells. FEBS Lett. *404*(1), 37-40.

Lanzetta, P.A., Alvarez, L.J., Reinach, P.S., Candia, O.A. (1979). An improved assay for nanomole amounts of inorganic phosphate. Anal. Biochem. *100*, 95-97.

Levy, J.B., Canoll, P.D., Silvennoinen, O., Barnea, G., Morse, B., Honegger, A.M., Huang, J.T., Cannizzaro, L.A., Park, S.H., Druck, T., *et al.* (1993). The cloning of a receptor-type protein tyrosine phosphatase expressed in the central nervous system. J. Biol. Chem. *268*(14), 10573-81.

Lim, W.A., Richards, F.M., Fox, R.O. (1994). Structural determinants of peptide-binding orientation and of sequence specficity in SH3 domains. Nature *372*, 375-379.

Liu, F., Hill D.E., Chernoff, J. (1996). Direct binding of the proline-rich region of protein tyrosine phosphatase 1B to the Src homology 3 domain of p130(Cas). J. Biol. Chem. *271*(49), 31290-5.

Maagdengerb, A.M.J.M., Hurk, H.H., Weghuis, D.O., Wieringa, B., Kessel, A.G., Hendriks, W.J.A. (1995). Genomics *30*,128-129.

Maehama, T., Dixon, J.E. (1998). The tumor suppressor, PTEN/MMAC1, dephosphorylates the lipid second messenger, phosphatidylinositol 3,4,5-trisphosphate. J. Biol. Chem. *273*(22), 13375-8.

Mathews, R.J., Cahir, E.D., and Thomas, M.L. (1990). Proc. Natl. Acad. Sci. *87*, 4444-4448.

Matsuyoshi, N., Hamaguchi, M., Taniguchi, S., Nagafuchi, A., Tsukita, S., Takeichi, M. (1992). Cadherin-mediated cell-cell adhesion is perturbed by v-src tyrosine phosphorylation in metastatic fibroblasts. J. Cell. Biol. *118*(3), 703-14.

McPhail, L.C. (1994). SH3-dependent Assembly of the Phagocyte NADPH Oxidase. J. Exp. Med. *180*, 2011-2015.

Melhado, I.G., Anderson, L.L., Duncan, A.M.V., Jirik, F.R. (1996). The gene encoding protein tyrosine phosphatase RPTPε (PTPRE) is assigned to human chromosome 10q26. Cytogen. Cell Gen. *73*, 168-178.

de Mendez, I., Adams, A.G., Sokolic, R.A., Malech, H.L., Leto, T.L. (1996). Multiple SH3 domain interactions regulate NADPH oxidase assembly in whole cells. EMBO J. *15*(6), 1211-20.

Milarski, K.L., Zhu, G., Pearl, C.G., McNamara, D.J., Dobrusin, E.M., MacLean, D., Thieme-Sefler, A., Zhang, Z.Y., Sawyer, T., Decker, S.J., et. al. (1993). Sequence specificity in recognition of the epidermal growth factor receptor by protein tyrosine phosphatase 1B. J. Biol. Chem. *268*(31), 23634-9.

Moller, N.P., Moller, K.B., Lammers, R., Kharitonenkov, A., Sures, I., Ullrich, A. (1994). Src kinase associates with a member of a distinct subfamily of protein-tyrosine phosphatases containing an ezrin-like domain. Proc. Natl. Acad. Sci. *91*(16), 7477-81.

Moller, N.P.H., Moller, K.B., Lammers, R., Kharitonenkov, A., Hoppe, E., Wiberg, C., Sures, I., and Ullrich, A. (1995). Selective Down-regulation of the Insulin Receptor Signal by Protein-tyrosine Phosphatases α and ε. J. Biol. Chem. *270*, 23126-131.

Musacchio, A., Noble, M., Pauptit, R., Wierenga, R., Saraste, M. (1992). Crystal structure of a Src-homology 3 (SH3) domain. Nature *359*,851-855.

Musacchio, A., Saraste, M., Wilmanns, M. (1994). High-resolution crystal structures of tyrosine kinase SH3 domains complexed with proline-rich peptides. Nat. Struct. Biol. *8*, 489- 491.

Mustelin, T., Coggeshall, K.M., Altman, A. (1989). Rapid activation of the T-cell tyrosine protein kinase pp56lck by the CD45 phosphotyrosine phosphatase. Proc. Natl. cad. Sci. *86*(16), 6302-6.

Mustelin, T., Altman, A. (1990). Dephosphorylation and activation of the T cell tyrosine kinase pp56lck by the leukocyte common antigen (CD45). Oncogene *5*(6), 809-13.

Neel, B.G., Tonks, N.K. (1997). Protein tyrosine phosphatases in signal transduction. Curr. Opin. Cell. Biol. *9*(2), 193-204.

Neel, B.G. (1997). Role of phosphatases in lymphocyte activation. Curr. Opin. Immunol. *9*(3), 405-20.

Okada, M., Howell, B.W., Broome, M.A., Cooper, J.A. (1994). Deletion of the SH3 Domain of Src Interferes with Regulation by the Phosphorylated carboxyl-terminal Tyrosine. J. Biol. Chem. *268*, 18070-18075.

Okada, S., Matsuda, M., Anafi, M., Pawson, T., Pessin, J.E. (1998). Insulin regulates the dynamic balance between Ras and Rap1 signaling by coordinating the assembly states of the Grb2-SOS and CrkII-C3G complexes. EMBO J. *17*(9), 2554-65.

Ostergaard, H.L., Shackelford, D.A., Hurley, T.R., Johnson, P., Hyman, R., Sefton, B., M., Trowbridge I.S. (1989). Expression of CD45 alters phosphorylation of the lck-encoded tyrosine protein kinase in murine lymphoma T-cell lines. Proc. Natl. Acad. Sci. *86*(22), 8959-63.

Pannifer, A.D., Flint, A.J., Tonks, N.K., Barford, D. (1998). Visualization of the cysteinyl-phosphate intermediate of a protein-tyrosine phosphatase by x-ray crystallography. J. Biol. Chem. *273*(17), 10454-62.

Pawson, T., Gish, G.D. (1992). SH2 and SH3 domains in signal transduction. Adv. Cancer. Res. *64*, 87-110.

Peles, E., Schlessinger, J., Grumet, M. (1998). Multi-ligand interactions with receptor-like protein tyrosine phosphatase beta: implications for intercellular signaling. Trends Biochem. Sci. *23*(4), 121-4.

Pingel, J.T., Thomas, M.L. (1989). Evidence that the leukocyte-common antigen is required for antigen-induced T lymphocyte proliferation. Cell *58*(6), 1055-65.

Pleiman, C.M., Hertz, W.M., Cambier, J.C. (1994). Activation of phosphatidylinositol-3' kinase by Src-family kinase SH3 binding to the p85 subunit. Science *263*, 1609-1612.

Posner, B.I., Faure, R., Burgess, J.W., Bevan, A.W., Lachance, D., Zhang-Sun, G., Fantus, I.G., Ng, J.B., Hall, D.A., Soo Lum, B., Shaver, A. (1994). Peroxovanadium compounds. A new class of potent phosphotyrosine phosphatase inhibitors which are insulin mimetics. J. Biol.Chem. *269*, 4596-4604.

Ralph, S.J., Thomas, M.L., Morton, C.C., Trowbridge, I.S. (1987). Structural variants of human T200 glycoprotein (leukocyte-common antigen). EMBO J. *6*(5), 1251-7.

Raschke, W.C., Baird, S., Ralph, P., Nakoinz, I. (1978). Functional macrophage cell lines transformed by Abelson leukemia virus. Cell *15*, 261-267.

Reedjik, M., Liu, X., Van der Geer, P., Letwin, K., Waterfield, M.D., Hunter, T., Pawson, T. (1992). Tyr721 regulates specific binding of the CSF-1 receptor kinase insert to PI 3'-kinase SH2 domains: a model for SH2-mediated receptor-target interactions. EMBO J.*11*, 1365-1372.

Renzoni, D.A., Pugh, D.J., Siligardi, G., Das, P., Morton, C.J., Rossi, C., Waterfield, M.D., Campbell, I.D., Ladbury, J.E. (1996). Structural and thermodynamic characterization of the interaction of the SH3 domain from Fyn with the proline-rich binding site on the p85 subunit of PI3-kinase. Biochemistry *35*(49), 15646-53,

Rivard, N., McKenzie, F.R., Brondello, J.M., Pouyssegur, J. (1995). The phosphotyrosine phosphatase PTP1D, but not PTP1C, is an essential mediator of fibroblast proliferation induced by tyrosine kinase and G protein-coupled receptors. J. Biol. Chem. *270*(18), 11017-24.

Rohrschneider, L.R., Eisenman, R.N., Leitch, C.R. (1979). Identification of a Rous sarcoma virus transformation-related protein in normal avian and mammalian cells. Proc. Natl. Acad. Sci. *76*(9), 4479-83.

Ruzzene, M., Donell-Deana, A., Marin, O., Perich, J.W., Ruzza, P., Borin, G., Calderan, A., Pinna, L.A. (1993). Sequence specificity of C-terminal Src kinase (CSK) a comparison with Src-related kinases c-Fgr and Lyn. Eur. J. Biochem. *211*, 289-295.

Sadowski, I., Stone, J.C., Pawson, T. (1986). A noncatalytic domain conserved among cytoplasmic protein-tyrosine kinases modifies the kinase function and transforming activity of Fujinami sarcoma virus P130gag-fps. Mol. Cell. Biol. *6*(12), 4396-408.

Sanger, F., Nicklen, S., Coulson, A.R. (1977). DNA sequencing with chain-terminating inhibitors. Proc. Natl. Acad. Sci. *74*(12),5463-7.

Sap, J., D'Eustachio, P., Givol, D., Schlesinger, J. (1990). Proc. Natl. Acad. Sci. *87*, 6112-6116.

Sato, T., Irie, S., Kitada, S., Reed, J., C. (1995). FAP-1: a protein tyrosine phosphatase that associates with Fas. Science *268*(5209), 411-5.

Schlessinger, J. (1994). SH2/SH3 signaling proteins. Curr. Opin. Genet. Dev. 4(1), 25-30.

Schroeter, E.H., Kisslinger, J.A., Kopan, R. (1998). Notch-1 signalling requires ligand-induced proteolytic release of intracellular domain. Nature. *393*, 382.

Secrist, J.P., Burns, L.A., Karnitz, L., Koretsky, G.A., Abraham, R.T. (1993). J. Biol. Chem. *268*, 5886-5893.

Sefton, B., M., Hunter, T., Beemon, K., and Eckhart, W. (1980). Evidence that the phosphorylation of tyrosine is essential for cellular transformation by Rous sarcoma virus. Cell *20*, 807.

Seimiya, H., Sawabe, T., Toho, M., and Tsuruo, T. (1995). Phorbol ester-resistant monoblastoid leukemia cells with a functional mitogen-activated protein kinase cascade but without responsive protein tyrosine phosphatases. Oncogene *11*, 2047-2054.

Shuai, K., Stark, G., R., Kerr, I., M., Darnell, Jr., J., E. (1993). A single phosphotyrosine residue of Stat91 required for gene activation by interferon-gamma. Science *261*, 1744-1746.

Serra-Pages, C., Medley, Q.G., Tang, M., Hart, A., Streuli, M. (1998). Liprins, a family of LAR transmembrane protein-tyrosine phosphatase-interacting proteins. J. Biol. Chem. *273*(25), 15611-20.

Smith, D.B., Johnson, K.S. (1988). Single-step purification of polypeptides expressed in Escherichia coli as fusions with glutathione S-transferase. Gene *67*(1), 31-40.

Soler, C., Rousselle, P., Damour, O. (1998). Cadherin mediated cell-cell adhesion is regulated by tyrosine phosphatases in human keratinocytes. Cell. Adhes. Commun. *5*(1), 13-25.

Su, L., Zhao, Z., Bouchard, P., Banville, D., Fischer, E.H., Krebs, E.G., Shen, S.H. (1996). Positive effect of overexpressed protein-tyrosine phosphatase PTP1C on mitogen-activated signaling in 293 cells. J. Biol. Chem. *271*(17), 10385-90.

Sun, H., Tonks, N.K., (1994). Trends in Biochem. Sci. *19*, 480-485.

Sun, H., Charles. C.H., Lau, L.F., Tonks, N.K. (1993). MKP-1 (3CH134), an immediate early gene product, is a dual specificity phosphatase that dephosphorylates MAP kinase in vivo. Cell *75*(3), 487-93.

Sundaresan, M., Yu, Z.X., Ferrans, V.J., Irani, K., Finkel, T. (1995). Requirement for generation of H_2O_2 for platelet-derived growth factor signal transduction. Science *270*(5234), 296-9.

Su, J., Batzer, A., Sap, J. (1994). Association between receptor protein-tyrosine phosphatase RPTPalpha and the Grb2 adaptor. Dual Src homology (SH) 2/SH3 domain requirement and functional consequences. J. Biol. Chem. *269*, 18731-18734.

Streuli, M., Hall, L.R., Saga, Y., Schlossman, S.F., Saito, H. (1987). Differential usage of three exons generates at least five different mRNAs encoding human leukocyte common antigens. J. Exp. Med. *166*(5), 1548-66.

Thomas, M.L., Reynolds, P.J., Chain, A., Ben-Neriah, Y., Trowbridge, I.S. (1987). B-cell variant of mouse T200 (Ly-5): evidence for alternative mRNA splicing. Proc. Natl. Acad. Sci. *84*(15), 5360-3.

Thomas, M.L., and Lefrancois, L. (1988). Differential expression of the leukocyte common antigen family. Immunol. Today *9*, 320-326.

Tomic, S., Greiser, U., Lammers, R., Kharitonenkov, A., Imyanitov, E., Ullrich, A., Bohmer, F., D. (1995). Association of SH2 domain protein tyrosine phosphatases with

the epidermal growth factor receptor in human tumor cells. Phosphatidic acid activates receptor dephosphorylation by PTP1C. J. Biol. Chem. *270*(36), 21277-84.

Uchida, T., Matoxaki, T., Matsuda, K., Suzuki, T., Matozaki, S., Nakano, O., Wada, K., Konda, Y., Sakamoto, C., and Kasuga, M. (1993). Phorbol ester stimulates the activity of a protein tyrosine phosphatase containing SH2 domains (PTP1C) in HL-60 leukemia cells by increasing gene expression. J. Biol. Chem. *268*, 11845-850.

Van der Geer, P., and Hunter, T. (1990). Identification of tyrosine 706 in the kinase insert as the major colony-stimulating factor 1 (CSF-1)-stimulated autophosphorylation site in the CSF-1 receptor in a murine macrophage cell line. Mol. Cell. Biol. *10*, 2991-3002.

Williamson, M. (1994). The structure and function of proline-rich regions in the proteins. Biochem. J. *297*, 249-260.

Yanagi, S., Sugawara, H., Kurosaki, M., Sabe, H., Yamamura, H., Kurosaki, T. (1996). CD45 modulates phosphorylation of both autophosphorylation and negative regulatory tyrosines of Lyn in B cells. J. Biol. Chem. *271*(48), 30487-92.

Yi, T., Cleveland, J., L., Ihle, J.N. (1991). Identification of novel protein tyrosine phosphatases of hematopoietic cells by polymerase chain reaction amplification. Blood *78*, 2222-2228.

Yoshida, M., Kawai, S., Toyoshima, K. (1980). Unifected avian cells contain structurally unrelated progenitors of viral sarcoma genes. Nature *287*(5783), 653-4.

Zhang, Z.Y. (1998). Protein-tyrosine phosphatases: biological function, structural characteristics, and mechanism of catalysis. Crit. Rev. Biochem. Mol. Biol. *33*(1), 1-52.

Zhang, Z.-Y., Thieme-Sefler, A.M., MacClean, D., McNamara, D., Dobrusin, E.M., Sawyer, T.K., Dixon, J.E. (1993). Proc. Natl. Acad. Sci. *90*, 4446-4450.

Zhao, Z., Shen, S.-H., and Fischer, E.H. (1994). Stimulation by phospholipids of a protein-tyrosine-phosphatase containing two src homology 2 domains. Proc. Natl. Acad. Sci. *91*, 5007-5011.

Zhao, Y., Wu, L., Noh, S., J., Guan, K.L., Zhang, Z.Y. (1998). Altering the nucleophile specificity of a protein-tyrosine phosphatase-catalyzed reaction. Probing the function of the invariant glutamine residues. J. Biol. Chem. *273*(10), 5484-92.

Zheng, X., M., Wang, Y., Pallen, C.J. (1992). Cell transformation and activation of pp60c-src by over-expression of a protein tyrosine phosphatase. Nature *359*, 336-339.

Ziegler, S.F., Levin, S.D., Perlmutter, R.M. (1989). Transformation of fibroblasts by an activated form of p59hck. Mol. Cell. Biol. *9*, 2724-2720.